POLITECNICO DI TORINO

Dipartimento di Elettronica e Telecomunicazioni

Corso di Laurea in Sistemi Elettronici

Master Degree Thesis

Physical simulations of molecular FCN technology

Supervisor
Prof. Gianluca PICCININI
Prof. Mariagrazia GRAZIANO

Candidate
Ugo ROMANO

Aprile 2018

"Everybody is a genius.
But if you judge a fish by
its ability to climb a tree
it will live its whole life
believing that it is stupid"
Albert Einstein

Acknowledgements

First of all, I would like to thank my parents for the support they have always given me, for their encouragement in the dark moments and for aling me, with sacrifices, to study here in Turin. Thanks also to my family and friends who tried to stay close despite the distance. Special thanks goes to my friend Chiara, for her patience during all these university years. But the deepest thanks goes to all those people who thought that I would never have done it because, if tI'm here, it is only thanks to them.

Summary

Nowadays the world is more "mobile" than ever. This mobility brings with it a very important technological problem: the miniaturization of electronic devices. Laptops and smartphones are more and more powerful meaning that bigger RAM and powerful processors must be placed within a small space. In order to achieve this goal, the miniaturization of single transistor might be the only solution. Until now the electronics industry has been based on Moore's Law which declare that "the number of transistors per square inch on integrated circuits had doubled every year since their invention". However, the ITRS roadmap predicted in 2015 that Moore's law will die in 2020, as matter of fact, we have now reached the physical limit of the semiconductor-based technology (few nanometer). There are some unmanageable problems at this level of miniaturization, for example the high power consumption due to leakage current. To overcome this problem we are aiming at other technologies, one of the most interesting is FCN (Field Coupled Nano-Computing): with this technology no more transistors, currents and voltage are used to transfer the information but alternately, via local field interactions between blocks of the circuit. In particular, the mQCA (molecular Quantum cellular automata) technology was studied in this thesis. Many solutions were proposed for QCA technology, for example semiconductor QCA, metal-dot QCA and magnetic-QCA. These technologies present some problems such as the working temperature and the working frequencies and for these reasons they have been left out. Therefore, the molecular technology is the most promising for QCA paradigms. The basic elements of this technology are the molecules, which can store information through the arrangement of the charge inside them. The basic cell is composed by two equal molecules. Each molecule has 2 or 3 redox centers, now called dots, in which is more probable that an electron is attracted or released. Furthermore, a basic cell is composed by 4 or 6 dots, and the charge displacement inside the cell determines its logic state. This cell has been designed to be bistable, then there are two states with lower energy and in these two states we encode the "0" or "1" logic. A clock field is needed to help the switching of the molecules. In literature many molecules have been proposed as candidates, in particular diallyl butane (4-dot molecule) whose behavior is considered the ideal one for this technology, but it presents two main problem: the absence of the third

dot necessary for the clock and the absence of the molecular binding element necessary for physical implementation. The University of Bologna and Polytechnic of Torino synthesized a new molecule *ad-hoc* for QCA computation: the bis-ferrocene molecule. In this work, three main molecules (diallyl butane, decatriene and bisferrocene) has been studied and analyzed throughout several ab-initio simulations with a computational chemistry software (GAMESS). This is the first time that this software has been used, in fact the software which has been used for this kind of work was gaussian09. For this reason, the first step of this thesis was studying and writing the manual of this software: all commands used in this work has been written and explained, for example the resolution method for Schrodinger equation (RHF, UHF, DFT), the basis-set (6,31g(d, p)), the total charge and so on. Then some simulations have been done to compare the results obtained by the two software to see if they converge. In particular the electric potential and the charge displacement were compared for the diallyl butane and decatriene molecules.

After this first step, the three candidate molecules have been analyzed. The steps were the same for each molecule:

- analysis of the molecule capability to encode binary information at equilibrium;

- simulation of the molecules with biasing conditions, in particular:

  - an external electric field (switching field);
  - a write-in system made by point charges;
  - clock field;

- post-processing with Matlab and C program.

The C program was written ad-hoc for this work: it reads the output file from the simulations then finds the atomic charges in this file and sums them to evaluate the dot charges. The first molecule studied was the diallyl butane: in its oxidized form it presents the perfect behavior for QCA computation. For this reason, it can be used as reference for other simulations. Then the bis-ferrocene molecule was simulated both in its neutral and oxidized version. In its neutral form, the bisferrocene is perfectly symmetrical, but the problem is that the slope is very small and consequently the switch also. To obtain a bigger slope, then, the molecule was oxidized by raising an electron from the HOMO (Highest Occupied Molecular Orbital) setting ICHARG = 1 MULT = 2. In this case, unlike gaussian09 which divided the charge equally between the two active ferrocene dots, GAMESS adds extra free charge only in one of the two dots. For this reason, the molecule is polarized at the equilibrium, this means that the molecule is not symmetrical. The difference in the results obtained with gaussian09 is due to the resolution method used and to the different basis-set. In fact, by setting two identical simulations

on both software (basis-set LANL2DZ and method DFT), GAMESS cannot solve the Schrodinger equation. Precisely for this reason the base 6,31-g (d, p) and the UHF method were used. Setting the potential (positions of the nuclei) and adding a number of electrons (with ICHARG), then the program tells you where the electrons are going to by solving the Schrˆdinger equation to some approximation (and under some restrictions, say total spin multiplicity). As can be seen from the figure, in these conditions the symmetry of the molecule is shifted to the right, in particular there is a switch from one state to another with an external electric field of 4.5 V/nm, this has a consequence also for simulations with the charge points. In fact, since the charge points placed at their ideal distance of 1 nm (the same distance of the two active dots) generate an electric field of just 0.5 V/nm, it does not allow the molecule to change the logic state. To allow this, it was found through iterative simulations that the distance from the molecule where to place the charge points is 0.3 nm. As future works, it would be interesting to study how the two software (GAMESS and gaussian09) manage the oxidation of the molecule, in particular GAMESS. Moreover, it would be interesting to study the molecules from a dynamic point of view during the switch, to simulate a QCA wire from a point of view of charge distribution and energy behavior.

Abstract

The work in this thesis is organized as follow:

- **Chapter 1: Introduction:**
  This chapter introduces the physical principles of QCA technology, in particular the clock system which is needed for the transportation of the information.

- **Chapter 2: Molecular QCA:**
  Many solutions were proposed for the QCA technology. For instance, metal-dot solution and semiconductor-solution which had the problem of working temperature (few mK). Another idea was the magnetic-solution, it seems promising but it has the problem of working frequency (too low). For these reason, the molecular-solution is considered the most promising and realistic solution to QCA technology. 3 candidate molecules are shown, in particular the bis-ferrocene molecule in which is focused this work.

- **Chapter 3: Methodology:**
  In this chapter the methodology of this work thesis is shown. The steps was: studying neutral molecule at the equilibrium, with an horizontal external electric field (*switching field*) and with the point charges to approximate a write-in system; then a vertical clock field is applied to the molecules; finally all these simulations are repeated with the oxidized molecole (total charge equal to 1). The results of these simulations was shown in Chapter 6.

- **Chapter 4: Tools Manual for MQCA simulation:**
  The software used in this work was mainly 2: GAMESS and gaussian09. This chapter shows a complete manual for these 2 software which are the most famous for the computational chemistry. All commands to be given as input to the program are described in detail, complete with input examples and explanations on how to read the output files. In addition, there is also a small manual of all programs used for post-processing (eg Avogadro, MacPlot). At the end of this chapter, the reader will be able to simulate accurately the molecular systems he or she prefers.

- **Chapter 5: Gamess vs Gaussian09**:
  As the main objective of this thesis was to find an alternative program to gaussian09, the results obtained using GAMESS were compared with the results obtained previously with gaussian. The molecules tested for this purpose were Diallyl Butane and Decatriene in different conditions (in equilibrium or in external electric field conditions).

- **Chapter 6: Charge distribution:** In this chapter the methodological steps explained in chapter 3 have been followed for each of the three candidate molecules. The diallyl butane molecule, which is also the simplest one, was studied for first, then the decatriene and the bis-ferrocene. For all three, both the neutral and the oxidized form were studied and a quick comparison was made with the results obtained with gaussian09. In particular the study is focused on the bis-ferrocene molecule.

- **Chapter 7: Conclusions and future study**: Some ideas for future studies are proposed.

Contents

List of Figures

List of Tables

Chapter 1

Introduction

Since the invention of the first transistor in 1947 at Bell Labs, the microelectronics industry has followed *Moore's Law* [1].This law takes its name from the engineer that enunciated it, Gordon Moore. Moore noted that the number of transistors on a chip had doubled in a time between 18 and 24 months. From there he formulated a hypothesis that semiconductor would double their capacity every 18 months, the original Moore's Law is shown in Fig. 1.1.
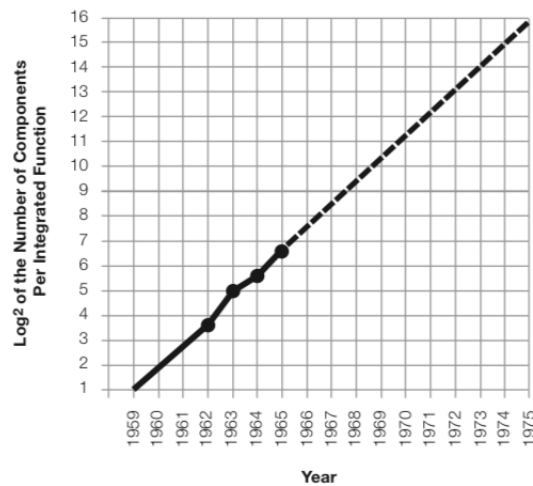
Figure 1.1: Original Moore's law [1]

This means that an integrated circuit would double the number of transistors it contains every 18 months and to follow this trend the area of single transistor would have to decrease. One consequence of Moore's Law is that the length of a transistor (as a channel length) decreases by 30% every two years, as shown in Fig. 1.2.
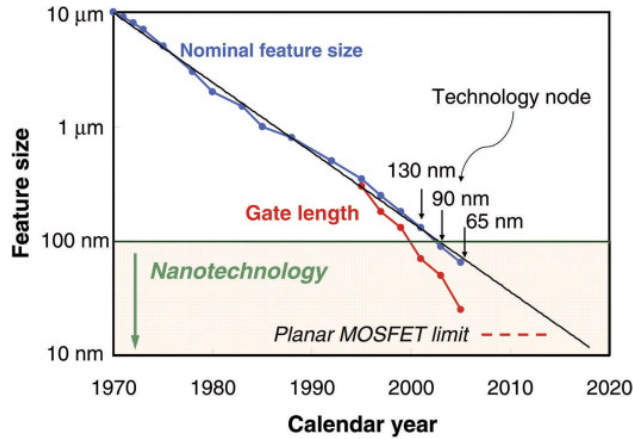
Figure 1.2: Channel lenght of a single transistor over the years [2]

Since the early '70s, the device of choice for high levels of integration has been the field effect transistor (FET). At gate lengths below 0.1 µm FETs will begin to encounter fundamental effects that make further scaling difficult. A possible way for the microelectronics industry to maintain growth in device density is to change from the FET-based paradigm to one based on nanostructures. One nanostructure paradigm, proposed by Lent in the early '90s is the quantum-dot cellular automata (QCA) [3],[4],[5],[6] which employs arrays of coupled quantum dots to implement Boolean logic functions. The advantage of QCA lies in the extremely high packing densities possible due to the small size of the dots, the simplified interconnection, and the extremely low power-delay product.

1.1 QCA

The ideal basic QCA cell is made of coupled quantum dots and a few free charges in a square array coupled by tunnel barriers. It consists of four quantum dots in the corners (called *working dots* or *active dots*) and two free charges in the middle. Let's consider half a QCA cell made by 2 active dots and one free charge, as shown in Fig. 1.3
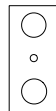
Figure 1.3: Basic half cell for QCA.

The electrons (as the charge) can stay in one of them depending on the external conditions. So, aligning another half QCA to obtain a complete cell, the electrons

in the first half cell force the electrons in the second half cell in the dots on opposite corners. For example, in Fig. 1.4 is shown what happens if two half cells with the charge in the same active dot are aligned.

(a)   (b)
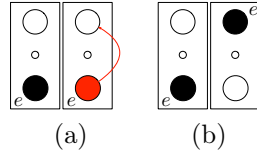
Figure 1.4: Re-arrangment of the charge between two nearby half cell.

What happens is the the charge in the second half cell re-arranges itself. This is due to the Coulomb interaction between them and to minimize the energy of the cell.

It is possible to have three different configurations for one QCA cell, which are shown in Fig. 1.5. Each configuration can encode the logic "0" or "1" if the free charges are confined in two opposite dots, while if the electrons are in the middle the state encoded is a *NULL state.* Electrons are able to tunnel between the dots, but cannot leave the cell.

"1"   "0"   "$NULL$"
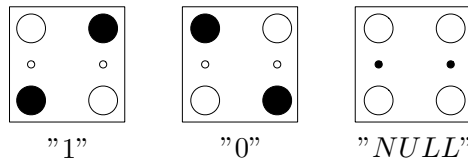
Figure 1.5: Basic cell and logic state encoding for QCA.

Two contiguous cells are placed at the same distance d that is between the two active dots of a half cell, as shown in Fig. 1.6. In this condition, the communication between two nearby cells is due to the Coulomb interaction between the working dots at the edge of the two nearby cells leading to a charge re-arrangement inside the second cell according to the previous cell state, as seen for two half cells.
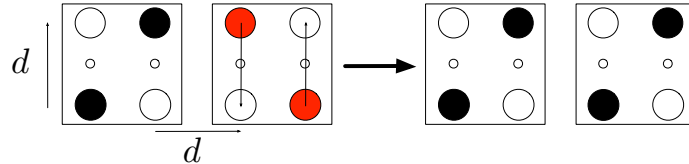
Figure 1.6: Interaction between QCA cells: re-arrangement of the charge in the second cell due to the Coulomb force.

Aligning many QCA cells we obtain the simplest and most fundamental block for QCA: a wire. In other words, a wire is simply a line of QCA cells, as in Fig. 1.7.
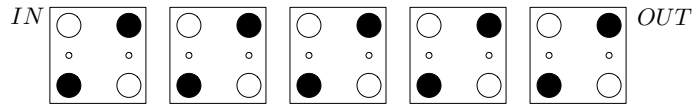
Figure 1.7: QCA wire.

At first, the line is at the ground state ′0′. An input, in this case ′1′, is applied to the left of the line and it forces the first cell to one polarization. Now the first and the second cell are of opposite polarization, ′1′ for the former and ′0′ for the latter. This means that two electrons are close together, the line is in a higher energy state and all successive cells must change their polarization to reach the new ground state.

QCA cells can implement all logic functions [7], multiplexor [8], alu [7], [9], [10] and also microprocessors [11],[12]. The basic logic functions NOT, AND and OR are shown in Fig. 1.8 and 1.9.
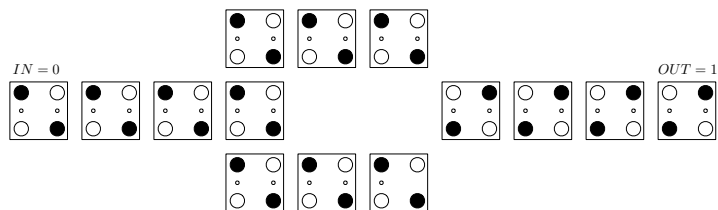
Figure 1.8: QCA inverter.
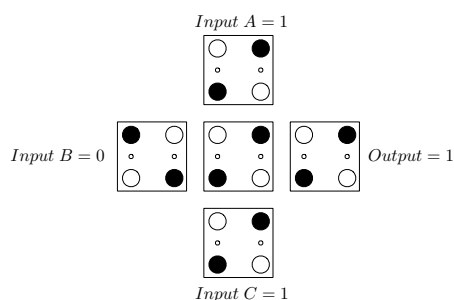
Figure 1.9: QCA AND or OR implemented by majority gate.

A	B	C	Output
0	0	0	0
0	0	1	0
0	1	0	0
0	1	1	1
1	0	0	0
1	0	1	1
1	1	0	1
1	1	1	1

Table 1.1: Majority gate truth table.

In the inverter, the input is split into two lines and then put together in a line placed at 45° angle with the two previous lines. This particular angle produces an opposite polarization to that in the two lines. For implementing AND and OR gates a topology called *majority gate* [7] is used. There are three inputs A, B and C. The central cell will have the polarization which prevails on the three inputs. Finally the polarization of the central cell is propagated at the output. One of the inputs can be used for selecting the function of the device, AND or OR. All combinational logic functions can be implemented by using only these 2 QCA blocks.

1.2   Clock system

In the previous paragraph we saw how a bit encoded in a molecule can be transmitted between two nearby molecules. However, this is not possible without a *clock* signal. The problem is that this clock signal can't be abrupt, in fact authors in [13] demonstrated that an abrupt clock can lead to metastability problems along the QCA circuit. For this reason, a new type of clock was developed for QCA technology, based on *Adiabatic Switching* [13],[14],[15],[16], which is the quantum version of the adiabatic theorem. Physically the clock is multi-phase [13], that is it consists of four consecutive phases with a different phase in a quarter of the period with respect to the signal in the previous zone, as shown in Fig. 1.10.
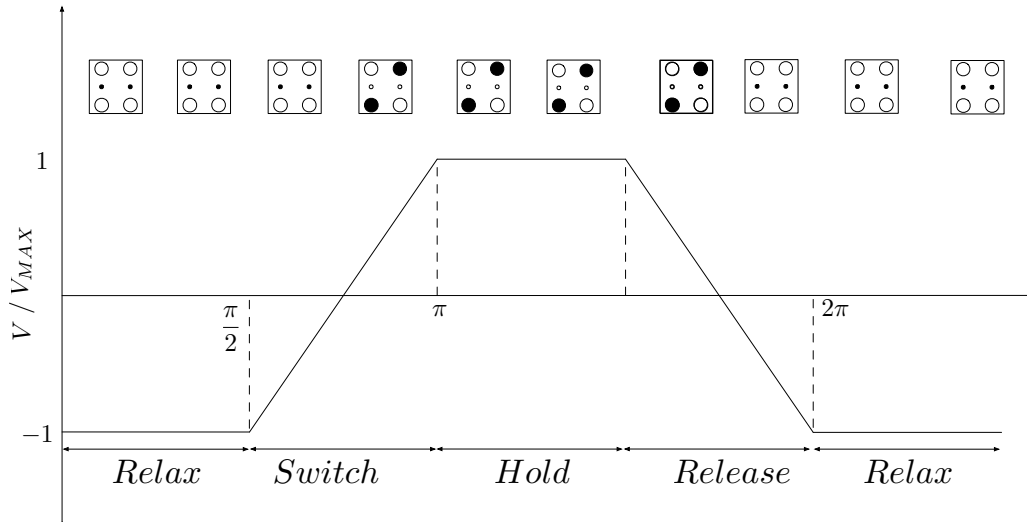
Figure 1.10: QCA clock.

The QCA circuit needs to be divided into *clock zones*, and each zone has a different phase of the clock.

These four phases of the clock are:

- switch;

- hold;

- release;

- relax.

In the *switch* phase, the inter-dot potential barrier is reduced so that the free charges in the molecule can move in one of two active dots depending on the external conditions (proximity of other molecules, external electric field, write-in system and so on) encoding the binary information; however in the second phase, *hold*, the potential between the dot is increased so that the charges are forced to stand still in the dot, so the next molecule (which will have the clock on the switch phase) will reallocate its free charge and so will all the others. In the *release* phase, the dot barrier potentials are lowered so that free charges can return to the initial position (*NULL* state) thus the molecule returns to have minimal energy and finally the *relax* phase in which the molecule remains stable in this condition.

Chapter 2

Molecular QCA

The molecular solution for the QCA technology is just the latest technology proposed and the most promising. But, many solutions were proposed and implemented before in the last two decades. In this chapter, some examples are listed.

2.1 Metal-Dot Solution

The metal-dot implementation was the first fabrication technology created to demonstrate the concept of QCA computing paradigm. The structure of this solution is based on metal Al islands, as shown in Fig. 2.1, over a silicon dioxide (SiO_2) substrate. The cell needs 2 capacitors to prevent charge exchanging.
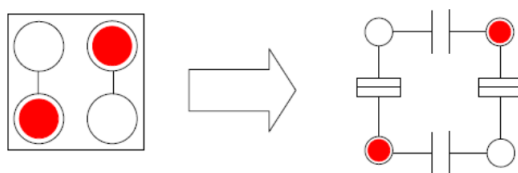
Figure 2.1: Metal-dot solution for QCA.

As we can see in the Fig. 2.2 we have four dots: two dots D_1 and D_2 in the left that can be associated with the others in the right (D_3 and D_4) by tunnel junctions which allow electrons to move between them [14], [5], [17].
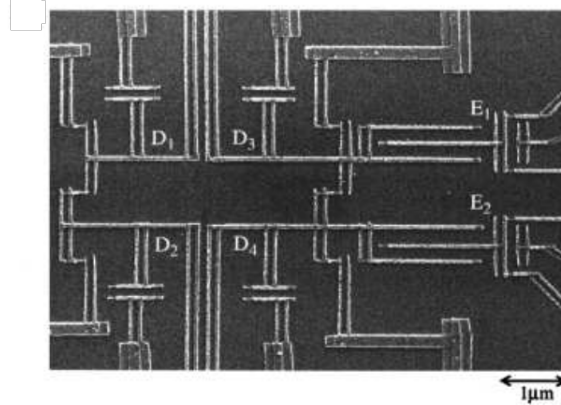
Figure 2.2: The QCA cell viewed with the scanning electron micrograph. [17].

The schematic cell structure is shown in Fig. 2.3.
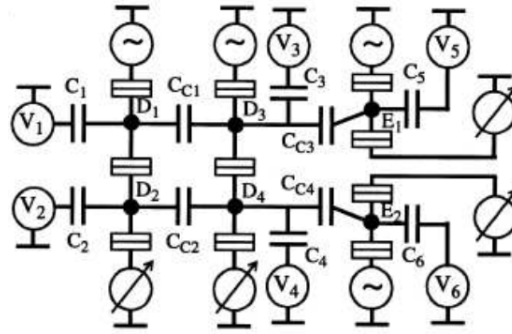
Figure 2.3: Schematic diagram of metal.-dot QCA cell.

This technology has two problems: the first one is that the metal islands are very large, so this device is not a nanodevice but it is in order to micrometers, the second problem is associated to the thermal energy. The metal-dots work only at the temperature of few mK because of quantum effects and so it is not realistic. Furthermore the maximum operating frequency is in the range of MHz.

In any case the principle has been demonstrated.

2.2   Semiconductor-Dot Solution

The second solution proposed in literature for the QCA was grounded on a semi-conductor structure [13] because semiconductors' technology is a well established technology. For example, a structure based on GaAs with several interleaved layers

of silicon, germanium or GaAs has been tested, as shown in Fig. 2.4. In this structure we have some dots that should be able to store charges. This structure, like the metal-dot solution has been tested but the results were not particularly successful because it should work at cryogenic temperature, it's highly defective and especially if nano-dimensions should be reached it has been proven that the defects prevent the feseability of this technology.
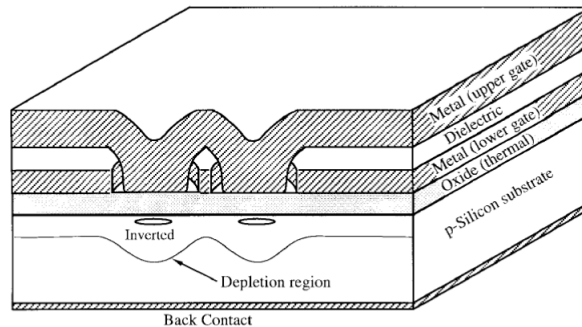
Figure 2.4: QCA cell implemented with semiconductor solution. [13].

2.3   Magnetic Solution

The real first successful implementation that is also currently adopted is the magnetic one. Here the cell is a nano-magnet [18] with a shape anisotropy in which the magnetization assumes a stable state in one direction or in the other direction, see Fig. 2.5.
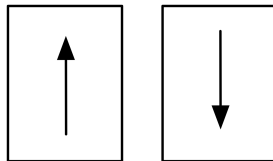
Figure 2.5: Two possibily states of magnetization for a nano-magnet.

These two directions that the nano-magnets can assume encode the logic states in the cells. Instead of electron-tunneling effects, the term "Quantum" refers to the quantum-mechanical nature of the magnetic exchange interactions. This information propagates among magnetic QCA devices due to the magnetic field coupling interaction (ferromagnetic or antiferromagnetic).

In this case we need a clock, a magnetic clock field, which is able to erase the magnetization and forces it in an horizontal state. As soon as the clock is released,

9

the magnetization goes up how has been proved and it is promising at least in terms of power dissipation. Because we are talking about magnetism, the speed is not very high but at least it can be implemented at room temperature.

2.4   Molecular QCA

Of all the solutions offered for QCA technology, the most promising is definitely the molecular one [19], [20], [21], [22]. This is due to several factors: the size that is on nanometers, the operating temperature (works correctly at room temperature), frequencies that can reach computing (THz) and higher density of devices.

Dots are represented by redox centers, which act as a loading container. The choice of redox centers as dots is due to the fact that it is possible to add or remove an electron (thus reduce or oxidize the molecule) from the redox centers without breaking the chemical bonds [21], in fact a redox center is a site of the molecule where is more probable to attract or to release an electron. The molecule condenses a 0 or 1 logic depending on the charge present in the two dots, as shown in the figure. The two (or three) redox centers are connected via a tunneling path that allows the electrons to pass from one point to another. As we will see later, in this thesis work we have dealt with either a molecule with two dots or three dots, the difference being basically that the third dot is needed to implement a system with a clock and to encode the NULL state. In order to obtain a complete QCA cell, two molecules must be joined together, making the cell then composed of 6 dots.
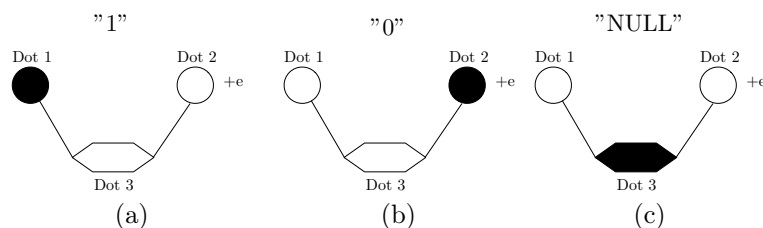
Figure 2.6: 3-dot molecule scheme: logic state encoding.

2.4.1   Candidate molecules

In literature, many ideal molecules [20], [21], [22], [23], [24], [25] have been studied as candidate for QCA device. They are ideal molecules because their behaviour has been studied only by means of simulations and they have been never been physically implemented.

This thesis only studies three different molecules for the QCA technology. The simplest molecule proposed for QCA computing is the diallyl butane [22]. As shown

in Fig. 5.1 it has two allyl groups (circled in the figure), that represent the dots (so they are the redox centers). The molecule proposed in literature has a free positive charge (an electron is missing). As said before, the single molecule represents half a QCA cell, so the complete cell could be implemented aligning two single molecules to form a square cell.
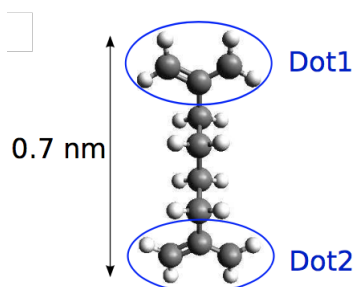
Figure 2.7: Diallyl butane molecule.

The second molecule studied in this thesis is decatriene. The decatriene molecule is a three dot molecule. These three dots, that are circled in Fig. 2.8(A), are ethylene groups. The molecule in the figure is a single molecule, this means that it represent half a QCA cell, so the two nearby molecules have to be aligned in order to have a complete QCA cell, as in the previous case. The authors in [26] used the electrostatic potential surface to identify the charge localization inside the molecule and so for the encoding of the three stable states ('1', '0' and 'NULL'), Fig. 2.8(B).
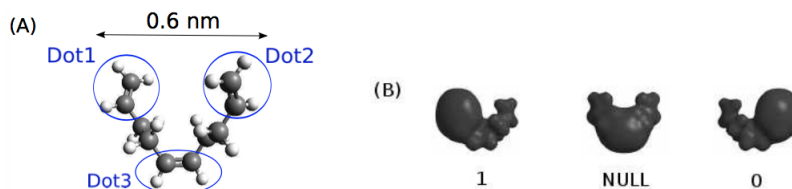
Figure 2.8: Decatriene molecule structure (a), and logical state encoding using HOMO visulazition (b).

The results discussed in [26] reveal that the decatriene molecule is a good candidate for QCA purpose, even though also in this case the molecule has no binding element necessary for physical implementation.

2.4.2 Bis-ferrocene molecule

The work of this thesis is focused on the bis-ferrocene molecule [27], [28], [29], [30], [31], which is considered the most promising molecule for the QCA technology. In

fact, this molecule has been synthesized by the University of Bologna and Politecnico di Torino ad hoc for QCA computation.

The structure of the molecule is reported in Fig 2.9: it consists in two ferrocenes and a central carbazole bridge.

(a)   (b)
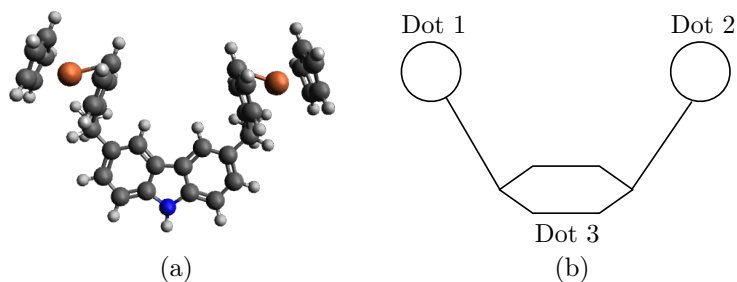
Figure 2.9: Bis-ferrocene molecule: (a) molecular structure, (b) 3-dot scheme.

The two ferrocenes are redox centers and function as working dots, while the central carbazole bridge works as third dot for the NULL state. This molecule has also an alkyl chain (a binding element), that in particular allows to attach the molecule to the thiol which is needed to put the molecule on a gold surface [27]. The complete structure is shown in Fig. 2.10.

(a)   (b)
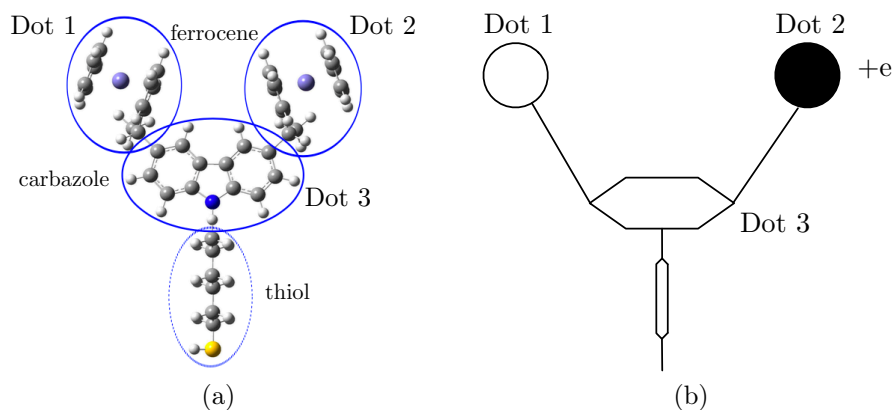
Figure 2.10: Bis-ferrocene molecule: dots definition (a) and equivalent 3-dot scheme (b).

The distance between the two working dot, dot1 and dot2, is 1.0 nm and, since the single molecule represents half a QCA cell, the ideal complete cell could be implemented placing two bis-ferrocenes at the distance of 1.0 nm.

Chapter 3

Methodology

The aim of this chapter is to understand how to study candidate molecules (diallyl butane, decatriene and bis-ferrocene) as QCA devices. In particular, we focused on the localization of the charges (electrons) in the molecules, which encode the binary information. To do this, simulations had to be made on computational chemistry software. In detail, the Gamess (US) [32], [33] software (the manual of which is in chapter 4) has been used instead of the most well known and most widely used Gaussian09 [34] which was used in [35].

The simulations of the candidate molecules were divided into two main steps:

- analysis of the molecules capability to encode binary information at equilibrium;

- simulation of the molecules with biasing conditions, in particular:

    - an external electric field [28];

    - a write-in system made by point charges [29].

- post-processing using Matlab and a C-program.

3.1 The steps

As said before, the first step of our analysis is to simulate a neutral molecule (total charge equal to 0) in equilibrium conditions. That means without any external field and far from other molecules (no interaction among them), as in Fig. 3.1.

Dot 1   Dot 2

Dot 3
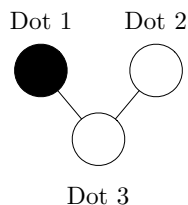
Figure 3.1: A 3 dot molecule scheme.

The first simulation that must be done is of the optimization type, this means that the software calculates the position of all the atoms of the molecule iteratively until it finds the geometry which minimizes the energy of the system. Once that the simulation is over, in the output file will be the new geometry of the molecule and it will be used as input for the following simulations. In particular, the molecular system for this first simulation is described by using the Z-matrix (see Chapter 4 for the description of input file). After this first simulation, some simulations with an external electric field and with two point charges have to be performed, paragraph 3.1.1 and 3.1.2. Then the output files are analyzed by using a C-program written to evaluate the dot charges, with Matlab to draw the charges characteristic (function of external electric field or polarization of the driver) and, last but not least with Avogadro to understand the behaviour of the molecules by seeing HOMO and LUMO. The workflow of this work is shown in Fig. 3.2.

Input file .inp → Optimization of the molecule → External electric field → Write-in system → Output .log → Post-processing on Matlab®
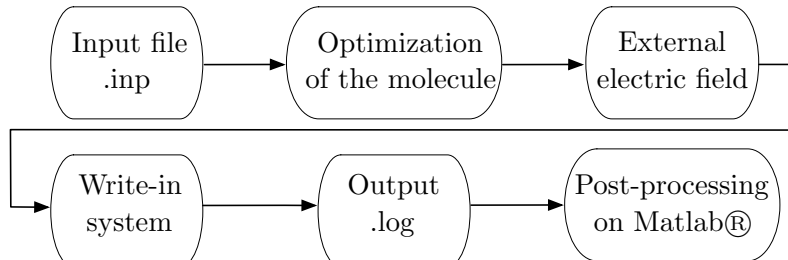
Figure 3.2: Workflow

3.1.1 External field

As explained in paragraph 3.1, after the optimization of the geometry of the molecule, a simulation with a finite external electric field has to be performed. This external electric field varies from $-5\,\mathrm{V/nm}$ to $5\,\mathrm{V/nm}$ to understand how the free charges inside the dots switch between them according to the electric field.

There are two types of external electric field: *Switching Field* [36] and *Clock Field* [21]. The switching field is parallel to the dot-axis. The idea is to put the molecule between two metal electrodes (yellow box in Fig. 3.3) and to apply a voltage difference between them ($V = V^+ - V^-$) [29]. The generated electric field has a direction

parallel to the working dot axis and lets the charges switch from one working dot to another one.
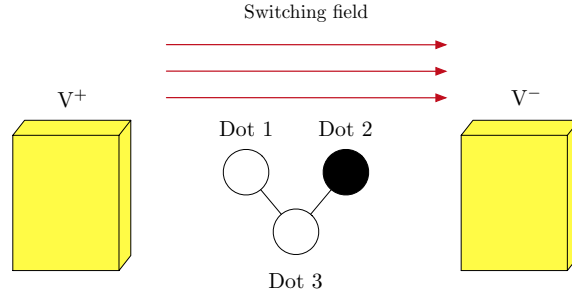
Figure 3.3: Switching field application system.
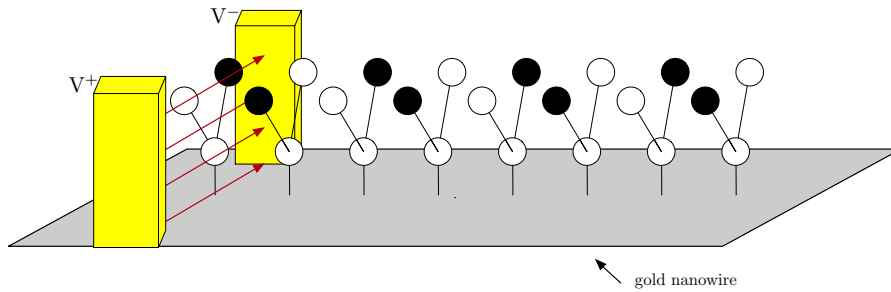
Figure 3.4: Switching field application system for a MQCA wire.

For instance, the charges in the molecule of the Fig. 3.3 switch to Dot 1 because of the direction of the switching field (from Dot 1 to Dot 2). Changing the sign of the switching field, the charge localization will be mostly in Dot 2. Basically, we can change the binary information encoded in the molecule by changing the sign of the switching field. In Fig. 6.4 is shown a simple example of this phenomenon for a diallyl butane molecule.

Figure 3.5: Displacement of the charge with an external electric field of: (a) $-5\,\mathrm{V/nm}$; (b) $5\,\mathrm{V/nm}$.

The clock field is a reference signal and it is perpendicular to the switching field, used to raise o lower the tunneling barriers during QCA computations. Schematically,

15

two metal electrodes are placed on the top and on the bottom of the molecule, and as for the switching field a voltage difference is applied, see Fig. 3.6.
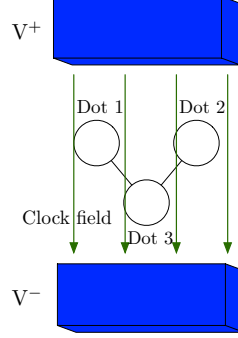
Figure 3.6: Clock field application system.

If the clock signal is negative, we are in the release and relax phases, this means that if we are considering a 3 dot molecule the charge would be into the lower central Dot3 keeping the molecule in NULL state, encoding no information. While if the clock signal is positive, we are in the switch and hold phases, this means that the charge is moving in the Dot 1 or 2 depending on the orientation of the switching field, encoding "0" or "1" logic.

3.1.2 Point charges

Authors in [29] demonstrated that setting two ideal point charges (atomic number and mass nuclear equal to 0) at distance d (the same distance from the two active dots) it is possible to polarize the molecule forcing the free charge to move in one of two dots, as in Fig. 3.7.
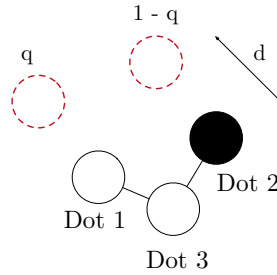
Figure 3.7: Driver-molecule interaction.

The driver is represented by two point charges with a value of q and $1 - q$, in this way the total charge is 1.

These point charges are named *Polarized Charge Driver* and are used as input for the system in a QCA wire, Fig. 3.8.
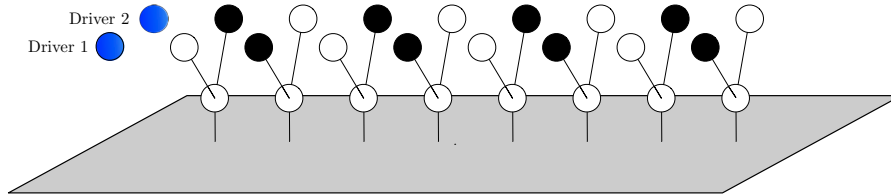
Figure 3.8: Point charges used as polarized driver for a MQCA wire.

Also in this case the localization of the charges inside the molecule is evaluated to understand the effect of the write-in system on the molecule.

Point charges can be useful, in addition to simulate the write-in system, also to simulate the behavior of the molecule in presence of a nearby molecule. In this case, the number of point charges must be equal to the number of dots of the molecule which has to be studied. This method is mainly used to simulate a QCA wire.

3.2   Figures of merit

Since we are analyzing the molecule from an electronic point of view, we have to understand how to study the charge localization inside the molecule. This can be done in two ways: one is a "chemical approach" and is the study of HOMO and LUMO orbitals; the second method is to define a new figures of merit, defined in [35], named *aggregated charge*, which is simply the sum of the atomic charge of each atom that forms a single dot. The choice of this new parameter means that the atomic charge is not a physical quantity, but a theoretical approximation. Even though the aggregated charge is strictly related to the atomic charge, it could represent the charge distribution inside a molecule from a macroscopic point of view and could be a readable quantity from an application perspective.
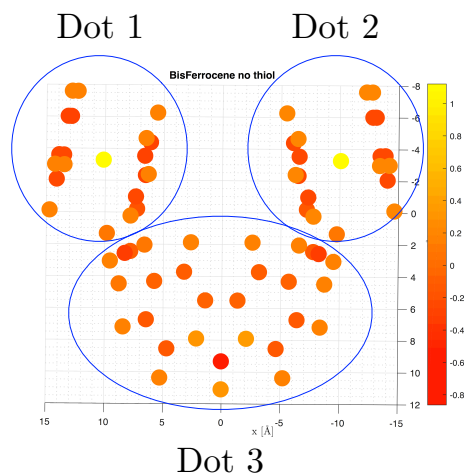
Figure 3.9: Definition of the aggregated charge for a bis-ferrocene molecule.

3.2.1 HOMO and LUMO

As we said in the previous paragraph, it is possible to see the charge configuration inside a molecule through the molecular orbital (MO). In particular, we have to see HOMO, HOMO-1, LUMO, LUMO+1. HOMO stands for Highest Occupied Molecular Orbital, so HOMO-1 is the second highest occupied molecular orbitals. Instead LUMO stands for Lowest Unoccupied Molecular Orbital. In particular, the HOMO-LUMO gap is defined as the energy difference between the HOMO's e LUMO's energy.

By definition, an orbital is the mathematical description of a region around a nucleus in an atom or molecule in which is more likely to find an electron. There are a maximum of 2 electrons in each orbital with opposite spin and the first occupied orbital is the one with the lowest energy (LUMO) up to the HOMO.

In the case studied in this work thesis, when a molecule is oxidized (which means that an electron is missing), this electron is removed by the HOMO.

3.3 Post-processing C-program

A C program has been written (see Appendix for the code) to automate the evaluation of the dots charge. In fact, at the end of simulation an output file is created, and this output file has more than 10k row. The C-program, called "*Mulliken charge*" ask for first which is the molecule to analyze, then ask to write the name of the .log file, see Fig. 3.10

(a)

(b)

Figure 3.10: Output of the c-program: selecting molecule and the writename (a) evaluation of the mulliken charge (b).

So it finds the mulliken charges in the .log file and perform some sums to evaluate the dots mulliken charges. This the "*one-shot*" version, which means that, after the first evaluation of the dots mulliken charge, it terminates. If you have more than one .log file to analyze you can use the *loop* version, which performs the same operation in a loop until an exit command is selected.

Finally the mulliken charge of every atoms is written in a .txt file called "*mulliken charge atoms.txt*" which can be useful for a successive visualization of the charge using Matlab.

Chapter 4

Tools Manual For Molecular QCA simulation

4.1 Ab-initio simulation

If we consider a polyatomic molecule, the electronic wave function depends on more than one parameter (bond distances, bond angles, dihedral angles of rotation about single bonds). In particular, for a molecular system, it's used to solve the Schroedinger equation defined as:

$$ih\frac{\partial}{\partial t}\Psi\left(\overrightarrow{r},t\right) = \hat{H}\left(\overrightarrow{r},t\right) \tag{4.1}$$

where $\Psi\left(\overrightarrow{r},t\right)$ is the wave function that depends on the position $\overrightarrow{r}$ and time t; h is the reduced Planck constant; $\hat{H}$ is the Hamiltonian defined as the sum of kinetic and potential energy operators:

$$\hat{H} = T + V \tag{4.2}$$

$$T = \frac{p^2}{2m} = -\frac{1}{2m}\nabla^2 \tag{4.3}$$

$$\rightarrow \hat{H} = -\frac{\nabla^2}{2m} + V\left(\overrightarrow{r}\right) \tag{4.4}$$

The chemical and physical properties of a generic molecular system are described by the solutions of the equation above. These properties are, for example the optimized physical geometrical molecular structure with the minimum total energy, the interaction energies, the electronic charge distributions. The Schrodinger equation

can be solved exactly for only a few particular cases, for example for the hydrogen atom. For other cases, we need some approximations. Computational chemistry provides this and we have three classes of approximation methods [37]:

- **Semi-empirical method**: this method uses a simpler Hamiltonian than the correct molecular Hamiltonian and use parameters whose values are adjusted to fit experimental data or the results of ab initio calculations;

- **Ab-initio method**: it uses the correct Hamiltonian and does not use experimental data other than the values of the fundamental physical constants.

- **Density Functional Theory (DFT) method**: they are similar to ab-initio methods, but they include the effects of electron correlation, which is the fact that electrons in a molecular system react to one another motion.

Each type of method is characterized by the combination of theoretical procedure (called *method*), a *basis set* and a description of the molecule which can be cartesian or by a *Z-matrix*. A basis set is a mathematical representation of the molecular orbitals within a molecule. The basis set can be interpreted as restricting each electron to a particular region of space. Larger basis sets impose more accurately approximated molecular orbitals and they require accordingly more computational resources, as more accurate methods become more computationally expensive.

4.1.1   Z-matrix

The most common way used to describe a molecular system in every chemistry computational tool is by using the Z-matrix. The Z-matrix specifies the position of atoms in a molecule relative to each other in terms of atomic types, bond lengths and bond angles and dihedral angles.

Let's consider the molecule in Fig. 4.1 It consists of three atoms, one of oxygen and two of hydrogen. If we represent the water molecule in a three-dimensional space, each atom has three coordinates $P(x, y, z)$.
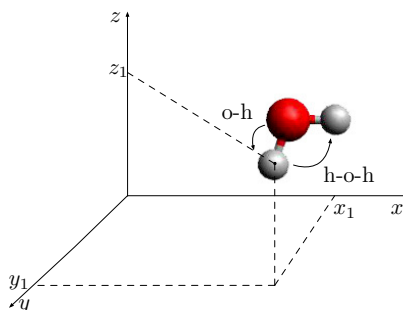
Figure 4.1: Water molecule.

The construction of the Z-matrix has to follow these simple rules:

1. choose the starting atom and place it conceptually at the origin of a three-dimensional space;

2. choose another atom linked to the first and position it along the z axis, specifying the label of the atom to which it is bound and the length of the link that connects them;

3. choose a third atom linked to one of the previous atoms and specify the binding angle formed by the two bonds;

4. Define the positions of the following atoms by specifying:

   - The atom label;
   - An atom to which it is bound and the bond length;
   - A third atom to which it is linked: label and value of the resulting binding angle;
   - A fourth atom and the value of the formed dihedral angle with the previous atoms.

It is possible to have two Z-matrix for each molecular system: one with the constant and another one with the variable. In particular, for the example in Fig. 4.1 we can have these two Z-matrix:

```
O
H  1  0.96
H  1  0.96  2  109.47


O
H  1  oh
H  1  oh  2  hoh
oh=0.96
hoh=109.47
```

In this work thesis, the input file for the optimization step has been written by using the Z-matrix, while all the others simulations by using the cartesian coordinates.

An example of an input file for a dially butane molecule is shown here:

```
$BASIS  GBASIS=STO  NGAUSS=3  $END
$CONTRL  SCFTYP=RHF  RUNTYP=FFIELD  COORD=ZMT  $END
$STATPT  OPTTOL=0.0001  NSTEP=20  $END
$EFIELD  EVEC(1)=0.002,0.001,0.001  $END

$DATA
Title
C1
C
C           1           B1
C           1           B2      2           A1
```

C	2	B3	1	A2	3	D1
H	3	B4	1	A3	2	D2
H	3	B5	1	A4	2	D3
H	4	B6	2	A5	1	D4
H	4	B7	2	A6	1	D5
H	1	B8	2	A7	4	D6
H	1	B9	2	A8	4	D7
H	2	B10	1	A9	3	D8
H	2	B11	1	A10	3	D9
C	4	B12	2	A11	1	D10
C	13	B13	4	A12	2	D11
C	13	B14	4	A13	2	D12
H	14	B15	13	A14	4	D13
H	14	B16	13	A15	4	D14
H	15	B17	13	A16	4	D15
H	15	B18	13	A17	4	D16
C	3	B19	1	A18	2	D17
C	20	B20	3	A19	1	D18
C	20	B21	3	A20	1	D19
H	21	B22	20	A21	3	D20
H	21	B23	20	A22	3	D21
H	22	B24	20	A23	3	D22
H	22	B25	20	A24	3	D23

B1	1.54219718
B2	1.54715028
B3	1.54715028
B4	1.08772095
B5	1.08771964
B6	1.08772095
B7	1.08771964
B8	1.08843697
B9	1.08843680
B10	1.08843697
B11	1.08843680
B12	1.53585525
B13	1.37770630
B14	1.37772504
B15	1.08001478
B16	1.08038854
B17	1.08001487
B18	1.08038819
B19	1.53585525
B20	1.37770630
B21	1.37772504
B22	1.08001478
B23	1.08038854
B24	1.08001487
B25	1.08038819
A1	112.18495797
A2	112.18495797
A3	109.25301425
A4	109.25298930
A5	109.25301425
A6	109.25298930
A7	109.48180141
A8	109.48122967
A9	109.48180141
A10	109.48122967
A11	111.24431029
A12	118.62285258
A13	118.61999817
A14	121.66720440

24

```
A15           121.41761015
A16           121.66666901
A17           121.41779191
A18           111.24431029
A19           118.62285258
A20           118.61999817
A21           121.66720440
A22           121.41761015
A23           121.66666901
A24           121.41779191
D1            180.00000000
D2            −58.69919355
D3             58.71180363
D4            −58.69919355
D5             58.71180363
D6            −58.61861781
D7             58.61814219
D8            −58.61861781
D9             58.61814219
D10          −179.99339158
D11           −88.92015591
D12            88.87856924
D13            −2.31385877
D14           178.35611866
D15             2.31545807
D16          −178.35545484
D17          −179.99339158
D18           −88.92015591
D19            88.87856924
D20            −2.31385877
D21           178.35611866
D22             2.31545807
D23          −178.35545484

$END
```

4.2   Gamess Manual

4.2.1   Introduction to Gamess

GAMESS [32] stands for General Atomic and Molecular Electronic Structure System (GAMESS (US)) and it is a computer software for computational chemistry. It is useful to solve the 4.1 by using RHF (restricted Hartee Fock), UHF (unrestricted Hartee Fock) and DFT (density functional theory). In this work the UHF has been used in all the simulations. The difference between UHF and DFT is that the latter considers the correlation between electron and electron. But it is much more expensive in terms of computational time. Because of this reason, we preferred to use the UHF, even though the results are less precise.
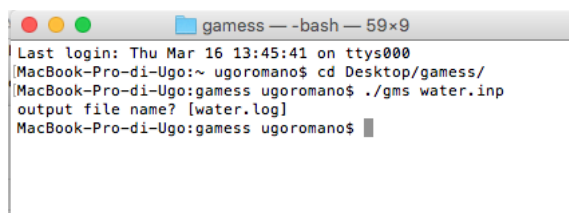
4.2.2   Download

Go to `http://www.msg.ameslab.gov/gamess/License_Agreement.html` and click on **"I agree to the above terms",** you will be addressed to a new website page where you can download the version of GAMESS that you need. GAMESS is available for Windows, OSX and Linux. An e-mail should arrive within one hour to one day with the link for downloading GAMESS and an username and password. If not, try again.

4.2.3   Run Gamess

- **MacOS**:
  To run Gamess an input file is needed which contains all the information that Gamess needs. An input file is a file with ".inp" extension, for example "water.inp". You have to copy the input file in the same folder where Gamess is located and then using the shell you have to type **cd/path** where "path" is the folder containing GAMESS. Then you can run **./gms water.inp** (see Figure 4.2).

Figure 4.2: Running Gamess.

  When the simulation is over, a file named "water.log" is created and it is the output file which cointains all the results from the simulation.

- **Linux**:
  To run Gamess in Linux the steps are the same for MacOs, the only difference is that when you are in the gamess folder you have to run **rungms** by typing: "/software/gamess/gamess20170420r1/gamess/rungms xxx.inp > xxx.log" where xxx is the name of the input file.

- **Windows:**

- **Through the server:**
  Before running Gamess we have to create in the folder /gamesstmp a subfolder named as the name of the user; then inside it, we need to create another folder named "scratch" where all the temporary files will be written. When a

simulation is over, these files will be deleted automatically . You need again a folder named "scratch" in your own home which will contain all the .dat files created during the simulations. If a simulation terminates abnormally you have to delete the .dat file in this folder before starting a new simulation.

Running Gamess through the server works exactly like on Linux, with the difference that on the server we have the possibility to run it in parallel. To do that we have to go in the folder where the .inp file is and type in the shell: "/software/gamess/gamess20170420r1/gamess/rungms xxx.inp YY Z > xxx.log" where xxx is the name of the input file, YY is the Gamess version (in our case "00") and Z is the number of processors we need. For example, there are 4 processors in the Micro&Nano server, so if we want to run Gamess in these 4 processors in parallel we have to type: /software/gamess/gamess20170420r1/gamess/rungms xxx.inp 00 4 > xxx.log.

A shell script has been written so that all files with extension .inp in the folder are identified and all sequentially simulated.

4.2.4 Input file

GAMESS [32] input takes the form of a list of groups. Each group controls some aspect of the calculation, from the choice of basis set to the kind of calculation to the format for structure input.

1. Each group has a name that begins with a $ sign, which must be in column 2 of the input line (you have to put a blank space at the start of the line);

2. The group must be terminated with $END;

3. The options within a group may be placed all on one line, or distributed over multiple lines. GAMESS recognizes the end of an input group by the $END;

4. Comment lines begin with a ! in column 1.

5. Each group consists of one or more keywords, depending on your choice.

Every group description are described accurately in [38] .

- **$CONTRL Group** [38]
  The control group handles the type of calculation, the type of SCF, the type of coordinates of the molecule and much more. A default GAMESS control group is RHF/UHF SCF, singlet state, a single point energy calculation and Cartesian coordinates in units of Angstroms. If these defaults are ok, then the $CONTRL group does not need to be provided.
  Below are some common options used in this work, specified by listing them following the $CONTRL:

- RUNTYP is the type of computation. In this work we used OPTIMIZE (optimize geometry using analytic energy gradients), FFIELD (applies finite electric fields) and ENERGY (single point energy);

- SCF calculation: SCFTYP=RHF for Restricted Hartree Fock calculation and UHF for Unrestricted Hartree Fock calculation.

- DFTTYP calculate the DFT (density functional theory), in particular B3LYP;

- Coordinates of the molecules: cartesians (COORD=CART) or by using the Z-matrix (COORD=ZMT), as seen in 4.1.1;

- MAXIT is the maximum number of SCF iteration cycles. This pertains only to RHF, UHF, ROHF runs (default = 30, maximum 200);

- ICHARG and MULT define the charge and the multiplicity of a molecule that can be neutral, oxidized (ICHARG=1 MULT=2) o reduced (ICHARG=-1 MULT=2).

- **$BASIS Group** [38]
  This group allows certain standard basis sets to be easily requested. Use GBASIS= to set the general type, and NGAUSS= to set the number of Gaussians. Here is a short list of basis presents in Gamess and used:

  - STO-3G: $BASIS GBASIS=STO NGAUSS=3 $END;

  - 6-31G: $BASIS GBASIS=N31 NGAUSS=6 $END;

  - 6-31G(d): $BASIS GBASIS=N31 NGAUSS=6 NDFUNC=1 $END;

  - 6-31G(d,p): $BASIS GBASIS=N31 NGAUSS=6 NDFUNC=1 NPFUNC=1 $END;

  Sometimes it may be necessary to use some basis that are not present in Gamess by default. For example, in the bis-ferrocene simulations in gaussian09 a basis (LANL2DZ) was used which is not present in Gamess. The procedure to use an external basis set consists in changing the $BASIS control to read an external file, and to modify rungms to read the external basis set file. Let's start with how to modify the rungms script. You have to modify the line "setenv EXTBAS" as follows:

```
set echo
setenv ERICFMT ./ericfmt.dat
setenv IRCDATA ./$JOB.irc
setenv   INPUT $SCR/$JOB.F05
setenv   PUNCH ./$JOB.dat
setenv  EXTBAS ./XXX.txt
setenv  AOINTS $SCR/$JOB.F08
```

  where XXX.txt is a random name of the basis. In this case the .txt file must be in the same folder as the rungms script, while if your file is in another folder

you have to specify the path. For example, if the basis file is in the desktop folder you have to write:

```
setenv  EXTBAS /Users/../Desktop/gamess/XXX.txt
```

Regarding the input file, the only noteworthy difference with the input file seen before is the $BASIS line: EXTFIL=.TRUE. tells GAMESS-US to use the external file and GBASIS=XXX to use external basis sets named XXX.

The external basis sets can be downloaded from `https://bse.pnl.gov/bse/portal`

An example of an external basis is shown here (LANL2DZ basis):

```
H LANL2DZ
  S    2
    1           1.309756377     0.4301284980
    2           0.233135974     0.6789135310

C LANL2DZ
S    7
    1    4233.0000000           0.0012200
    2     634.9000000           0.0093420
    3     146.1000000           0.0454520
    4      42.5000000           0.1546570
    5      14.1900000           0.3588660
    6       5.1480000           0.4386320
    7       1.9670000           0.1459180
S    2
    1       5.1480000          -0.1683670
    2       0.4962000           1.0600910
S    1
    1       0.1533000           1.0000000
P    4
    1      18.1600000           0.0185390
    2       3.9860000           0.1154360
    3       1.1430000           0.3861880
    4       0.3594000           0.6401140
P    1
    1       0.1146000           1.0000000


N LANL2DZ
S    7
    1    5909.0000000           0.0011900
    2     887.5000000           0.0090990
    3     204.7000000           0.0441450
    4      59.8400000           0.1504640
    5      20.0000000           0.3567410
    6       7.1930000           0.4465330
    7       2.6860000           0.1456030
S    2
    1       7.1930000          -0.1604050
    2       0.7000000           1.0582150
S    1
    1       0.2133000           1.0000000
P    4
    1      26.7900000           0.0182540
    2       5.9560000           0.1164610
    3       1.7070000           0.3901780
    4       0.5314000           0.6371020
```

```
P    1
   1         0.1654000              1.0000000


Fe  LANL2DZ
S    3
   1         6.4220000             −0.3927882
   2         1.8260000              0.7712643
   3         0.7135000              0.4920228
S    4
   1         6.4220000              0.1786877
   2         1.8260000             −0.4194032
   3         0.7135000             −0.4568185
   4         0.1021000              1.1035048
S    1
   1         0.0363000              1.0000000
P    3
   1        19.4800000             −0.0470282
   2         2.3890000              0.6248841
   3         0.7795000              0.4722542
P    1
   1         0.0740000              1.0000000
P    1
   1         0.0220000              1.0000000
D    4
   1        37.0800000              0.0329000
   2        10.1000000              0.1787418
   3         3.2200000              0.4487657
   4         0.9628000              0.5876361
D    1
   1         0.2262000              1.0000000


Au  LANL2DZ
S    3
   1         2.8090000             −1.2021556
   2         1.5950000              1.6741578
   3         0.5327000              0.3526593
S    4
   1         2.8090000              1.1608481
   2         1.5950000             −1.8642846
   3         0.5327000             −1.0356230
   4         0.2826000              1.3064399
S    1
   1         0.0598000              1.0000000
P    3
   1         3.6840000             −0.2802681
   2         1.6660000              0.7818398
   3         0.5989000              0.4804776
P    2
   1         0.6838000             −0.0952078
   2         0.0977000              1.0299147
P    1
   1         0.0279000              1.0000000
D    2
   1         1.2870000              0.5844273
   2         0.4335000              0.5298161
D    1
   1         0.1396000              1.0000000
```

- **$STATPT Group** [38]

This group is used for RUNTYP = OPTIMIZE. In particular it controls the search for optimized points. The parameter OPTTOL is the gradient convergence tolerance, in Hartree/Bohr. The simulation converges when the convergence of a geometry search requires the largest component of the gradient to be less than OPTTOL, and the root mean square gradient less than 1/3 of OPTTOL (default=0.0001). NSTEP is the maximum number of steps to take. The default is 50 steps for a minimum search, but only 20 for a transition state search, which benefit from relatively frequent Hessian re-evaluations.

- **$EFIELD Group** [38]
  This group introduces an external electric field on the system. It is composed by two parameters, but we used just one:

  - EVEC = an array of the three (x, y, z) components of the applied electric field, in a.u;

- **$SYSTEM Group** [38]
  This group provides global control information for your computer's operation. If you don't specify this group, Gamess uses 1000000 words of memory by default. 1 word is 8 byte, so 8 MB of RAM

  $SYSTEM MWORDS=1 $END

  MWORDS is the maximum replicated memory which your job can use, on every node and it can only be integers (1, 2, 3, ..). This is given in units of 1000000 words (as opposed to $1024 \cdot 1024$ words). There are some simulations which need more than 8 MB of RAM, in this case there will be an error in the output file (***** ERROR: MEMORY REQUEST EXCEEDS AVAILABLE MEMORY). The memory used by Gamess can be improved with the command $SYSTEM. Here is the simplest way to deal with memory: if your current laptop computer has 4 GB of RAM, and you use it for other things while GAMESS is running, so you can give GAMESS a maximum of roughly 2 or 3 GB of RAM. This translates to:

  $$2 \, \text{GB} = 2.000 \, \text{MB} = 250 \, MWORDS$$

  In this case, you have to add the following command in all your input files:

  $SYSTEM MWORDS=250 $END

  Here there is a simple example of a first part of an input file:

```
$BASIS  GBASIS=N31  NGAUSS=6  NDFUNC=1  NPFUNC=1  $END
$CONTRL  SCFTYP=RHF  RUNTYP=OPTIMIZE  COORD=ZMT  $END
$STATPT  OPTTOL=0.0001  NSTEP=20  $END
$SYSTEM  MWORDS=50  $END
```

- **$ELPOT Group** [38]
  This group controls electrostatic potential calculation, if IEPOT=0 Gamess skips this property, while if IEPOT=1 calculates electric potential. It is possible calculate the electric potential in several points by the keyword WHERE which can be equal to:

  - COMASS: center of mass;
  - NUCLEI: at each nucleus (default);
  - POINTS: at points given in $POINTS;
  - GRID : at grid given in $GRID;

  This first card in the $POINT group must contain the string ANGS or BOHR, followed by an integer NPOINT, the number of points to be used. The next NPOINT cards are read in free format, containing the X, Y, and Z coordinates of each desired point.
  The $GRID group is used to input a plane or cube on which properties will be calculated (in our case the electric potential). It is composed of:

  - MODGRD = 0 orthonormalize the grid vectors or 1 normalize the grid vectors;
  - ORIGIN(i) = coordinates of one corner of the grid/cube;
  - XVEC(i) = vector from ORIGIN to an adjacent corner "X" of the grid (or cube); the XVEC direction need not be parallel to the X-axis of the molecule.
  - YVEC(i) = vector to the adjacent corner "Y" of grid/cube;
  - ZVEC(i) = vector to the adjacent corner "Z" of the cube, given if and only if MODGRD=1;
  - SIZE = grid increment in all directions (default 0.25);
  - UNITS = units of the above five values, it can be either ANGS (the default) or BOHR.

  In this way a cube is created in a three-dimensional space, and the electrostatic potential is calculated at each point where two lines intersect. This method is used since the value of the electrostatic potential around the molecule is needed in the algorithm used in [39] for the calculation of the ESP charges.

- **$GUESS and VEC Group** [38]
  You may have to use the results of a simulation as the starting point for a second simulation. For example, when the SCF does not converge after 200 iterations, you can start from the two hundredth iteration to get 400 iterations

and so on. The second example is that, for particularly complex molecules (for example bis-ferrocene), it is necessary to give as input the MOs calculated in a previous optimization simulation because otherwise the calculation of the SCF oscillates. At the end of an optimization simulation, GAMESS creates a .dat file with a section called $VEC, where all the calculated MOs are described by a list of vectors. To use these vectors in the input file you must write the command:

```
$GUESS GUESS=MOREAD NORB=154 $END
```

where MOREAD tells GAMESS that the molecular orbitals must read and NORB is the number of molecular orbitals to read. This number can be found in the .log file:

```
NUMBER OF OCCUPIED ORBITALS (ALPHA)        =   154
NUMBER OF OCCUPIED ORBITALS (BETA )        =   153
TOTAL NUMBER OF ATOMS                      =    72
```

At the end of the file the $VEC group must be written with all the orbital vectors (more than 50000 lines). If geometry optimization was calculated using SCFTYP = UHF, you have two different values for alpha and beta orbitals. In the case in the example, you have to copy the 154th alpha orbitals after the 153th beta orbitals and set NORB=154.

- **Effective fragment potential (EFP)** [38]
  The only way to include two or more points charge in the simulations found up to now is to use EFP (Effective Fragment Potential). The basic idea behind the EFP method is to replace the chemically inert part of a system by EFPs (points charge), while performing a regular ab-initio calculation on the chemically active part (the molecule). Here "inert" means that no covalent bond breaking process occurs. This "spectator region" consists of one or more "fragments", which interact with the ab initio "active region" through non-bonded interactions, and so of course these EFP interactions affect the ab initio wavefunction. Let's consider the following molecular system:
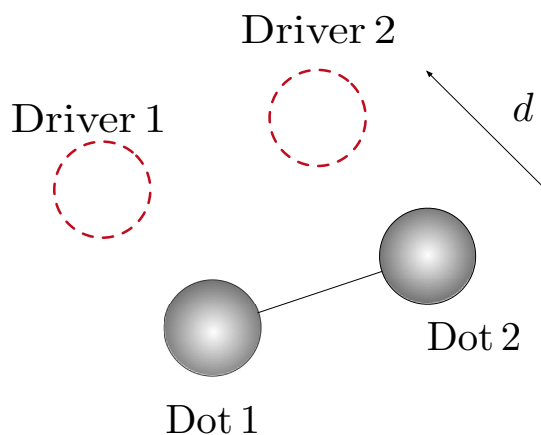
Figure 4.3: Diallyl butane with 2 points charge.

To describe this molecular system we have to write the following input file:

```
$BASIS GBASIS=N31 NGAUSS=6 NDFUNC=1 NPFUNC=1 $END
$CONTRL SCFTYP=RHF RUNTYP=ENERGY COORD=CART UNITS=BOHR
  MAXIT=200 $END
$SCF CONV=1d−5 $END
$STATPT OPTTOL=0.0001 NSTEP=20 $END
$SYSTEM MWORDS=50 $END

$DATA
Title
C1
C     6.0    1.3332368711   −0.0002526451   −0.5880556204
C     6.0   −1.3332368711   −0.0002526451    0.5880556204
C     6.0    3.4358660887   −0.0002526451    1.4434251503
C     6.0   −3.4358660887   −0.0002526451   −1.4434251503
H     1.0    3.2227946107    1.6578397290    2.6394134677
H     1.0    3.2230477325   −1.6585651191    2.6391490900
H     1.0   −3.2227946107    1.6578397290   −2.6394134677
H     1.0   −3.2230477325   −1.6585651191   −2.6391490900
H     1.0    1.5533761233   −1.6556908607   −1.7887575775
H     1.0    1.5533514007    1.6551827736   −1.7887654158
H     1.0   −1.5533761233   −1.6556908607    1.7887575775
H     1.0   −1.5533514007    1.6551827736    1.7887654158
C     6.0   −6.0717882763    0.0000593591   −0.2287136680
C     6.0   −7.1866398826   −2.2847192418    0.3325699278
C     6.0   −7.1854907850    2.2851711012    0.3336581671
H     1.0   −6.2846283303   −4.0578002243   −0.1234590242
H     1.0   −9.0163919699   −2.3834287213    1.2328758142
H     1.0   −6.2825836824    4.0579984242   −0.1215847979
H     1.0   −9.0151818102    2.3843934114    1.2340302771
C     6.0    6.0717882763    0.0000593591    0.2287136680
C     6.0    7.1866398826   −2.2847192418   −0.3325699278
C     6.0    7.1854907850    2.2851711012   −0.3336581671
H     1.0    6.2846283303   −4.0578002243    0.1234590242
H     1.0    9.0163919699   −2.3834287213   −1.2328758142
H     1.0    6.2825836824    4.0579984242    0.1215847979
H     1.0    9.0151818102    2.3843934114   −1.2340302771
 $END
 $EFRAG
 POSITION=FIXED COORD=CART
 fragname=WATER1
```

```
W1O1   −7.1861  −14.372  −0.333
W1H2   −3.2131  5.376  −0.12
W1H3   −3.2131  4.763  −0.23
 fragname=CO21
C1C1   7.1861  −14.372  −0.333
C1O2   −6.3131  5.376  −0.12
C1O3   −6.2131  4.763  −0.23
 $END
 $WATER1
WATER1 as DR1
COORDINATES(BOHR)
W1O1   −7.1861  −14.372  −0.333 0.0  0.0
W1H2   −3.2131  5.376  −0.12   0.0  0.0
W1H3   −3.2131  4.763  −0.23   0.0  0.0
 STOP
 MONOPOLES
W1O1 0.7  0.0
W1H2 0.0  0.0
W1H3 0.0  0.0
 STOP
 REPULSIVE POTENTIAL
W1O1
0 ,0
 STOP
 $END
 $CO21
Carbon as DR2
COORDINATES(BOHR)
C1C1   7.1861  −14.372  −0.333 0.0  0.0
C1O2   −6.3131  5.376  −0.12 0.0  0.0
C1O3   −6.2131  4.763  −0.23 0.0  0.0
 STOP
 MONOPOLES
C1C1 0.3  0.0
C1O2 0.0  0.0
C1O3 0.0  0.0
 STOP
 REPULSIVE POTENTIAL
C1C1
0 ,0
 STOP
 $END
 $FRGRPL
 PAIR=WATER1 CO21
W1O1 C1C1  0  0
 STOP
 $END
```

After the coordinates of the molecule we have the EFRAG group so formed:

- line 1: POSITION=FIXED COORD=CART
  This means that the position of the fragments are fixed and that we are considering cartesian coordinates;
- line 2: fragname=XXX
  This the name of the fragment for a future use;
- line 3: Gamess needs at least three atoms to define each fragment, since we need just one atom for each fragment we set the coordinates for the first atom. The second and third atoms are dummy values;

– line 4: There is a group with the name of the fragment where we specify again the coordinates and the value of charges in MONOPOLES.

– line 5: REPULSIVE POTENTIAL signals the start of the subgroup containing the fitted exchange repulsion potential, for the interaction between the fragment and the ab initio part of the system;

– line 6: This group defines the inter-fragment repulsive potential for EFP1 potentials; it accounts primarily for exchange repulsions, but also includes charge transfer. Note that the functional form used for the fragment-fragment repulsion differs from that used for the ab initio-fragment repulsion, which is defined in the $FRAGNAME input.

- **Creating an input file by using Avogadro**
  Avogadro is an advanced molecule editor and visualizer designed for cross-platform use in computational chemistry, you can download it from this link: `https://sourceforge.net/projects/avogadro/files/latest/download` and some manuals are available here: `https://avogadro.cc/docs/` and here `https://www.gitbook.com/book/ghutchis/avogadro/details`. Select the pencil to begin drawing, like in Fig. 4.4:
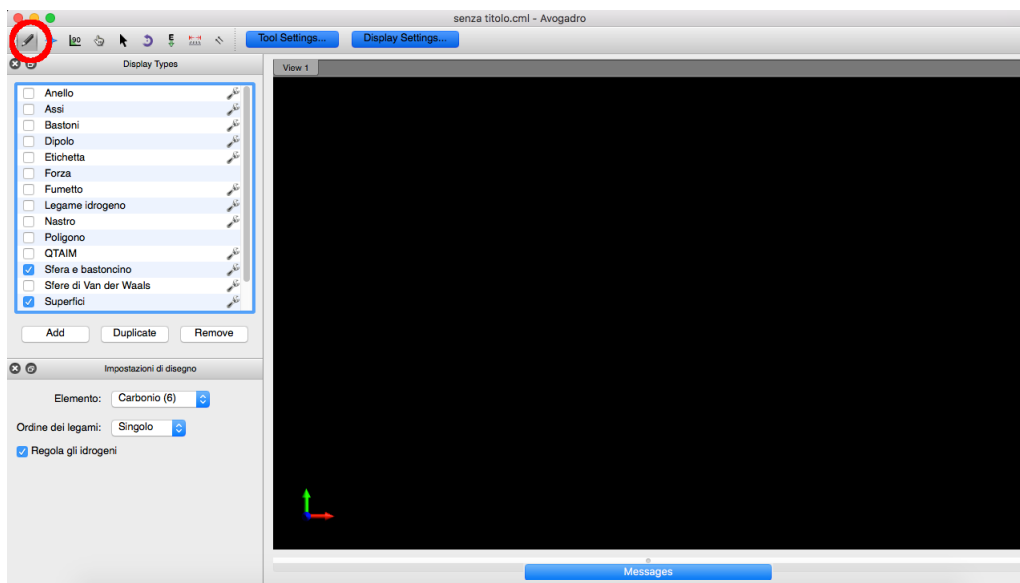
Figure 4.4: Avogadro

Note that the red, green, and blue arrows represent the x, y, and z axes respectively. You can select the element you want from "Draw settings" on the left; if you work with organic molecules you have to select "satura con idrogeni".
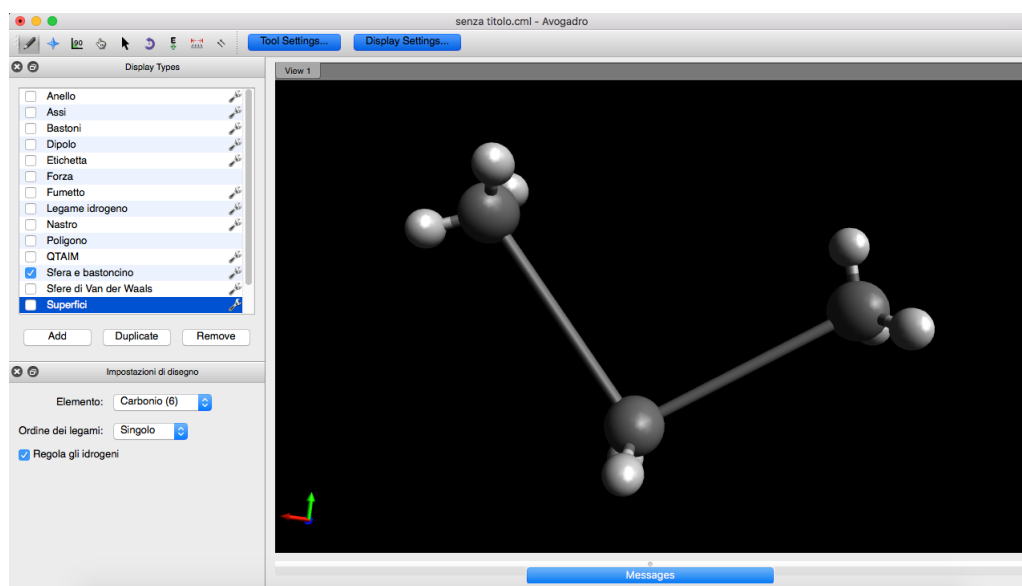
Figure 4.5: Drawing a molecul with Avogadro.

After you have drawn your molecule you can optimize it. To do this, go to Estensione → Ottimizza la geometria.
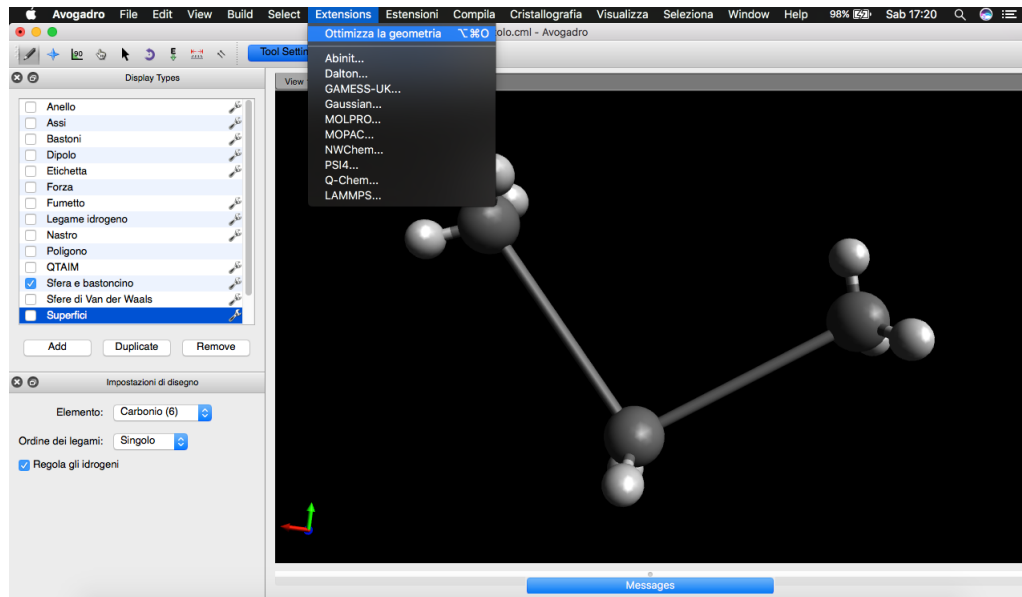
Figure 4.6: Optimize geometry.

You can also change the "ordine dei legami", as in Fig. 4.7.

37
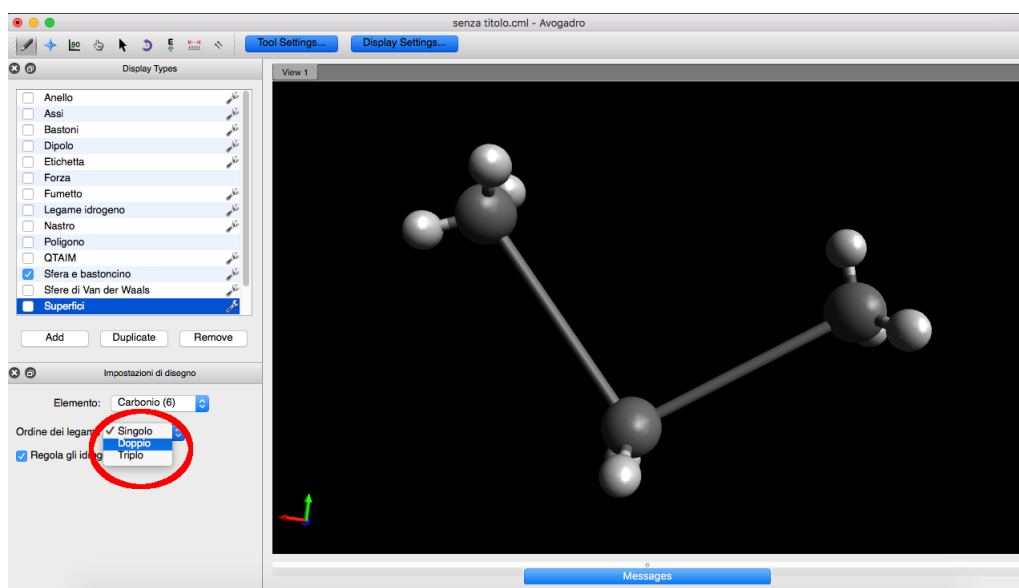
Figure 4.7: Bond order.

Now you can generate the Gamess input file. Go to Estensioni → Gamess → Generatori di input.
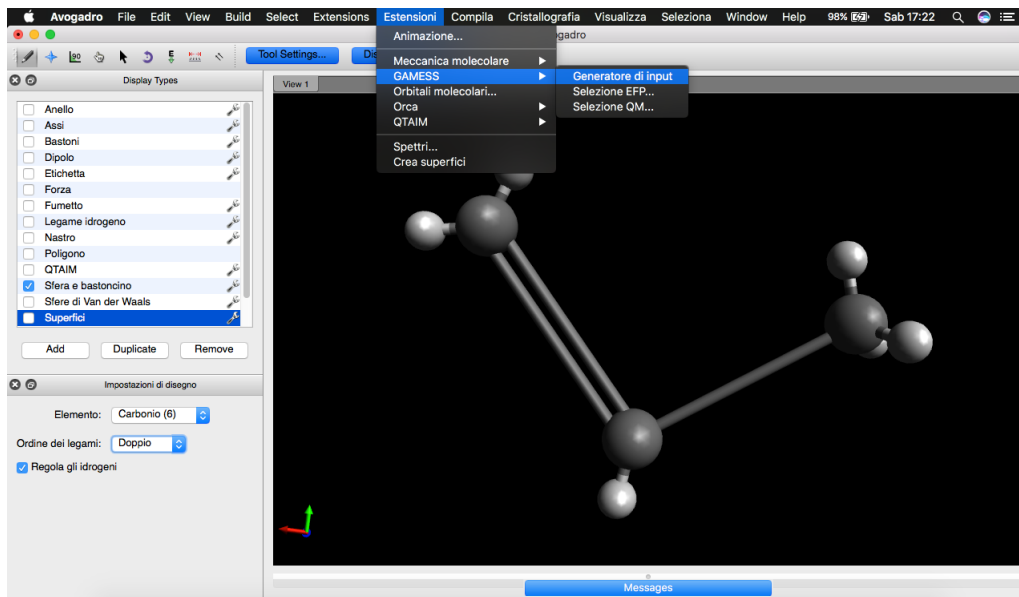
Figure 4.8: Gamess input generator.

Then you can choose all the parameters for your simulation, for example basis

sets, what you want to calculate and the representation of the molecule (Z-Matrix or cartesian axis).
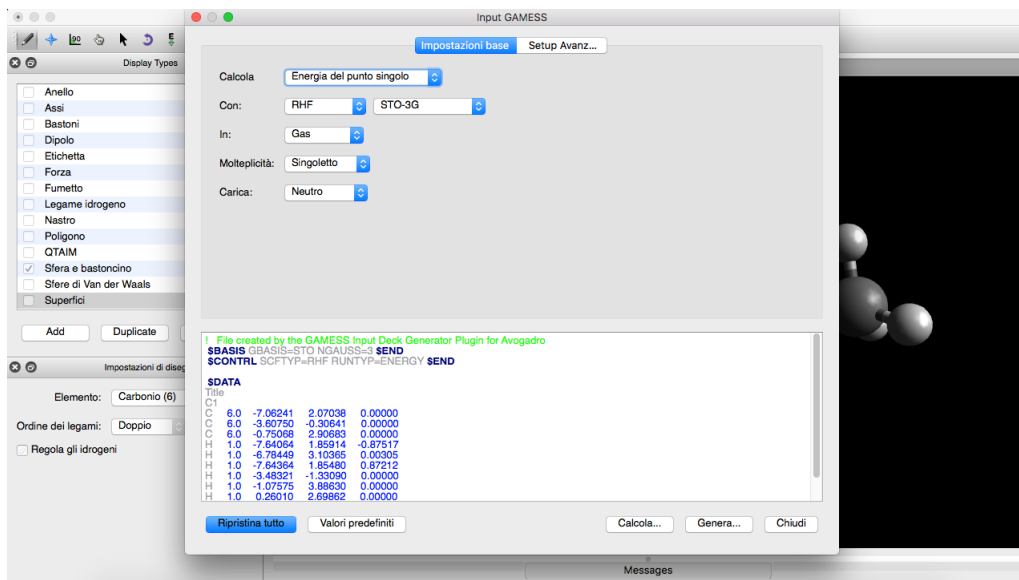
Figure 4.9: Input generator settings (A).
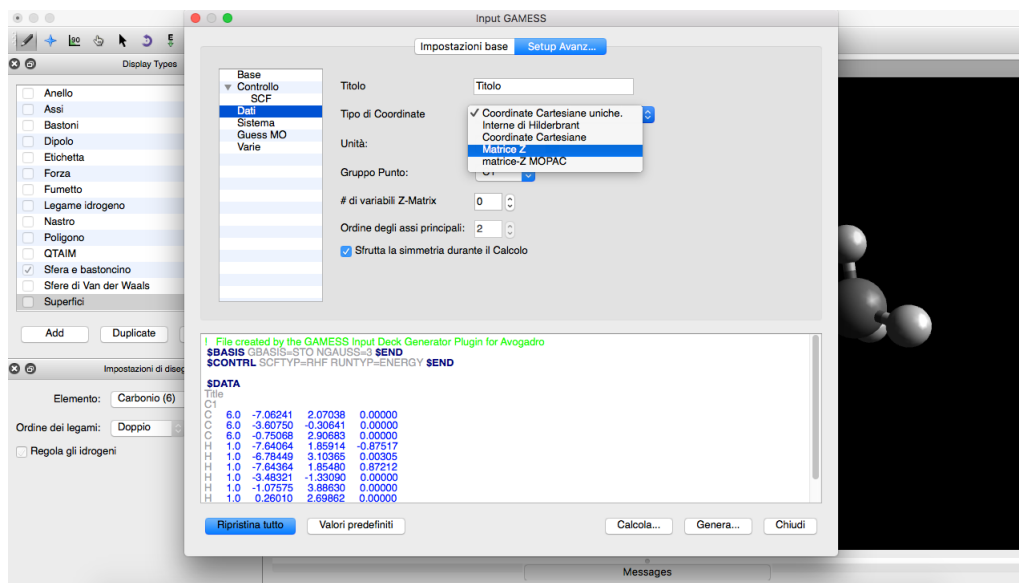
Figure 4.10: Input generator settings (B).

Finally click on "Genera...".

4.2.5   Output file

When the simulation is over, an output file is created. This file has a .log extension and it contains all the results from the simulation. Starting from the input file for Dially Butane seen before, now the output file is reported here. Some portions of the output file are reported here.

The INPUT CARD section at the start shows the first few lines of the input file. Here it shows the entire input:

```
   ECHO OF THE FIRST FEW INPUT CARDS −
INPUT CARD> $BASIS GBASIS=STO NGAUSS=3 $END
INPUT CARD> $CONTRL SCFTYP=RHF RUNTYP=OPTIMIZE COORD=ZMT $END
INPUT CARD> $STATPT OPTTOL=0.0001 NSTEP=20 $END
INPUT CARD>
INPUT CARD> $DATA
INPUT CARD>Title
INPUT CARD> C1
INPUT CARD> C
INPUT CARD> C       1            B1
INPUT CARD> C       1            B2      2        A1
INPUT CARD> C       2            B3      1        A2      3        D1
INPUT CARD> H       3            B4      1        A3      2        D2
INPUT CARD> H       3            B5      1        A4      2        D3
INPUT CARD> H       4            B6      2        A5      1        D4
INPUT CARD> H       4            B7      2        A6      1        D5
INPUT CARD> H       1            B8      2        A7      4        D6
INPUT CARD> H       1            B9      2        A8      4        D7
INPUT CARD> H       2            B10     1        A9      3        D8
INPUT CARD> H       2            B11     1        A10     3        D9
INPUT CARD> C       4            B12     2        A11     1        D10
INPUT CARD> C       13           B13     4        A12     2        D11
INPUT CARD> C       13           B14     4        A13     2        D12
INPUT CARD> H       14           B15     13       A14     4        D13
INPUT CARD> H       14           B16     13       A15     4        D14
INPUT CARD> H       15           B17     13       A16     4        D15
INPUT CARD> H       15           B18     13       A17     4        D16
INPUT CARD> C       3            B19     1        A18     2        D17
INPUT CARD> C       20           B20     3        A19     1        D18
INPUT CARD> C       20           B21     3        A20     1        D19
INPUT CARD> H       21           B22     20       A21     3        D20
INPUT CARD> H       21           B23     20       A22     3        D21
INPUT CARD> H       22           B24     20       A23     3        D22
INPUT CARD> H       22           B25     20       A24     3        D23
INPUT CARD>
INPUT CARD>      B1              1.54219718
INPUT CARD>      B2              1.54715028
INPUT CARD>      B3              1.54715028
INPUT CARD>      B4              1.08772095
INPUT CARD>      B5              1.08771964
INPUT CARD>      B6              1.08772095
INPUT CARD>      B7              1.08771964
INPUT CARD>      B8              1.08843697
INPUT CARD>      B9              1.08843680
INPUT CARD>      B10             1.08843697
INPUT CARD>      B11             1.08843680
INPUT CARD>      B12             1.53585525
INPUT CARD>      B13             1.37770630
INPUT CARD>      B14             1.37772504
INPUT CARD>      B15             1.08001478
    1000000 WORDS OF MEMORY AVAILABLE
```

BASIS OPTIONS
————————————

GBASIS=STO		IGAUSS=	3	POLAR=NONE	
NDFUNC=	0	NFFUNC=	0	DIFFSP=	F
NPFUNC=	0	DIFFS=	F	BASNAM=	

Then there is a section called "Coordinates of all atoms (angs)" that lists the coordinate system used internally by the program:

COORDINATES OF ALL ATOMS ARE (ANGS)

ATOM	CHARGE	X	Y	Z
C	6.0	0.7055186200	−0.0001336940	−0.3111856556
C	6.0	−0.7055186200	−0.0001336940	0.3111856556
C	6.0	1.8181821656	−0.0001336940	0.7638277505
C	6.0	−1.8181821656	−0.0001336940	−0.7638277505
H	1.0	1.7054295870	0.8772910675	1.3967175585
H	1.0	1.7055635332	−0.8776749274	1.3965776558
H	1.0	−1.7054295870	0.8772910675	−1.3967175585
H	1.0	−1.7055635332	−0.8776749274	−1.3965776558
H	1.0	0.8220113040	−0.8761539353	−0.9465698144
H	1.0	0.8219982213	0.8758850671	−0.9465739622
H	1.0	−0.8220113040	−0.8761539353	0.9465698144
H	1.0	−0.8219982213	0.8758850671	0.9465739622
C	6.0	−3.2130522180	0.0000314115	−0.1210300697
C	6.0	−3.8030063244	−1.2090214437	0.1759884396
C	6.0	−3.8023982480	1.2092605574	0.1765643111
H	1.0	−3.3256823323	−2.1472955607	−0.0653317068
H	1.0	−4.7712695007	−1.2612562545	0.6524098320
H	1.0	−3.3246003512	2.1474004435	−0.0643399089
H	1.0	−4.7706291117	1.2617667465	0.6530207475
C	6.0	3.2130522180	0.0000314115	0.1210300697
C	6.0	3.8030063244	−1.2090214437	−0.1759884396
C	6.0	3.8023982480	1.2092605574	−0.1765643111
H	1.0	3.3256823323	−2.1472955607	0.0653317068
H	1.0	4.7712695007	−1.2612562545	−0.6524098320
H	1.0	3.3246003512	2.1474004435	0.0643399089
H	1.0	4.7706291117	1.2617667465	−0.6530207475

The first analysis of the tools is to calculate the SCF convergence. This calculation is made by iterative steps (maximum of 200), and if it is converge means that it has calculated the MOs correctly.

————————————————
UHF SCF CALCULATION
————————————————

NUCLEAR ENERGY = 472.1093670933
MAXIT =200   NPUNCH= 2   MULT= 2
EXTRAP=T DAMP=F SHIFT=F RSTRCT=F DIIS=F SOSCF=T
DENSITY MATRIX CONV= 1.00E−08
SOSCF WILL OPTIMIZE   7296 ALPHA AND   7141 BETA ROTATION ANGLES.
SOGTOL= 2.500E−01
MEMORY REQUIRED FOR UHF/ROHF ITERS=   663739 WORDS.

ITER	EX	TOTAL ENERGY	E CHANGE	DENSITY CHANGE	ORB. GRAD
1	0	−386.506..	−386.506...	0.158841616	0.000000000
		————————START SECOND ORDER SCF————————			
2	1	−387.552..	−1.046...	0.083271087	0.046839021
3	2	−387.636..	−0.083...	0.033275224	0.035754195

4	3	−387.664..	−0.028...	0.034107009	0.014857162
5	4	−387.672..	−0.007...	0.014524410	0.007080819
6	5	−387.674..	−0.001...	0.006631104	0.003996855
7	6	−387.674..	−0.000...	0.002796382	0.001823908
8	7	−387.675..	−0.000...	0.001608628	0.000739862
9	8	−387.675..	−0.000...	0.000499825	0.000252934
10	9	−387.675..	−0.000...	0.000369083	0.000188611
11	10	−387.675..	−0.000...	0.000573632	0.000193212
12	11	−387.675..	−0.000...	0.001555634	0.000204483
13	12	−387.675..	−0.000...	0.004079090	0.000207224
14	13	−387.675..	−0.000...	0.010511500	0.000343003
15	14	−387.675..	−0.000...	0.013124786	0.000625395
16	15	−387.675..	−0.000...	0.003925157	0.000734568
17	16	−387.675..	−0.000...	0.001459006	0.000479828
18	17	−387.675..	−0.000...	0.002360579	0.000078118
19	18	−387.675..	−0.000...	0.000660724	0.000030537
20	19	−387.675..	−0.000...	0.000153743	0.000016381
21	20	−387.675..	−0.000...	0.000037904	0.000005277
22	21	−387.675..	−0.000...	0.000026781	0.000002305
23	22	−387.675..	−0.000...	0.000003936	0.000001063
24	23	−387.675..	−0.000...	0.000002720	0.000000491
25	24	−387.675..	−0.000...	0.000001486	0.000000226
26	25	−387.675..	−0.000...	0.000000319	0.000000108
27	26	−387.675..	−0.000...	0.000000200	0.000000035
28	27	−387.675..	−0.000...	0.000000133	0.000000026
29	28	−387.675..	−0.000...	0.000000060	0.000000024
30	29	−387.675..	0.000...	0.000000086	0.000000022
31	30	−387.675..	0.000...	0.000000184	0.000000019
32	31	−387.675..	−0.000...	0.000000326	0.000000018
33	32	−387.675..	0.000...	0.000000435	0.000000024
34	33	−387.675..	−0.000...	0.000000354	0.000000024
35	34	−387.675..	0.000...	0.000000128	0.000000017
36	35	−387.675..	0.000...	0.000000031	0.000000006
37	36	−387.675..	−0.000...	0.000000015	0.000000002
38	37	−387.675..	0.000...	0.000000006	0.000000001

The Mulliken and Lowdin population analyses is needed to calculate the charge of all atoms in the given system. The atomic charge is one of the most important figure in this work. This analysis is shown above:

MULLIKEN AND LOWDIN POPULATION ANALYSES

ATOMIC MULLIKEN POPULATION IN EACH MOLECULAR ORBITAL

	1	2	3	4	5
	2.000000	2.000000	2.000000	2.000000	2.000000
1	0.002960	0.005305	0.997891	0.995717	0.000028
2	0.002960	0.005305	0.997891	0.995717	0.000028
3	0.998141	0.995793	0.002986	0.005276	−0.000097
4	0.998141	0.995793	0.002986	0.005276	−0.000097
5	0.000490	−0.000488	−0.000004	−0.000006	−0.000001
6	0.000490	−0.000488	−0.000004	−0.000006	−0.000001
7	0.000490	−0.000488	−0.000004	−0.000006	−0.000001
8	0.000490	−0.000488	−0.000004	−0.000006	−0.000001
9	0.000001	0.000001	−0.000454	−0.000535	−0.000000
10	0.000001	0.000001	−0.000454	−0.000535	−0.000000
11	0.000001	0.000001	−0.000454	−0.000535	−0.000000
12	0.000001	0.000001	−0.000454	−0.000535	−0.000000
13	0.000123	−0.000126	0.000038	0.000090	1.001317

14	0.000001	0.000001	−0.000000	−0.000000	−0.000623
15	0.000001	0.000001	−0.000000	−0.000000	−0.000623
16	0.000000	−0.000000	0.000000	0.000000	0.000000
17	0.000000	0.000000	−0.000000	0.000000	0.000001
18	0.000000	−0.000000	0.000000	0.000000	0.000000
19	0.000000	0.000000	−0.000000	0.000000	0.000001
20	0.000123	−0.000126	0.000038	0.000090	1.001317
21	0.000001	0.000001	−0.000000	−0.000000	−0.000623
22	0.000001	0.000001	−0.000000	−0.000000	−0.000623
23	0.000000	−0.000000	0.000000	0.000000	0.000000
24	0.000000	0.000000	−0.000000	0.000000	0.000001
25	0.000000	−0.000000	0.000000	0.000000	0.000000
26	0.000000	0.000000	−0.000000	0.000000	0.000001

	6	7	8	9	10
	2.000000	2.000000	2.000000	2.000000	2.000000
1	0.000073	0.000000	0.000000	0.000000	0.000000
2	0.000073	0.000000	0.000000	0.000000	0.000000
3	0.000090	−0.000000	−0.000000	0.000002	0.000002
4	0.000090	−0.000000	−0.000000	0.000002	0.000002
5	0.000001	−0.000000	−0.000000	−0.000000	−0.000000
6	0.000001	−0.000000	−0.000000	−0.000000	−0.000000
7	0.000001	−0.000000	−0.000000	−0.000000	−0.000000
8	0.000001	−0.000000	−0.000000	−0.000000	−0.000000
9	0.000000	−0.000000	−0.000000	−0.000000	−0.000000
10	0.000000	−0.000000	−0.000000	−0.000000	−0.000000
11	0.000000	−0.000000	−0.000000	−0.000000	−0.000000
12	0.000000	−0.000000	−0.000000	−0.000000	−0.000000
13	1.001265	−0.000506	−0.000506	−0.000724	−0.000724
14	0.000623	0.500765	0.500773	0.500832	0.500825
15	0.000623	0.500701	0.500694	0.500897	0.500904
16	0.000000	−0.000242	−0.000242	−0.000249	−0.000249
17	0.000001	−0.000238	−0.000238	−0.000254	−0.000254
18	0.000000	−0.000242	−0.000242	−0.000249	−0.000249
19	0.000001	−0.000238	−0.000238	−0.000254	−0.000254
20	1.001265	−0.000506	−0.000506	−0.000724	−0.000724
21	0.000623	0.500765	0.500773	0.500832	0.500825
22	0.000623	0.500701	0.500694	0.500897	0.500904
23	0.000000	−0.000242	−0.000242	−0.000249	−0.000249
24	0.000001	−0.000238	−0.000238	−0.000254	−0.000254
25	0.000000	−0.000242	−0.000242	−0.000249	−0.000249
26	0.000001	−0.000238	−0.000238	−0.000254	−0.000254

	11	12	13	14	15
	2.000000	2.000000	2.000000	2.000000	2.000000
1	0.255847	0.041522	0.326683	0.177713	0.000787
2	0.255847	0.041522	0.326683	0.177713	0.000787
3	0.240847	0.194306	0.060093	0.320610	0.007633
4	0.240847	0.194306	0.060093	0.320610	0.007633
5	0.025669	0.020014	0.002807	0.052071	0.001905
6	0.025669	0.020014	0.002807	0.052070	0.001910
7	0.025669	0.020014	0.002807	0.052071	0.001905
8	0.025669	0.020014	0.002807	0.052070	0.001910
9	0.028696	0.003284	0.038823	0.017743	0.000323
10	0.028697	0.003285	0.038821	0.017742	0.000324
11	0.028696	0.003284	0.038823	0.017743	0.000323
12	0.028697	0.003285	0.038821	0.017742	0.000324
13	0.212049	0.355797	0.205191	0.113051	0.160194
14	0.079224	0.155568	0.135117	0.095594	0.286542

15	0.079226	0.155564	0.135093	0.095554	0.286601
16	0.006526	0.012897	0.011470	0.008649	0.074979
17	0.005512	0.012427	0.015816	0.020284	0.051898
18	0.006527	0.012897	0.011466	0.008642	0.074991
19	0.005512	0.012426	0.015814	0.020277	0.051913
20	0.212049	0.355797	0.205191	0.113051	0.160194
21	0.079224	0.155568	0.135117	0.095594	0.286542
22	0.079226	0.155564	0.135093	0.095554	0.286601
23	0.006526	0.012897	0.011470	0.008649	0.074979
24	0.005512	0.012427	0.015816	0.020284	0.051898
25	0.006527	0.012897	0.011466	0.008642	0.074991
26	0.005512	0.012426	0.015814	0.020277	0.051913

	16	17	18	19	20
	2.000000	2.000000	2.000000	2.000000	2.000000
1	0.000371	0.187315	0.426944	0.026639	0.016436
2	0.000371	0.187315	0.426944	0.026639	0.016436
3	0.007294	0.329478	0.140537	0.107598	0.114665
4	0.007294	0.329478	0.140537	0.107598	0.114665
5	0.001808	0.075705	0.042111	0.019860	0.037940
6	0.001814	0.075703	0.042099	0.019862	0.037945
7	0.001808	0.075705	0.042111	0.019860	0.037940
8	0.001814	0.075703	0.042099	0.019862	0.037945
9	0.000170	0.030761	0.148814	0.001554	0.005111
10	0.000171	0.030762	0.148814	0.001554	0.005112
11	0.000170	0.030761	0.148814	0.001554	0.005111
12	0.000171	0.030762	0.148814	0.001554	0.005112
13	0.160203	0.102436	0.023334	0.164917	0.148500
14	0.286977	0.055694	0.008455	0.191325	0.185925
15	0.287036	0.055653	0.008439	0.191322	0.185943
16	0.075051	0.005799	0.000948	0.060174	0.065612
17	0.052013	0.022458	0.004284	0.077510	0.065594
18	0.075063	0.005793	0.000946	0.060171	0.065611
19	0.052028	0.022444	0.004276	0.077511	0.065607
20	0.160203	0.102436	0.023334	0.164917	0.148500
21	0.286977	0.055694	0.008455	0.191325	0.185925
22	0.287036	0.055653	0.008439	0.191322	0.185943
23	0.075051	0.005799	0.000948	0.060174	0.065612
24	0.052013	0.022458	0.004284	0.077510	0.065594
25	0.075063	0.005793	0.000946	0.060171	0.065611
26	0.052028	0.022444	0.004276	0.077511	0.065607

	21	22	23	24	25
	2.000000	2.000000	2.000000	2.000000	2.000000
1	0.318257	0.040583	0.052167	0.039419	0.141526
2	0.318257	0.040583	0.052167	0.039419	0.141526
3	0.186725	0.096963	0.121483	0.223542	0.007685
4	0.186725	0.096963	0.121483	0.223542	0.007685
5	0.067580	0.003959	0.024643	0.084066	0.002952
6	0.067594	0.003959	0.024604	0.084093	0.002958
7	0.067580	0.003959	0.024643	0.084066	0.002952
8	0.067594	0.003959	0.024604	0.084093	0.002958
9	0.111881	0.001456	0.007787	0.013856	0.055878
10	0.111879	0.001461	0.007779	0.013845	0.055873
11	0.111881	0.001456	0.007787	0.013856	0.055878
12	0.111879	0.001461	0.007779	0.013845	0.055873
13	0.021370	0.132305	0.121571	0.103560	0.141203
14	0.034747	0.204565	0.182783	0.134713	0.183167
15	0.034752	0.204561	0.182776	0.134713	0.183076

16	0.000227	0.120789	0.108176	0.000005	0.001798
17	0.022378	0.034305	0.029031	0.084092	0.111077
18	0.000224	0.120788	0.108174	0.000005	0.001795
19	0.022388	0.034305	0.029027	0.084092	0.111013
20	0.021370	0.132305	0.121571	0.103560	0.141203
21	0.034747	0.204565	0.182783	0.134713	0.183167
22	0.034752	0.204561	0.182776	0.134713	0.183076
23	0.000227	0.120789	0.108176	0.000005	0.001798
24	0.022378	0.034305	0.029031	0.084092	0.111077
25	0.000224	0.120788	0.108174	0.000005	0.001795
26	0.022388	0.034305	0.029027	0.084092	0.111013

	26	27	28	29	30
	2.000000	2.000000	2.000000	2.000000	2.000000
1	0.350342	0.406154	0.110857	0.011042	0.020748
2	0.350342	0.406154	0.110857	0.011042	0.020748
3	0.343779	0.150858	0.163617	0.028573	0.003155
4	0.343779	0.150858	0.163617	0.028573	0.003155
5	0.052509	0.011375	0.072454	0.011101	0.002757
6	0.052107	0.011337	0.072814	0.011108	0.002761
7	0.052509	0.011375	0.072454	0.011101	0.002757
8	0.052107	0.011337	0.072814	0.011108	0.002761
9	0.038591	0.010713	0.047324	0.006096	0.011464
10	0.038831	0.010755	0.047088	0.006101	0.011457
11	0.038591	0.010713	0.047324	0.006096	0.011464
12	0.038831	0.010755	0.047088	0.006101	0.011457
13	0.052100	0.065637	0.043371	0.090948	0.163248
14	0.022941	0.088716	0.122553	0.221153	0.230586
15	0.023135	0.088776	0.122338	0.221146	0.230593
16	0.004711	0.019691	0.019032	0.159643	0.149572
17	0.008034	0.058120	0.079857	0.036722	0.012023
18	0.004750	0.019708	0.018982	0.159642	0.149598
19	0.008168	0.058160	0.079710	0.036726	0.012038
20	0.052100	0.065637	0.043371	0.090948	0.163248
21	0.022941	0.088716	0.122553	0.221153	0.230586
22	0.023135	0.088776	0.122338	0.221146	0.230593
23	0.004711	0.019691	0.019032	0.159643	0.149572
24	0.008034	0.058120	0.079857	0.036722	0.012023
25	0.004750	0.019708	0.018982	0.159642	0.149598
26	0.008168	0.058160	0.079710	0.036726	0.012038

	31	32	33	34	35
	2.000000	2.000000	2.000000	2.000000	2.000000
1	0.086425	0.392655	0.008051	0.281929	0.209125
2	0.086425	0.392655	0.008051	0.281929	0.209125
3	0.275794	0.250811	0.281261	0.109654	0.228707
4	0.275794	0.250811	0.281261	0.109654	0.228707
5	0.162810	0.021951	0.023575	0.084622	0.020686
6	0.162746	0.022116	0.023513	0.084736	0.020645
7	0.162810	0.021951	0.023575	0.084622	0.020686
8	0.162746	0.022116	0.023513	0.084736	0.020645
9	0.046791	0.104192	0.002427	0.200288	0.012459
10	0.046582	0.104376	0.002390	0.200338	0.012450
11	0.046791	0.104192	0.002427	0.200288	0.012459
12	0.046582	0.104376	0.002390	0.200338	0.012450
13	0.067292	0.061053	0.244286	0.010571	0.260781
14	0.060163	0.018676	0.103033	0.011221	0.065762
15	0.060245	0.018649	0.103016	0.011265	0.065734
16	0.007933	0.000824	0.019342	0.000912	0.009241

45

17	0.007633	0.001938	0.084896	0.001770	0.042596
18	0.007918	0.000832	0.019332	0.000907	0.009238
19	0.007667	0.001926	0.084876	0.001787	0.042577
20	0.067292	0.061053	0.244286	0.010571	0.260781
21	0.060163	0.018676	0.103033	0.011221	0.065762
22	0.060245	0.018649	0.103016	0.011265	0.065734
23	0.007933	0.000824	0.019342	0.000912	0.009241
24	0.007633	0.001938	0.084896	0.001770	0.042596
25	0.007918	0.000832	0.019332	0.000907	0.009238
26	0.007667	0.001926	0.084876	0.001787	0.042577

	36	37	38
	2.000000	2.000000	2.000000
1	0.038418	0.125940	0.000347
2	0.038418	0.125940	0.000347
3	0.023647	0.081052	0.000243
4	0.023647	0.081052	0.000243
5	0.012027	0.006195	0.000005
6	0.011993	0.006178	0.000005
7	0.012027	0.006195	0.000005
8	0.011993	0.006178	0.000005
9	0.000975	0.000900	0.000000
10	0.000970	0.000898	0.000000
11	0.000975	0.000900	0.000000
12	0.000970	0.000898	0.000000
13	0.428541	0.345371	0.000009
14	0.241410	0.215109	0.499662
15	0.241371	0.215081	0.499724
16	0.000043	0.000358	0.000001
17	0.000281	0.001281	0.000000
18	0.000043	0.000358	0.000001
19	0.000281	0.001280	0.000000
20	0.428541	0.345371	0.000009
21	0.241410	0.215109	0.499662
22	0.241371	0.215081	0.499724
23	0.000043	0.000358	0.000001
24	0.000281	0.001281	0.000000
25	0.000043	0.000358	0.000001
26	0.000281	0.001280	0.000000

After this, the charge of each atom is listed:

ATOM		MULL.POP.	CHARGE	LOW.POP.	CHARGE
		TOTAL MULLIKEN AND LOWDIN ATOMIC POPULATIONS			
1	C	6.311074	−0.311074	6.182458	−0.182458
2	C	6.311076	−0.311076	6.182460	−0.182460
3	C	6.267563	−0.267563	6.156002	−0.156002
4	C	6.267563	−0.267563	6.156002	−0.156002
5	C	5.965556	0.034444	5.858663	0.141337
6	C	5.965557	0.034443	5.858663	0.141337
7	C	6.115265	−0.115265	6.122202	−0.122202
8	C	6.115260	−0.115260	6.122203	−0.122203
9	C	6.263573	−0.263573	6.203562	−0.203562
10	C	6.263575	−0.263575	6.203560	−0.203560
11	H	0.795061	0.204939	0.855144	0.144856
12	H	0.815910	0.184090	0.872539	0.127461
13	H	0.795060	0.204940	0.855143	0.144857
14	H	0.815909	0.184091	0.872539	0.127461
15	H	0.850290	0.149710	0.892064	0.107936
16	H	0.837496	0.162504	0.885043	0.114957
17	H	0.850291	0.149709	0.892065	0.107935

```
18 H   0.837496    0.162504    0.885042    0.114958
19 H   0.744216    0.255784    0.836773    0.163227
20 H   0.744216    0.255784    0.836773    0.163227
21 H   0.838142    0.161858    0.881292    0.118708
22 H   0.838143    0.161857    0.881293    0.118707
23 H   0.837857    0.162143    0.869659    0.130341
24 H   0.857995    0.142005    0.884599    0.115401
25 H   0.837857    0.162143    0.869659    0.130341
26 H   0.857996    0.142004    0.884599    0.115401
```

4.3   Gaussian tutorial

Gaussian09 is another computational chemistry program. Maybe it is the most well-known and the most developed. Unlike Gamess (which is an open source program), gaussian09 requires to purchase a license in order to use it. In the second part of this chapter will be a brief introduction to the program, the main commands will be listed and the output file will be introduced. For common arguments with Gamess (for example the Z-matrix or the meaning of some specific terms, for example SCF), refer to the Gamess manual.

A brief introduction of this software has already been written in [35], [40], [41].

4.3.1   Input file

The gaussian09 input file is very similar to the gamess one. There is a first part where the commands are given, such as the basis sets, the type of calculation to perform and so on. After the command section the Z-matrix is written 4.1.1. The portion of input file commands is shown below:

```
%NProc=6
%Chk=rs3_opt_b3lyp_LANL2DZ_ch1_field_x+1.chk
# b3lyp/lanl2dz geom=connectivity scf=maxcycle=1000
field=x+20 pop=(mk,readradii)

rs3 B3LYP/TZVP field

1 2
 C
 C     1      B1
 C     2      B2    1     A1
 C     3      B3    2     A2    1     D1
 C     4      B4    3     A3    2     D2
 Fe    1      B5    2     A4    3     D3
 C     6      B6    1     A5    2     D4
 C     7      B7    6     A6    1     D5
 C     8      B8    7     A7    6     D6
 C     9      B9    8     A8    7     D7
 C    10      B10   9     A9    8     D8
 C     8      B11   7     A10   6     D9
 C    12      B12   8     A11   7     D10
 C    12      B13   8     A12   7     D11
 C    14      B14   12    A13   8     D12
```

C	15	B15	14	A14	12	D13	
C	16	B16	15	A15	14	D14	
C	17	B17	16	A16	15	D15	
C	18	B18	17	A17	16	D16	
C	16	B19	15	A18	14	D17	
C	20	B20	16	A19	15	D18	
N	21	B21	20	A20	16	D19	
C	20	B22	16	A21	15	D20	
C	23	B23	20	A22	16	D21	
C	24	B24	23	A23	20	D22	
C	21	B25	20	A24	16	D23	
C	24	B26	23	A25	20	D24	
C	27	B27	24	A26	23	D25	
C	27	B28	24	A27	23	D26	
C	29	B29	27	A28	24	D27	
C	30	B30	29	A29	27	D28	
C	31	B31	30	A30	29	D29	
C	29	B32	27	A31	24	D30	
Fe	32	B33	31	A32	30	D31	
C	34	B34	32	A33	31	D32	
C	35	B35	34	A34	32	D33	
C	36	B36	35	A35	34	D34	
C	37	B37	36	A36	35	D35	
C	38	B38	37	A37	36	D36	
H	12	B39	8	A38	7	D37	
H	13	B40	12	A39	8	D38	
H	13	B41	12	A40	8	D39	
H	13	B42	12	A41	8	D40	
H	28	B43	27	A42	24	D41	
H	28	B44	27	A43	24	D42	
H	28	B45	27	A44	24	D43	
H	36	B46	35	A45	34	D44	
H	37	B47	36	A46	35	D45	
H	38	B48	37	A47	36	D46	
H	39	B49	38	A48	37	D47	
H	35	B50	34	A49	32	D48	
H	30	B51	29	A50	27	D49	
H	33	B52	29	A51	27	D50	
H	32	B53	31	A52	30	D51	
H	31	B54	30	A53	29	D52	
H	9	B55	8	A54	7	D53	
H	10	B56	9	A55	8	D54	
H	11	B57	10	A56	9	D55	
H	7	B58	6	A57	1	D56	
H	1	B59	2	A58	3	D57	
H	5	B60	4	A59	3	D58	
H	4	B61	3	A60	2	D59	
H	3	B62	2	A61	1	D60	
H	2	B63	1	A62	5	D61	
H	15	B64	14	A63	12	D62	
H	19	B65	18	A64	17	D63	
H	18	B66	17	A65	16	D64	
H	22	B67	21	A66	20	D65	
H	26	B68	21	A67	20	D66	
H	25	B69	24	A68	23	D67	
H	23	B70	20	A69	16	D68	
H	27	B71	24	A70	23	D69	

B1	1.44327819
B2	1.44047882
B3	1.44067328
B4	1.44219375
.	

```
   .
   .
   .
  D68              −0.64353627
  D69             −168.54682503

1 2 1.5 5 1.5 60 1.0
2 3 1.5 64 1.0
3 4 1.5 63 1.0
4 5 1.5 62 1.0
 .
 .
 .
 .
 70
 71
 72
```

```
Fe 1.3
```

The first line of the input file specifies the number of processors to use in order to do a parallel computation using the % symbol. In the VLSI laboratory there are 14 processors, in that of Micro & Nano 4. Obviously the number of the values of # can not exceed the physucall number of processors. The second line instead the name of the file checkpoint. This file serves mainly two purposes: it is used as a starting point for a second simulation and it is the file that is used by software like Avogadro for the molecule visualization.

In the third row, however, there are all the other commands to be given to gaussian09 to obtain the required results.

- **Method and basis sets**:
  It corresponds to \$SCFTYP and \$GBASIS group in Gamess. Gaussian09 can also perform RHF, UHF and DFT calculations. In the example, the calculations are ub3lyp (DFT) and the basis is lanl2dz but they are optional.

- **Geom=connectivity** :
  The Geom keyword specifies the source of the molecule specification input, options related to coordinate definitions, and geometry related output.

- **Scf=maxcylce=N** :
  This keyword specifies the maximum number of steps for SCF. Usually, N is equal to 2000.

- **Pop=(mk, readradii)**:
  It is the type of calculation for the atomic charge. In particular, this command set Merz-Singh-Kollman (MK) scheme for evaluating the atomic charge distribution with the calculation of Mulliken and ESP charges.

- **Charge**:
  To add a point charge driver we have to specify the keyword "charge" in the

command line. The coordinates and the value of the point charge driver will be at the end of the input file (Fe 1.3 in the example): we can add as many point driver as we want.

- **External electric field field:**
  It is possible to insert an external electric field also with gaussian09. In this case, the syntax is *field = D±N* . *D* is the direction (x, y, z) , in the example is x and N is the magnitude of the field in atomic unit ($1\,\mathrm{a\,u} = 5.14 \cdot 102\,\mathrm{V/nm}$). In the input file listed above, we have an electric field with a modulus of $1.028\,\mathrm{V/nm}$ and oriented along the positive X axes.

4.3.2   Running Gaussian Through Gaussian User Interface

After the input file of Gaussian simulation is properly set-up, we could run the software to perform the simulation in order to solve the Schrodinger Equation mentioned in the previous section. But until now, it is needed to point out that we have two ways to perform the running procedure: one is through the Gaussian Viewer Software user interface (could be installed on personal computer) and the other is through the online server of Politecnico di Torino.

One could run the Gaussian simulation through the Gaussian user interface, in this part, a detailed procedure is described. First we run the Gaussian software, which is provided in Windows, on the personal computer where it was installed and open an input file we just defined. Then the pop-up window is shown in Fig. 4.11, from this figure we can observe that, in the pop-up window we can modify every command that was mentioned in the last section, like the method/basis and value of the uniform electric field applied to the molecule, etc. Also the Z-matrix is available in the window and can be changed freely according to the requirement of the user. After configuring the input file, we could run the software by simply clicking the icon RUN on the right of the window and the simulation is performed. As shown in Fig. 4.11 , the software is running and the content of the output file is updated frequently as it runs. About the output file, we have perform the detailed analysis later on in the following section.
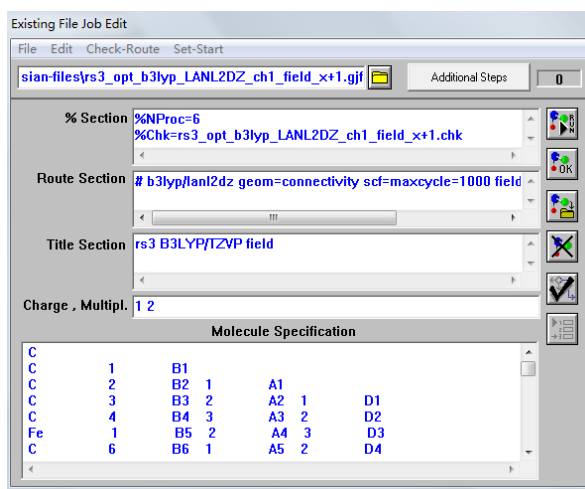
Figure 4.11: Gaussian input file configuration through Gaussian User Interface.

This method is simple and easily used without internet connection, but generally speaking, while you set at first that the number of processors is 14, usually personal computers has only one or few processors; as a consequence of that, the time needed for the simulation in this situation is large. So in order to improve the simulation procedure and save the time, we need a more powerful environment to work with, which brings us to the following section about the online server.

4.3.3   Running Gaussian through online server

- Login:
  This server is run in a Linux environment and once you have got the user id and the password, you can login into the server. A screen shot of the server interface is shown in Fig 4.12. Then create a folder which contains the input Gaussian simula- tion files. We could name the input folder as the title of the simulation, for example, rs3:._x 200.gjf. In the Fig 4.13 there are some already named input file ready to be executed.
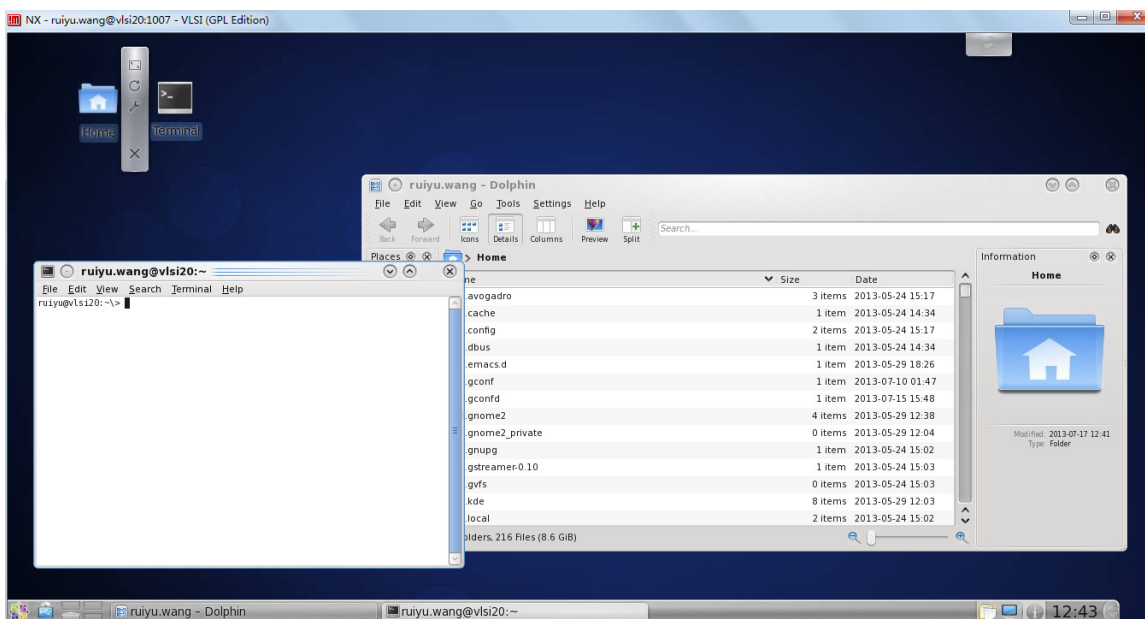
Figure 4.12: The interface of the server after login.
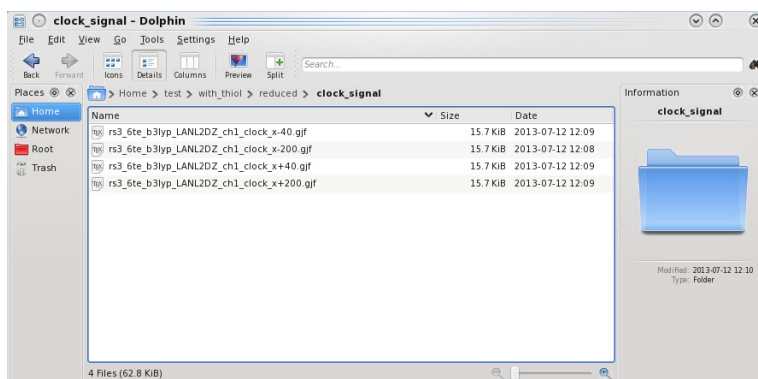
Figure 4.13: Some input Gaussian file in the folder of the server.

- Initialize the Gaussian software:
  After preparing the input files, we need to initialize the Gaussian software. First open the terminal on the server and type the command source /software/scripts/init_g09 to initialize the Gaussian software on the server. Then the return instruction tells us that we could use all the commands that contains in the /g09 directory.

- Run Gaussian software:
  After initializing Gaussian software, we could perform the simulation. Change

the current directory to the folder which contains the input files that needed to be executed, mentioned previously. Then type the command g09 input file name to run the Gaussian software on the server; for example, g09 rs3 ... _x-200.gjf. The Gaussian software will generate the checkpoint file (.chk) and the output Gaussian file (.log) immediately and updatethem frequently until the simulation is finished. And at the same time we could perform also the inspection of the content at the output file and state of our current simulation job. By typing the command tail -f file name, for example, tail -f rs3_6te_b3lyp_LANL2DZ_ch1_clock_x-200.gjf, one could see the content at the very end of the corresponding output file and it updates. Furthermore, by typing the command top, one could see the current simulation jobs existing on the server right now the occupancy of cpu processors and memories, etc. Usually, the simulation would take few hours to finish the job depending the requirements that you have put in the input file, for example, the simulation time decreases as the number of processors increases and if we have defined a more accuracy simulations with lower convergency error, and the time consumed will be larger. During simulation, Gaussian have written all the relevant information, such as the optimized structure, the charge distribution, the energy distribution, etc, into the output file. So an detailed analysis of the output Gaussian file is necessary and provided in the next section.

4.3.4 Gaussian Output file

In this section the interisting parts of the gaussian09 output file will be analyzed. The first part of the output file is a summary of all commands given in the input file. After that, the software will calculate the convergence of the SCF and, once finished, will displays the optimized geometry of the system under the heading "Standard orientation".

```
SCF Done:   E(UB3LYP) =    −1934.75497408
A.U. after   137 cycles
Convg  =     0.5178D−05      −V/T =   2.0627
```

Standard orientation:

Center Number	Atomic Number	Atomic Type	Coordinates (Angstroms)		
			X	Y	Z
1	6	0	−4.918827	−6.503165	−0.858753
2	6	0	−3.579317	−6.985817	−0.896848
3	6	0	−3.081190	−7.006256	0.436876
4	6	0	−4.112678	−6.535603	1.299485
5	6	0	−5.248466	−6.225703	0.498685
6	26	0	−3.621776	−5.061555	−0.093920
7	6	0	−3.050836	−3.321389	0.899548
8	6	0	−1.962576	−3.796463	0.105018
9	6	0	−2.416639	−3.822346	−1.249553
10	6	0	−3.763476	−3.365730	−1.289245

11	6	0	-4.158567	-3.058639	0.042877
12	6	0	-0.558257	-4.131058	0.553616
13	6	0	-0.465246	-4.439280	2.058170
14	6	0	0.444124	-3.044541	0.163909
15	6	0	0.139553	-1.691654	0.283352
16	6	0	1.096090	-0.729637	-0.041332
17	6	0	2.373864	-1.140125	-0.491853
18	6	0	2.696541	-2.486842	-0.619626
19	6	0	1.721577	-3.418903	-0.288960
20	6	0	1.100825	0.719432	-0.041284
21	6	0	2.381274	1.121592	-0.491743
22	7	0	3.133515	-0.011731	-0.755438
23	6	0	0.150634	1.687664	0.283527
24	6	0	0.464079	3.038546	0.164253
25	6	0	1.743936	3.404577	-0.288609
26	6	0	2.712770	2.466172	-0.619380
27	6	0	-0.531171	4.131502	0.554190
28	6	0	-0.436340	4.438604	2.058855
29	6	0	-1.937621	3.806277	0.105337
30	6	0	-2.391378	3.835498	-1.249267
31	6	0	-3.741277	3.388017	-1.289156
32	6	0	-4.138545	3.083330	0.042875
33	6	0	-3.029135	3.338416	0.899689
34	26	0	-3.588201	5.082574	-0.093538
35	6	0	-5.207203	6.257731	0.498493
36	6	0	-4.875391	6.532672	-0.858928
37	6	0	-3.532675	7.006339	-0.896808
38	6	0	-3.034728	7.023719	0.437034
39	6	0	-4.069553	6.560177	1.299498
40	1	0	-0.259057	-5.036331	0.016672
41	1	0	-1.146080	-5.245724	2.336993
42	1	0	0.550987	-4.738287	2.319920
43	1	0	-0.710502	-3.559217	2.656141
44	1	0	-1.111879	5.249435	2.337833
45	1	0	-0.687484	3.559987	2.656509
46	1	0	0.581807	4.730823	2.320838
47	1	0	-5.520928	6.389455	-1.710657
48	1	0	-2.983376	7.283984	-1.782307
49	1	0	-2.043784	7.323560	0.739444
50	1	0	-3.999349	6.443893	2.369292
51	1	0	-6.147953	5.869248	0.854797
52	1	0	-1.803305	4.150818	-2.097183
53	1	0	-3.027230	3.221106	1.971365
54	1	0	-5.112695	2.740301	0.353495
55	1	0	-4.361577	3.319262	-2.168613
56	1	0	-1.830752	-4.141442	-2.097570
57	1	0	-4.383356	-3.292640	-2.168648
58	1	0	-5.130361	-2.709120	0.353637
59	1	0	-3.048081	-3.204310	1.971248
60	1	0	-5.563611	-6.355854	-1.710355
61	1	0	-6.186526	-5.830903	0.855138
62	1	0	-4.041421	-6.419502	2.369229
63	1	0	-2.092175	-7.312560	0.739115
64	1	0	-3.032123	-7.267338	-1.782426
65	1	0	-0.845996	-1.386579	0.613822
66	1	0	1.953001	-4.473914	-0.387597
67	1	0	3.670610	-2.804973	-0.971993
68	1	0	3.688901	2.777953	-0.971720
69	1	0	1.982274	4.458058	-0.387130
70	1	0	-0.836888	1.389033	0.614000
71	1	0	-0.225977	5.034977	0.017593
72	6	0	5.077530	-0.018064	-1.466538
73	6	0	5.972919	-0.023851	-0.364428

74	1	0	5.247605	0.856108	−2.059664
75	1	0	5.240630	−0.891176	−2.063173
76	1	0	5.809820	0.849262	0.232206
77	1	0	5.802845	−0.898023	0.228698
78	6	0	7.310461	−0.028233	−0.841252
79	1	0	7.473558	−0.901343	−1.437891
80	1	0	7.480537	0.845943	−1.434372
81	6	0	8.205850	−0.034020	0.260858
82	6	0	9.543380	−0.041005	−0.215969
83	1	0	8.034463	−0.907207	0.855056
84	1	0	8.044074	0.840068	0.856423
85	1	0	9.714769	0.832186	−0.810162
86	1	0	9.705154	−0.915090	−0.811540
87	6	0	10.438768	−0.046792	0.886140
88	1	0	10.276994	0.827298	1.481704
89	1	0	10.267380	−0.919978	1.480339
90	16	0	11.776298	−0.053777	0.409313
91	1	0	11.712547	0.943917	0.027943

After this, the software calculates both the mulliken and ESP charge for each atom:

```
Mulliken atomic charges:
             1
   1   C    −0.221124
   2   C    −0.223534
   3   C    −0.238507
   4   C    −0.228625
   5   C    −0.225585
   6   Fe   −0.199686
   7   C    −0.372597
   8   C     0.410068
   9   C    −0.392602
  10   C    −0.226502
  11   C    −0.254862
  12   C    −0.352958
  13   C    −0.728372
  14   C     0.617275
  15   C    −0.554318
  16   C     0.147861
  17   C     0.105610
  18   C    −0.369091
  19   C    −0.486003
  20   C     0.141926
  21   C     0.106513
  22   N    −0.197087
  23   C    −0.548822
  24   C     0.621526
  25   C    −0.487745
  26   C    −0.368574
  27   C    −0.349308
  28   C    −0.694479
  29   C     0.387699
  30   C    −0.354662
  31   C    −0.192878
  32   C    −0.216721
  33   C    −0.329718
  34   Fe   −0.148018
  35   C    −0.200374
  36   C    −0.198491
  37   C    −0.199462
  38   C    −0.209320
  39   C    −0.196901
```

```
40   H      0.205347
41   H      0.227280
42   H      0.211820
43   H      0.201264
44   H      0.211844
45   H      0.213162
46   H      0.230596
47   H      0.309987
48   H      0.293477
49   H      0.283917
50   H      0.295778
51   H      0.310899
52   H      0.300403
53   H      0.298723
54   H      0.300730
55   H      0.301375
56   H      0.269161
57   H      0.271757
58   H      0.266463
59   H      0.253300
60   H      0.279294
61   H      0.273935
62   H      0.240110
63   H      0.245803
64   H      0.262697
65   H      0.252826
66   H      0.232094
67   H      0.213693
68   H      0.216624
69   H      0.228475
70   H      0.242723
71   H      0.199395
72   C     −0.239049
73   C     −0.372663
74   H      0.193982
75   H      0.197360
76   H      0.220536
77   H      0.222355
78   C     −0.352521
79   H      0.193135
80   H      0.188875
81   C     −0.353446
82   C     −0.356126
83   H      0.201132
84   H      0.195466
85   H      0.200221
86   H      0.223291
87   C     −0.981432
88   H      0.265158
89   H      0.290753
90   S      0.342422
91   H      0.004046
```

```
Charges from ESP fit , RMS=    0.00241 RRMS=    0.03237:
Charge=    1.00000 Dipole=   −14.9919      17.8193      −2.3172 Tot=      23.4020
                     1
    1   C     −0.080041
    2   C     −0.145153
    3   C     −0.117293
    4   C     −0.124639
    5   C     −0.095515
    6   Fe    −0.035222
    7   C     −0.218018
```

8	C	0.087472
9	C	−0.216355
10	C	−0.102856
11	C	−0.198681
12	C	0.055317
13	C	−0.478739
14	C	0.116963
15	C	−0.204041
16	C	−0.090490
17	C	0.379271
18	C	−0.361242
19	C	−0.237414
20	C	−0.060053
21	C	0.375767
22	N	−0.474431
23	C	−0.215194
24	C	0.090075
25	C	−0.252744
26	C	−0.343626
27	C	−0.009742
28	C	−0.384757
29	C	0.147562
30	C	−0.164260
31	C	−0.039338
32	C	−0.144109
33	C	−0.144862
34	Fe	−0.028176
35	C	−0.057776
36	C	−0.036953
37	C	−0.098178
38	C	−0.061542
39	C	−0.061836
40	H	0.079417
41	H	0.139449
42	H	0.127097
43	H	0.106225
44	H	0.106470
45	H	0.102009
46	H	0.133709
47	H	0.159295
48	H	0.161503
49	H	0.146875
50	H	0.151044
51	H	0.163618
52	H	0.161341
53	H	0.176733
54	H	0.188968
55	H	0.166931
56	H	0.149563
57	H	0.160822
58	H	0.174733
59	H	0.159330
60	H	0.145478
61	H	0.141611
62	H	0.118465
63	H	0.129092
64	H	0.148758
65	H	0.171063
66	H	0.151108
67	H	0.207316
68	H	0.209188
69	H	0.154750
70	H	0.169135

71	H	0.087156
72	C	−0.132970
73	C	0.091021
74	H	0.111644
75	H	0.118075
76	H	−0.003851
77	H	0.010561
78	C	0.266237
79	H	−0.065648
80	H	−0.062238
81	C	−0.021247
82	C	0.317494
83	H	−0.069288
84	H	−0.035506
85	H	−0.101566
86	H	−0.065233
87	C	0.092996
88	H	−0.006425
89	H	0.120334
90	S	−0.603377
91	H	0.321584

4.4   Avogadro

When the simulation is over for both Gamess and Gaussian, you can analyze the simulation results using Avogadro. Avogadro is an advanced molecule editor and visualizer designed for cross-platform use in computational chemistry, molecular modeling, bio-informatics, materials science, and related areas. It offers flexible high quality rendering and a powerful plug-in architecture.

Now you have two possibilities: either install Avogadro on your laptop or use Avogadro through the server. In the first case, when the software is opened you have to click on File → Import → Molecule File and then select GAMESS output or the checkpoint file of Gaussian. In the second case you have to type the command *avogadro &* in the terminal of the server that we have mentioned before. The molecule will be visualized in the user interface:

58
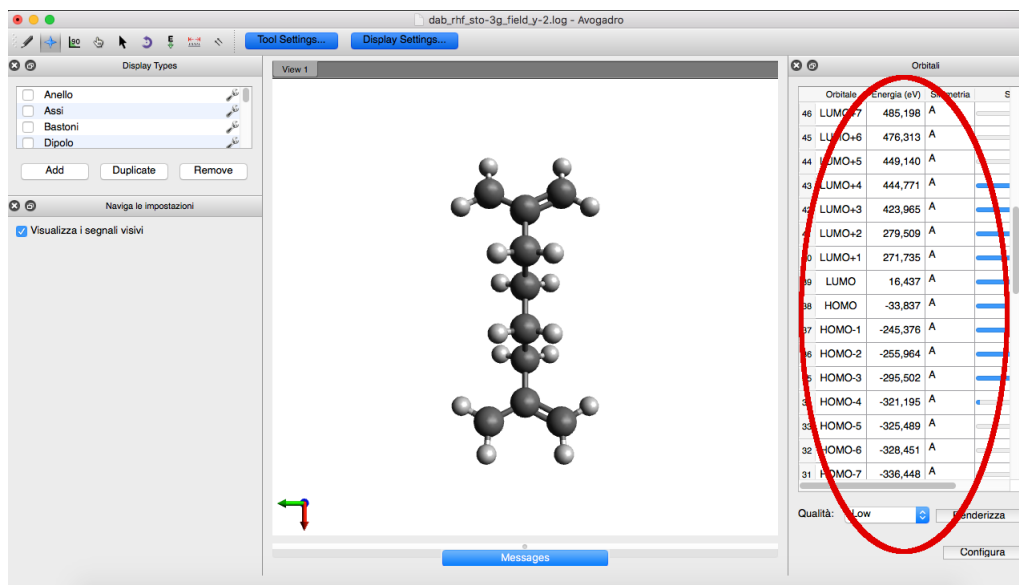
Figure 4.14: Visualizing the molecule with Avogadro.

The tables to the right lists all molecular orbitals. If the status bar is full, you can click on the row of the orbital and a quick low quality rendition of the orbital will be created. An example of HOMO (Highest Occupied Molecular Orbital) is shown in Fig. 4.15.
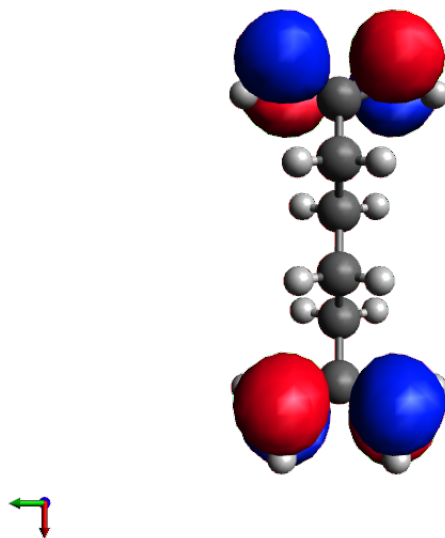
Figure 4.15: HOMO orbitals.

Chapter 5

Gamess VS Gaussian09

One of the purposes of this work thesis is to compare the results obtained by using GAMESS with those obtained with Gaussian09 in the previous thesis. It is important to understand which results have to be compared. The results of a simulation depends on the input file, changing it you can have every kind of results. But there are some type of computation that a specific tools can not do. For example, you can not calculate the ESP charges in Gamess, but just the Mulliken and Lodwin population. This is an important constraint for this work and, in this case, a post-processing work has to be done for evaluating it [39].

Since we are focused on the charge localization in this thesis, just the Mulliken and Lodwin population and the electrostatic potential (for the ESP algorithm [39]) have been analyzed for both Gaussian09 and Gamess for two candidate molecules (diallyl butane and decatriene) in two different conditions:

- at the equilibrium;

- with a switching field.

The bis-ferrocene molecule was not analyzed in this first phase of the work since, given the complexity of itself and the very high computational cost especially in terms of time, would not have been convenient.

5.1 Mulliken population analysis

Before starting with the comparison between Gamess and Gaussian09 results, let's review what Mulliken population is [42]. Population analysis is the study of charge distribution within molecules. Mulliken population analysis is by default always performed both in Gamess and in Gaussian.

Let's suppose that we have N number of electrons within a molecule. In this case N can be expressed as [43]

$$N = \sum_{j}^{electrons} \left(\sum_{r} c_{jr}^2 + \sum_{r \neq s} c_{jr} c_{js} S_{rs} \right) \tag{5.1}$$

The problem of the Mulliken population analysis is that it splits the shared electrons from two atoms to fifty-fifty. The advantages of this model is that it is computationally cheap. It works well for comparing changes in partial charge assignment between two different geometries when the same size basis set is used. The main disadvantage is that the partial charges assigned to atoms varies significantly for the same system when different size basis sets are used, so computations using different basis sets cannot be compared.

5.2 Electrostatic potential

For the evaluation of the electrostatic potential in a nucleus, that nucleus is ignored, avoiding a singularity. All other atoms in the molecule contribute to the calculation of electrostatic potential except for the nucleus where the electrostatic potential is calculated [32]. The analysis of electrostatic potential is very important since author in [39] starts from this result for the ESP calculation.

5.3 Diallyl butane

Let's consider a Diallyl butane molecule as in Fig. 5.1.
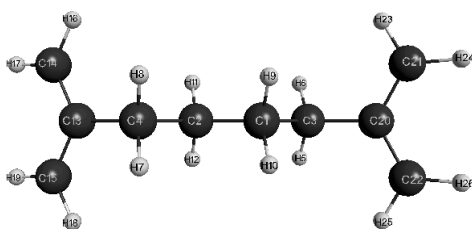
Figure 5.1: Diallyl butane molecule.

As mentioned before, we have to study two configuration: at the equilibrium and with the switching field.

5.3.1   At the equilibrium

First, the Mulliken charges and the electrostatic potential are analyzed at the equilibrium condition. This means that the molecule is neutral (total charge equal to 0) and there is not an external electric field. The geometry of the molecule is optimized to have the minimum possible energy in the system.

The input files for both Gamess and Gaussian are listed here:

- Gamess input:

  ```
  $BASIS  GBASIS=STO NGAUSS=3 $END
  $CONTRL SCFTYP=RHF RUNTYP=OPTIMIZE COORD=ZMT $END
  $STATPT OPTTOL=0.0001  NSTEP=20  $END
  ```

- Gaussian input:

  ```
  %chk=1−4_diallyl_butane_opt.chk
  # opt rhf/sto−3g geom=connectivity
  ```

In Fig. 5.2 and 5.3 the results of these comparable simulation and the absolute error (evaluated as $|V_{gamess} - V_{gaussian09}|$), for all the values see Appendix A.
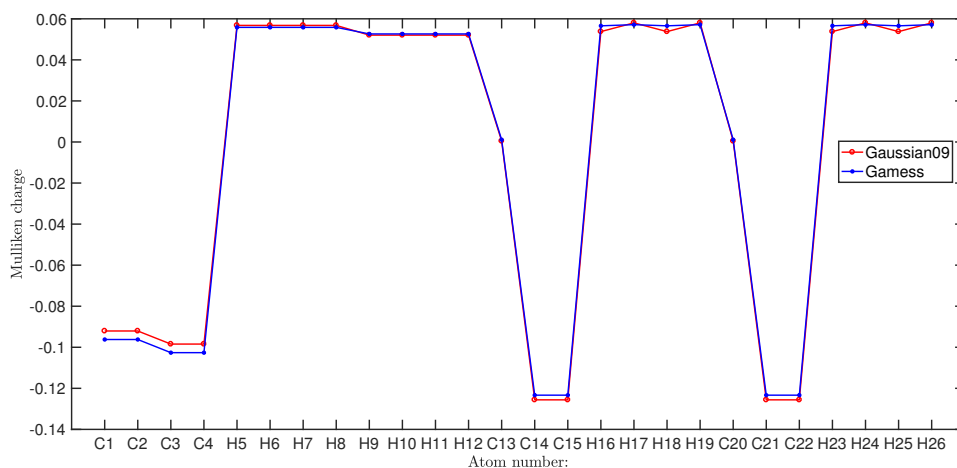
Figure 5.2: Comparison of Mulliken charges for a molecule of Diallyl butane at the equilibrium.
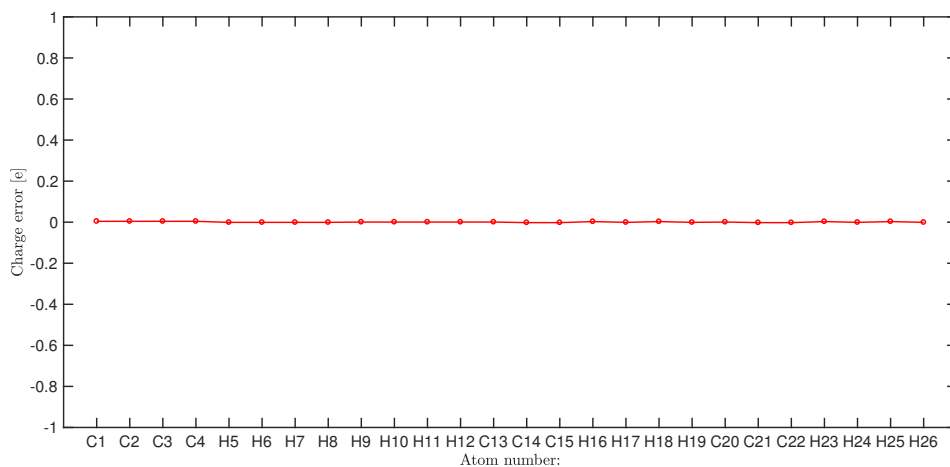
Figure 5.3: Error in che computation of Mulliken charges for a molecule of Diallyl butane at the equilibrium between Gaussian09 and Gamess.

5.3.2 Switching field

In this second case, a switching field of $0.001 \, \mathrm{a\,u} = 0.514 \, \mathrm{V/nm}$ is applied, as shown in Fig. 5.1. Again the results are listed in Appendix B and shown in Fig. 5.4 and 5.5.
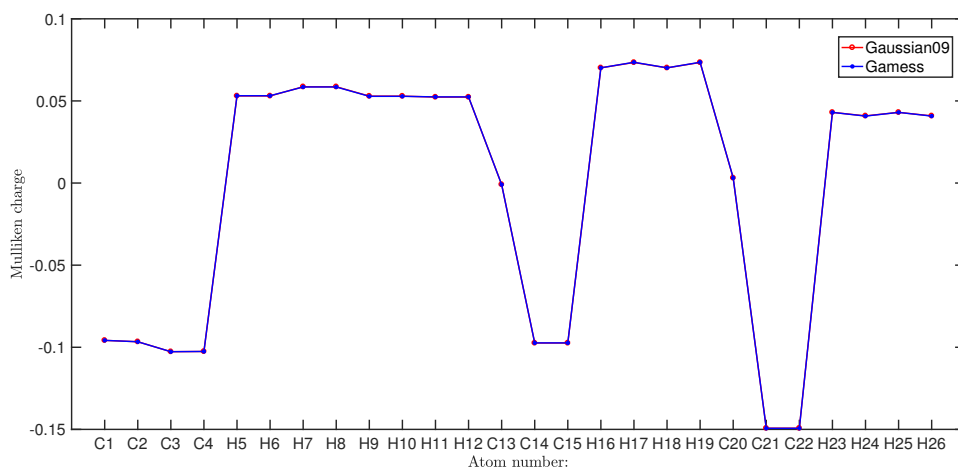
Figure 5.4: Comparison of Mulliken charges for a molecule of Diallyl butane with an external electric field of $0.514 \, \mathrm{V/nm}$.
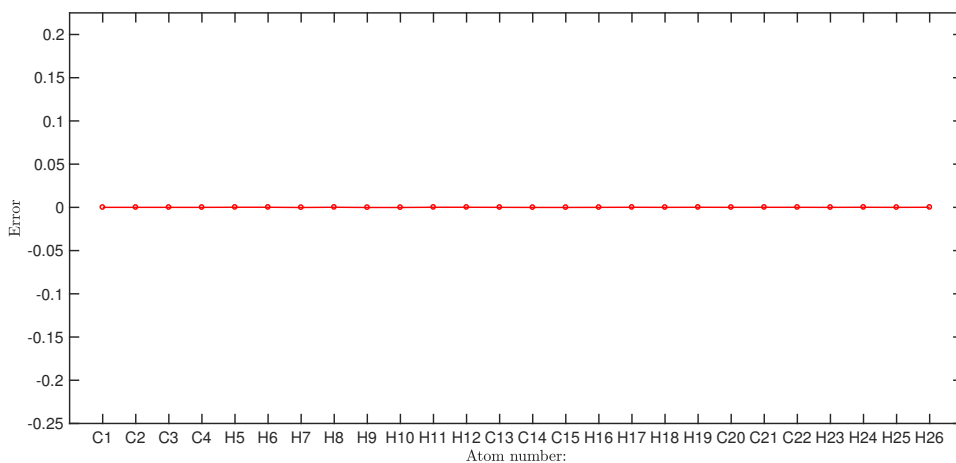
Figure 5.5: Error in che computation of Mulliken charges for a molecule of Diallyl butane with an external electric field of $0.514\,\text{V/nm}$ between Gaussian09 and Gamess.

Here the electrostatic potential at the nuclei is shown, table in Appendix C:
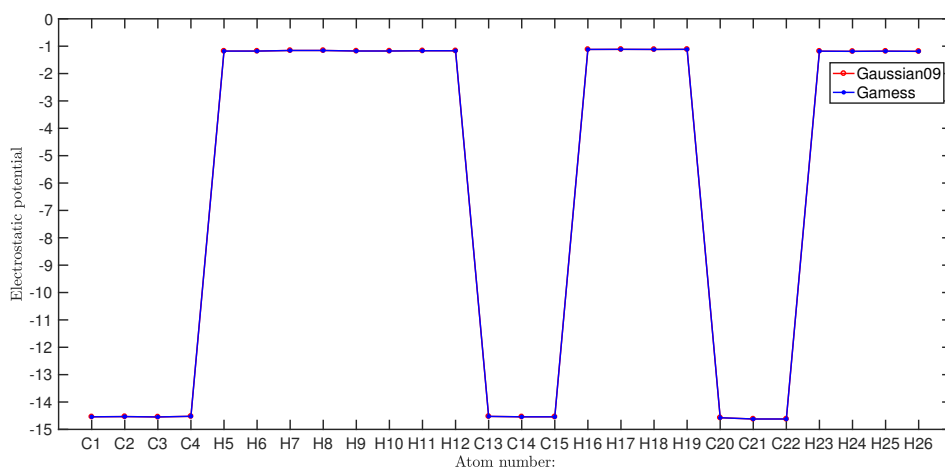
Figure 5.6: Comparison of electrostatic potential for a molecule of Diallyl butane with an external electric field of $0.514\,\text{V/nm}$.
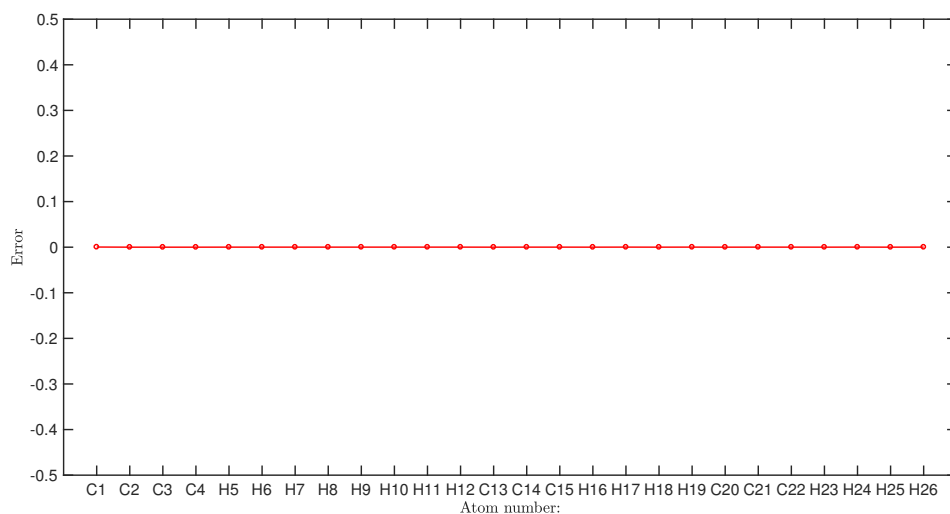
Figure 5.7: Error in che computation of the electrostatic potential for a molecule of Diallyl butane with an external electric field of $0.514\,\mathrm{V/nm}$ between Gaussian09 and Gamess.

5.4 Decatriene

Now, let's consider the second molecule candidate for the QCA technology, Fig. 5.8.
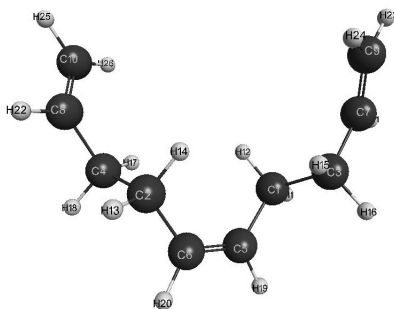
Figure 5.8: Decatriene molecule.

In this second case, we are evaluating the *aggregate charge* instead to the charge for each atom. Tor do this, we have to define the three dots of the Decatriene. Fig. 6.2shows a molecule of Decatriene with the three dots.
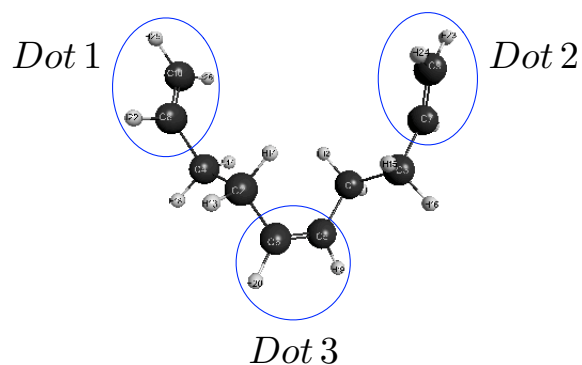
Figure 5.9: Decatriene molecule and dots definition.

Dot 1 is made up of C8, C10, H22, H25 and H26 atoms, Dot 2 is made up of C7, C9, H21, H23 and H24, finally Dot 3 is made up of C5, C6, H19 and H20 atoms, see table 5.1.

	Atoms
Dot 1	C8, C10, H22, H25, H26
Dot 2	C7, C9, H21, H23, H24
Dot 3	C5, C6, H19, H20

Table 5.1: Dots definition.

5.4.1   @ the equilibrium

Once we defined the Dot for the decatriene, we can calculate the charges in every dot of the molecule, as listed in table 5.2:

	Gaussian09	Gamess	Error
Dot 1	0.011968	0.01124	0.000728
Dot 2	0.011974	0.012778	0.000804
Dot 3	0.011974	0.03182	0.00855

Table 5.2: Dot charge comparison for a Decatriene molecule at the equilibrium.
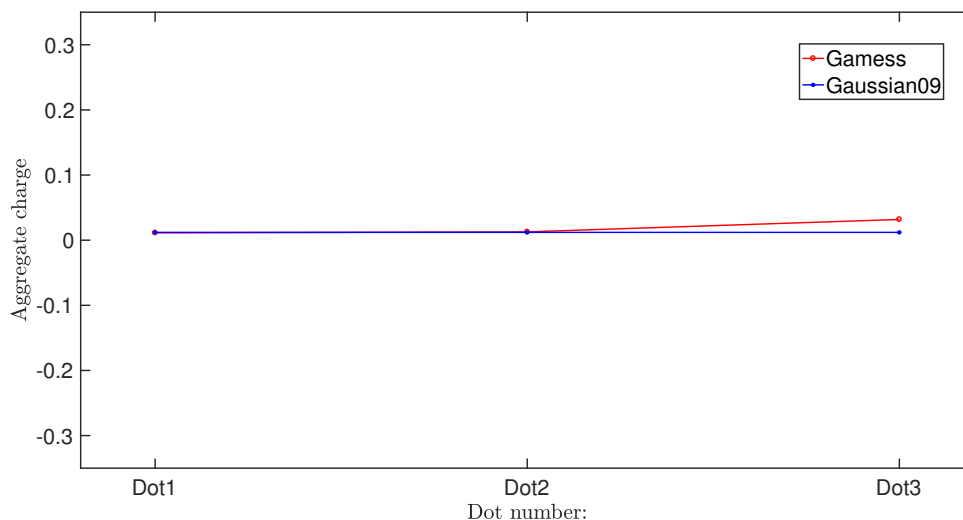
Figure 5.10: Dot charge comparison for a Decatriene molecule at the equilibrium.

5.4.2   Switching field

Now, let's focus on a Decatriene molecule inside a switching field of magnitude of $0.514\,\mathrm{V/nm}$, as seen before for the Dially butane molecule, Fig. 5.11. Again, the Dot charges is listed in the table 5.3.
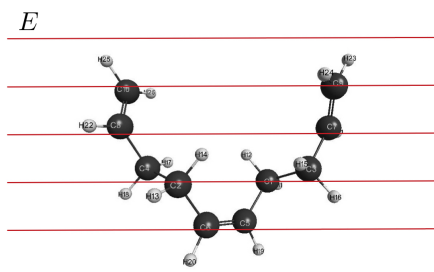
Figure 5.11: Decatriene molecule in presence of a switching field of $0.514\,\mathrm{V/nm}$.

	Gaussian09	Gamess	Error
Dot 1	0.001929	0.003675	0.001746
Dot 2	0.022024	0.01933	0.002694
Dot 3	0.023303	0.031792	0.008489

Table 5.3: Dot charge comparison for a Decatriene molecule with a switching field of $0.514\,\mathrm{V/nm}$.
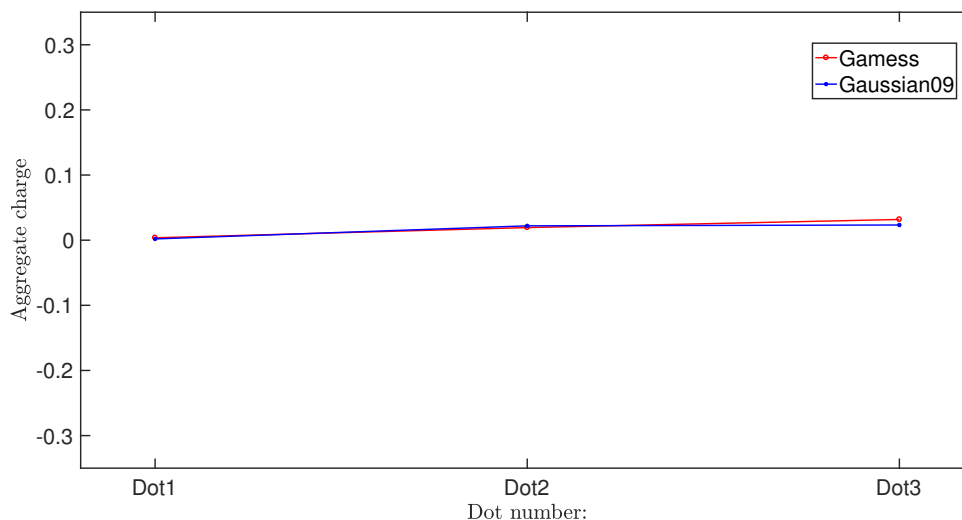
Figure 5.12: Dot charge comparison for a Decatriene molecule with an external electric field of $0.514\,\text{V/nm}$.

5.5 Final considerations

As can be seen from a first analysis, the results obtained from this comparison between GAMESS and gaussian09 are almost identical. Since the molecules are very simple and do not need many steps for SCF convergence, the approximation introduced by the algorithm is negligible. Despite this, the results obtained with Gamess regarding the distribution of the charges in the molecule are not very precise, as we recall that the ESP charges are much more precise. Moreover, during the simulation Gamess creates temporary files much bigger than gaussian09 (in particular for the bis-ferrocene there is a ratio of 32:1) and finally there is no clear and default procedure to handle the ideal point charge, while there is one in gaussian09 and other software. The advantage of Gamess is the ease of use for simulating systems that are not too complex and the fact that it is open source.

69

Chapter 6

Charge distribution

As we said in Chapter 1, a single molecule represents just half a QCA cell, since it has just 2 or 3 dots instead of 4 (for the Diallyl butane) and 6 (for decatriene and bis-ferrocene molecules). In this thesis we have analyzed the properties of half a QCA cell (single molecule) through ab initio simulations.

6.1   Diallyl butane and decatriene

The first molecule that has been analyzed is the Diallyl Butane [21], shown in Fig. 6.1. The two allyl groups represent the dots (circled in the figure) and so they encode the two logic state '0' and '1' depending on where the aggregate charge is localized.

The second molecule analyzed in this work is the decatriene, Fig. 6.2 . It has three dots respect of the diallyl butane, which are ethylene groups. These two molecules have been analyzed in two configurations: neutral and oxidized. By definition "a neutral molecule is a molecule in which the number of electrons surrounding the nuclei is the same as the total number of protons in the nuclei, so that there is no net electric charge" [44] while if the molecule is oxidized it has a free positive charge, that is to say:

$$Total\, charge = \begin{cases} 0 & neutral\, molecule \\ 1 & oxidized\, molecule \end{cases}$$

71
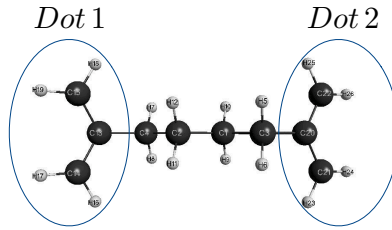
Figure 6.1: Diallyl Butane molecule and dots definition.
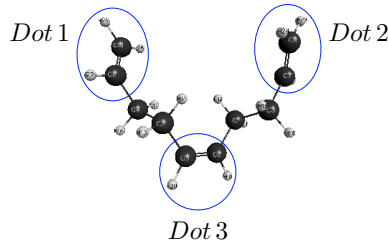
Figure 6.2: Decatriene molecule and dots definition.

6.1.1 Neutral molecules

The diallyl butane and the decatriene neutral molecules, which are ideal molecules for the QCA technology, have been studied in order to evaluate the effects of the switching field and of the point charges on them; in this way we can evaluate the effectiveness of this method on real molecules (the bis-ferrocene).

First, in the Table 6.1, we listed the aggregated charges of Dot1 and Dot2 for the diallyl butane as function of the switching field ($\pm 3 \, \text{V/nm}$). The graph in Fig. 6.3 shows that the molecule, also if it is neutral, has a strong internal charge displacement as a function of the switching field. In particular, we can notice from table 6.1 that the module of the aggregated charges in the two dots is equal and just the sign changes. This means that the diallyl butane is an idea candidate in terms of charge localization for our technology. The problem with this molecule is that we have just 2 dots instead of 3, necessary for the clock.

Switching field [V/nm]	Dot 1	Dot 2
-3.0	0.3115	-0.3476
-2.0	0.2016	-0.2378
-1.0	0.0918	-0.128
0	-0.0181	-0.0181
+1.0	-0.128	0.0918
+2.0	-0.2378	0.2016
+3.0	-0.3476	0.3115

Table 6.1: Diallyl butane molecule: dot charges as function of the switching field.
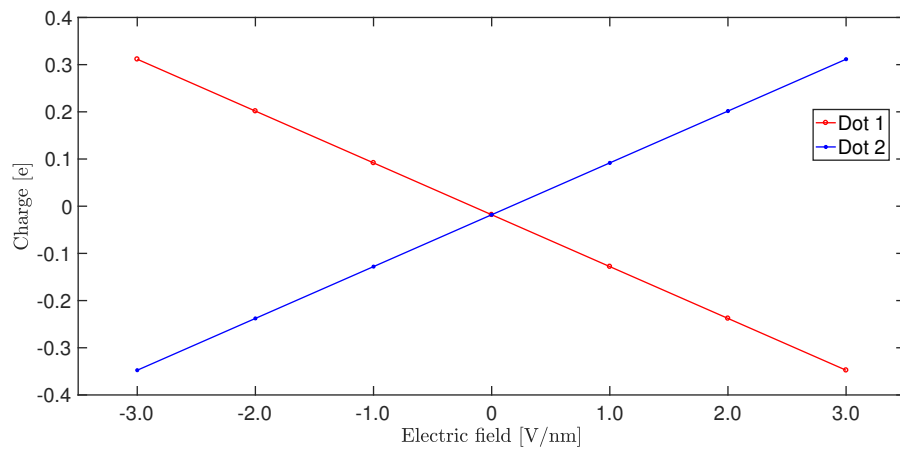
Figure 6.3: Diallyl butane: dot charges as function of the switching field.
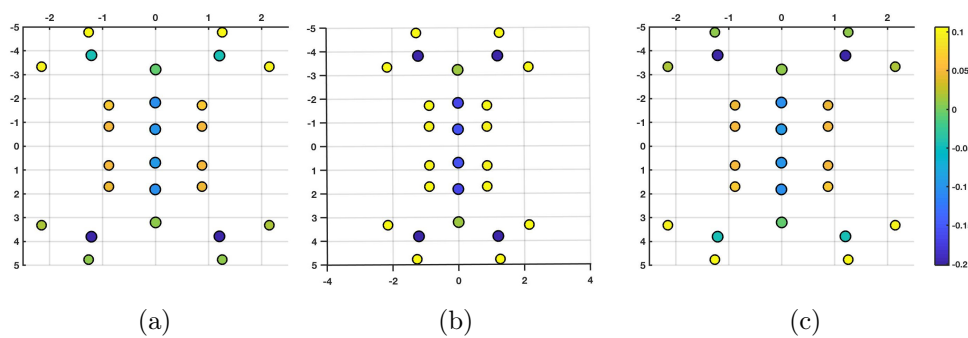
Figure 6.4: Displacement of the charge inside the diallyl butane molecule at the equilibrium (a) and with a switching field of -3 (b) and $+3\,\mathrm{V/nm}$ (c).
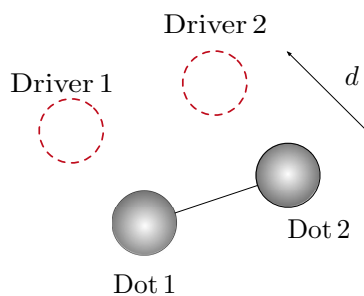
Figure 6.5: Diallyl butane with point charges configuration.

Driver 1	Driver 2	Dot 1	Dot 2
0.1	0.9	0.0512	-0.0858
0.2	0.8	0.0341	-0.0687
0.3	0.7	0.0171	-0.0517
0.4	0.6	≈ 0	-0.0346
0.5	0.5	-0.0170	-0.0175
0.6	0.4	-0.0341	≈ 0
0.7	0.3	-0.0511	0.0166
0.8	0.2	-0.0682	0.0336
0.9	0.1	-0.0852	0.0507

Table 6.2: Diallyl butane molecule : dot charges as function of the driver polarization.
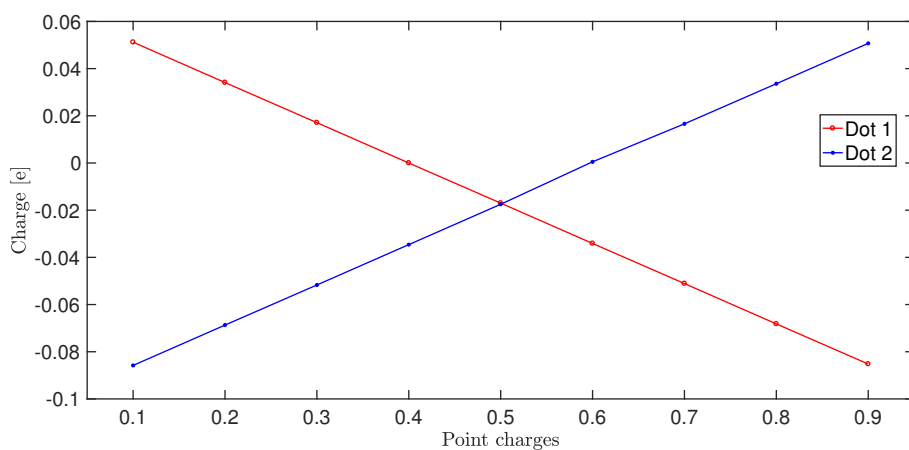
Figure 6.6: Diallyl butane: dot charges as function of the polarization of the driver.

The same type of analysis was done for the neutral decatriene molecule. Also in

74

this case, as shown in the table 6.3and in the Fig. 6.7 the charge values present in Dot1 and Dot2 are almost perfectly symmetrical. The difference with the butane molecule is the presence of the third dot; in fact, in this case all the charge is not in the two dots but is divided among three. This fact will however be clearer when the molecule is oxidized. As we can see in Fig. 6.7 and table 6.3 the charge on the central dot remains almost constant, this is due to the fact that the electric field is parallel to the axis that joins the two dots and therefore the third dot is not affected by it. To interest the third dot on the charge switching, you have to use a *clock field* that is perpendicular to the axis that joins dot1 and 2 and that helps to move the charge present in the third dot in the two dots during the clock phase and to move most of the charge in Dot1 and 2 in the third dot in the relax phase.

Switching field [V/nm]	Dot 1	Dot 2	Dot 3
-4.0	-0.0196	0.0430	0.0334
-3.0	-0.0119	0.0351	0.0328
-2.0	-0.0041	0.0272	0.0323
-1.0	0.0037	0.0193	0.0317
0	0.0115	0.0115	0.0313
+1.0	0.0192	0.0036	0.0308
+2.0	0.0270	-0.0042	0.0305
+3.0	0.0349	-0.0121	0.0301
+4.0	0.0427	-0.0199	0.0298

Table 6.3: Neutral decatriene molecule : dot charges as function of the switching field.
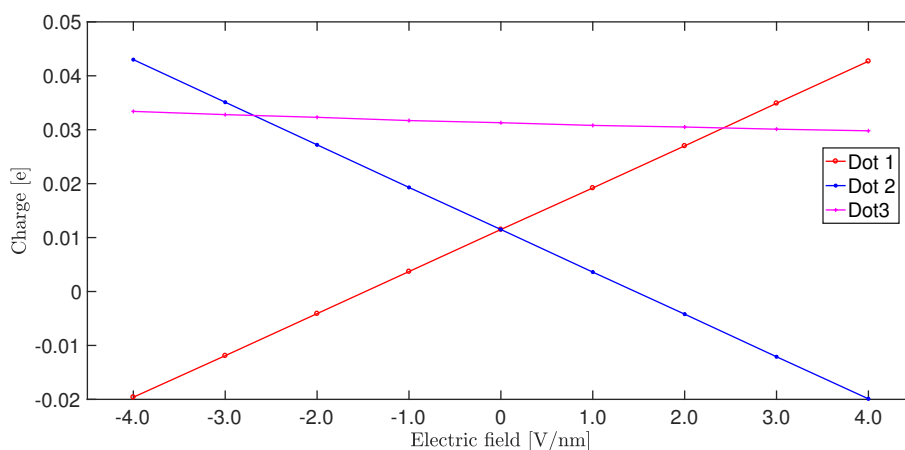
Figure 6.7: Decatriene: dot charges as function of the switching field.

6.1.2 Oxidized molecules

Since in the neutral molecules analyzed up to now the charge that could switch was small, the oxidation technique of a molecule was used. In this way, a charge has been added inside the molecule so that the total charge quantity is 1. As we can see from Fig. 6.8, the oxidized diallyl butane shows a greater charge switching than the neutral molecules and this means a greater V_{out}. The diallyl butane shows the ideal case since there are only two dots; this free charge is distributed equally between them. In this case, as we can see from the Fig. 6.8, the trend of the charge in the molecule undergoes a sharp variation between ± 1 V, this means that a field of 2 V is enough to change the molecule status.

Switching Field [V/nm]	Dot 1	Dot 2
-5.0	-0.0217	0.8651
-4.0	-0.0139	0.8550
-3.0	-0.0060	0.8449
-2.0	0.0018	0.8346
-1.0	0.0097	0.8242
0	0.4358	0.4358
+1.0	0.8242	0.0097
+2.0	0.8346	0.0018
+3.0	0.8449	-0.0060
+4.0	0.8550	-0.0139
+5.0	0.8651	-0.0217

Table 6.4: Oxidized Diallyl butane molecule : dot charges as function of the switching field.
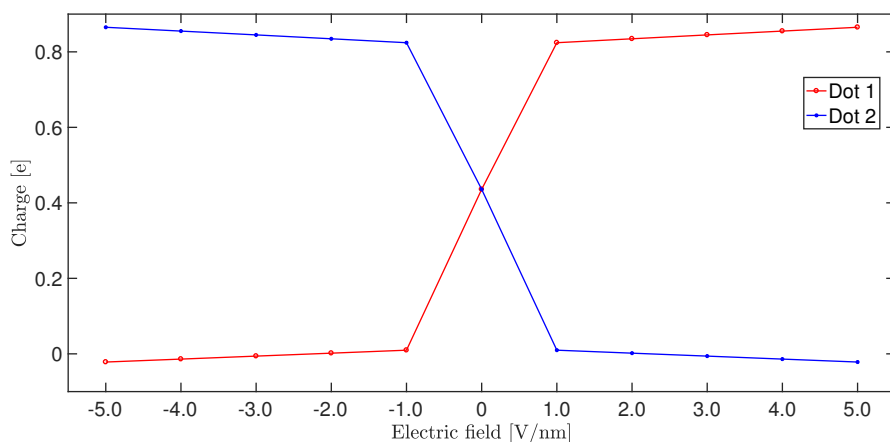
Figure 6.8: Oxidizied diallyl butane: dot charges as function of the switching field.

For the Decatriene molecule, and as we will also see for the bis-ferrocene, the same does not happen. In this case, because of the greater complexity of the molecule due to the presence of the third dot, the extra free charge is not equally distributed. To be precise it goes almost entirely on the third dot, making the switch almost equal to the case of the neutral molecule. As can be seen from the gaussian graph instead [35], Fig. 6.9

this distributed the charge in the two active dots and therefore the molecule switch was much better for our purposes. In reality, where to put the extra charge is in no way manageable by us but it is the software, through an energy simulation, to understand where to put it to minimize the energy of the molecule and therefore make it more stable.
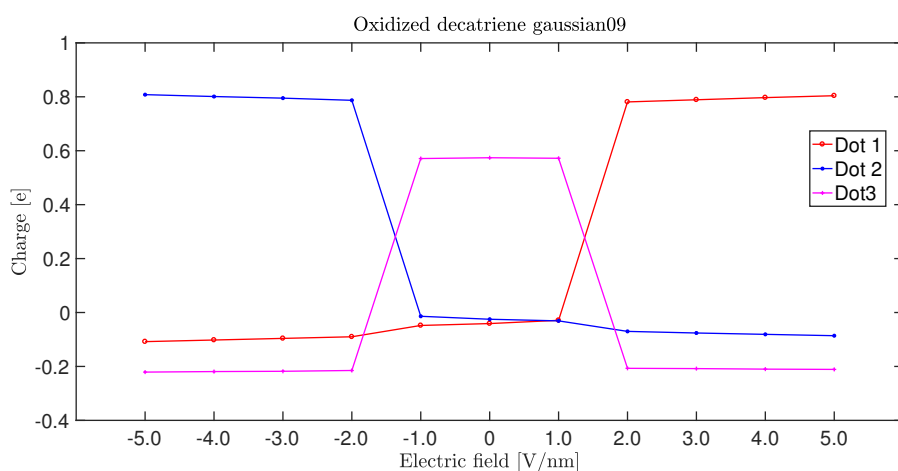
Figure 6.9: Oxidizied decatriene: dot charges as function of the switching field [35].

Fig. 6.10 shows the comparison between the HOMO, HOMO-1 and HOMO-2 orbitals of the neutral or oxidized decatriene. As you can see, the HOMO orbital (which is where the extra charge of oxidation goes) is present only in the third dot.

(a) Neutral HOMO

(b) Neutral HOMO-1

(c) Neutral HOMO-2

(d) Oxidized HOMO

(e) Oxidized HOMO-1

(f) HOMO-2
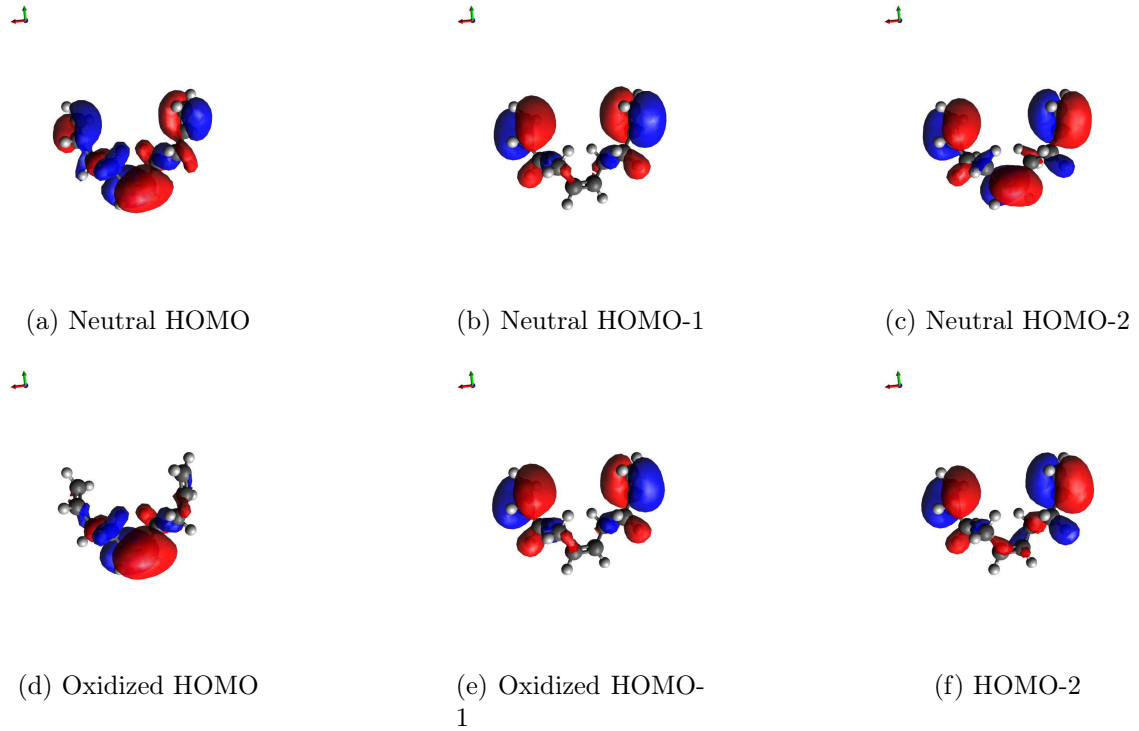
Figure 6.10: HOMO visualization in a decatriene molecule.

Switching Field [V/nm]	Dot 1	Dot 2	Dot 3
-4.0	0.1629	0.0864	0.4923
-3.0	0.1522	0.0954	0.4956
-2.0	0.1421	0.1044	0.4982
-1.0	0.1324	0.1134	0.5003
0	0.1230	0.1227	0.5020
+1.0	0.1138	0.1321	0.5034
+2.0	0.1048	0.1418	0.5043
+3.0	0.0959	0.1520	0.5048
+4.0	0.0870	0.1628	0.5048

Table 6.5: Oxidized decatriene molecule : dot charges (mulliken) as function of the switching field.
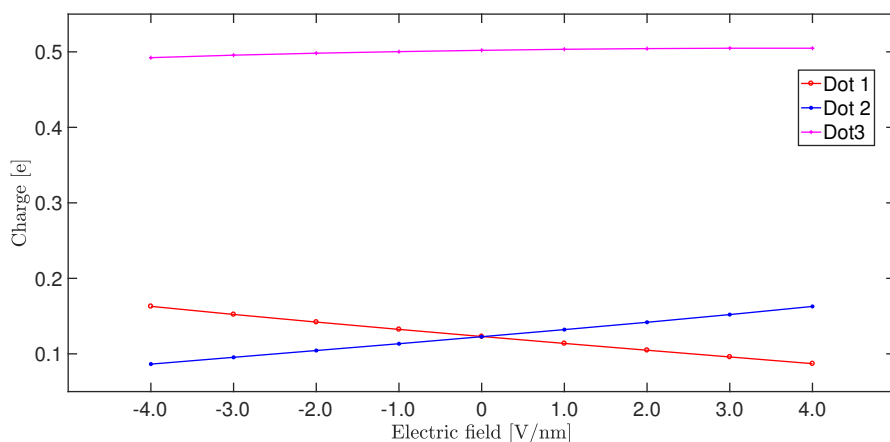
Figure 6.11: Oxidized decatriene: dot charges as function of the switching field.

In Fig. 6.13 and in table 6.6 the results of the simulation are shown with the write-in system. As already explained in Chapter 3, the two ideal charge points are placed at the distance d equal to the distance between the two active dots of the molecule. All the possible values between 0 and 1 for the two charge points were taken into consideration so that the total charge of the driver is equal to 1. Again, the graph is symmetrical and a better switch is obtained than in the case of the switching field. This is due to the fact that, unlike the electric field which is directed parallel to the axis between the two dots, the charge points create an electric field in all directions, ??as shown in figure 22??, this means that there will be a component of this electric field that moves the charge from the third dots to one of the two active dots.
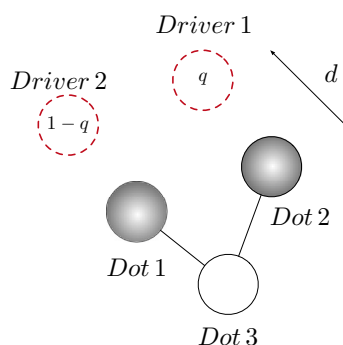
Figure 6.12: Oxidized decatriene with point charges configuration.

79

Driver 1	Driver 2	Dot 1	Dot 2	Dot 3
0.0	1.0	0.1050	0.8035	0.0154
0.1	0.9	0.1024	0.8054	0.0159
0.2	0.8	0.1855	0.1762	0.4712
0.3	0.7	0.1840	0.1766	0.4720
0.4	0.6	0.1827	0.1771	0.4723
0.5	0.5	0.1815	0.1778	0.4723
0.6	0.4	0.1805	0.1786	0.4718
0.7	0.3	0.1797	0.1796	0.4710
0.8	0.2	0.1791	0.1807	0.4698
0.9	0.1	0.8068	0.0980	0.0143
1.0	0.0	0.8046	0.1003	0.0136

Table 6.6: Oxidized decatriene molecule : dot charges as function of the driver polarization.
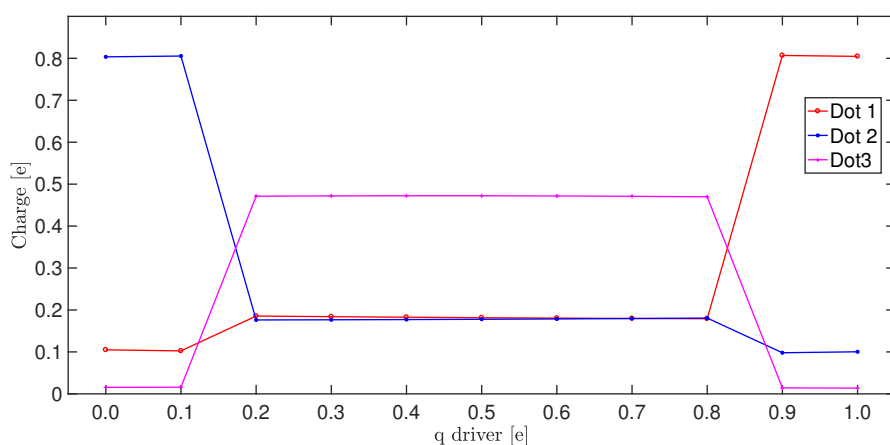
Figure 6.13: Oxidized decatriene: dot charges as function of the polarization of the driver.

6.2 The bis-ferrocene molecule

6.2.1 Neutral molecule

What has been done up to now for ideal but not synthesizable molecules such as diallyl butane and decatriene will be repeated now for the bis-ferrocene molecule. This molecule, as already mentioned, has already been synthesized by the PoliTo in

collaboration with the University of Bologna and it is the most promising molecule for QCA technology.

Also in this case, a first optimization simulation of the geometry of the neutral molecule was performed, in this case with the base *6,31g (d, p),* which is a basis with polarization functions on both heavy and light atoms. Unlike the two previous molecules, which had only 26 atoms between carbon and hydrogen, this molecule in its version without thiol has 72 atoms, including two iron atoms and one of nitrogen. This fact causes that a single optimization simulation to last from 8 to 12 days, depending on whether it is neutral or oxidized. As can be seen from table 6.7 and Fig. 6.14, in its neutral form, this molecule behaves exactly like the ideal molecules. The switch is almost perfectly symmetrical and the charge on the third dot (carbazole) is almost 0. Since even in this case the switch is not very strong we need to oxidize the molecule.

Switching Field [V/nm]	Dot 1	Dot 2	Dot 3
-5.0	0.0676	-0.0702	0.0026
-4.0	0.0540	-0.0561	0.0021
-3.0	0.0403	-0.0421	0.0018
-2.0	0.0267	-0.0282	0.0015
-1.0	0.0144	-0.0130	0.0014
0	0	0	0.0013
+1.0	-0.0144	0.0130	0.0014
+2.0	-0.0282	0.0266	0.0015
+3.0	-0.0420	0.0403	0.0018
+4.0	-0.0546	0.0546	0.0021
+5.0	-0.0686	0.0686	0.0026

Table 6.7: Neutral bis-ferrocene molecule : dot charges (mulliken) as function of the switching field.
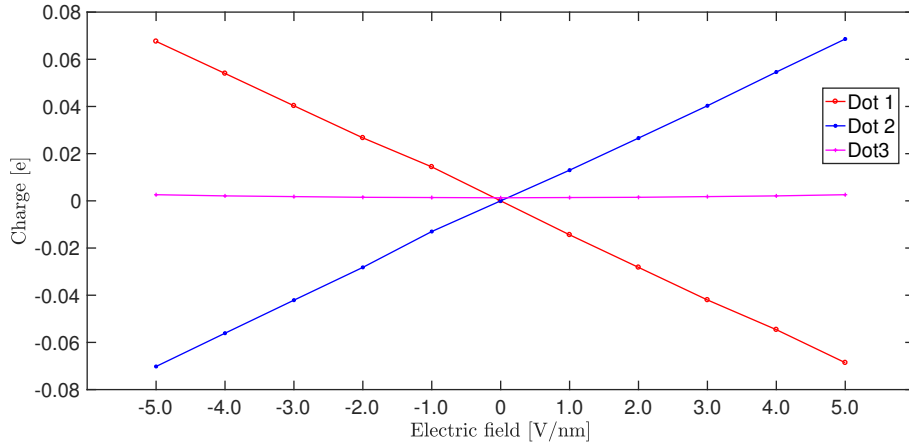
Figure 6.14: Neutral bis-ferrocene: dot charges as function of the switching field.

6.2.2 Oxidized molecule

For the bis-ferrocene, like for the decatriene, the extra charge obtained by oxidizing the molecule is not equally distributed between the two active dots as we hoped. Indeed, in this case, the extra charge is almost completely distributed on just one of the two active dots, practically polarizing the molecule. This behavior by the simulator causes the molecule to already codify a logical state to equilibrium and an electric field of $5\,\mathrm{V/nm}$ is required to change the state to the molecule.

	Dot 1	Dot 2	Dot 3
neutral	0	0	0.0013
oxidized	0.0163	0.9154	0.0683

Table 6.8: Comparison between neutral and oxidized bis-ferrocene molecule : dot charges (mulliken) at the equilibrium.
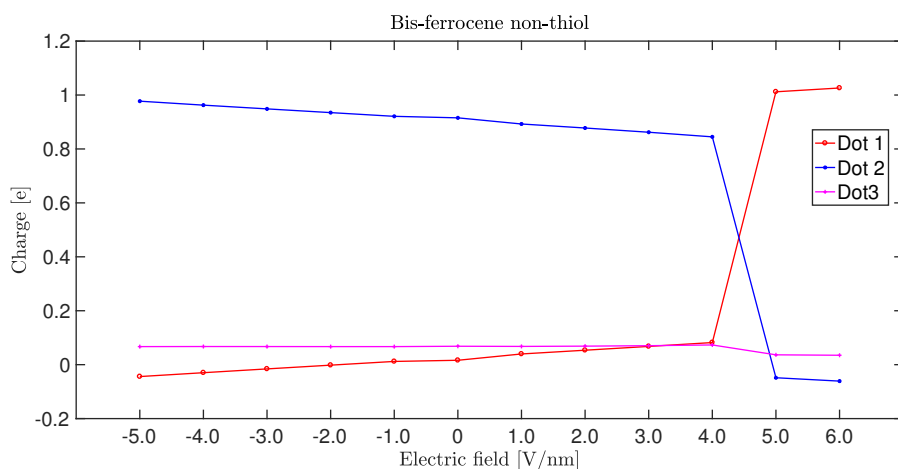
Figure 6.15: Oxidized bis-ferrocene: dot charges as function of the switching field.

Switching Field [V/nm]	Dot 1	Dot 2	Dot 3
-6.0	1.0261	-0.0610	0.0349
-5.0	1.0120	-0.0485	0.0365
-4.0	0.0820	0.8449	0.0731
-3.0	0.0677	0.8620	0.0704
-2.0	0.0536	0.8777	0.0687
-1.0	0.0397	0.8926	0.0677
0	0.0163	0.9154	0.0683
+1.0	0.0120	0.9210	0.0670
+2.0	-0.0018	0.9348	0.0670
+3.0	-0.0157	0.9486	0.0672
+4.0	-0.0298	0.9625	0.0673
+5.0	-0.0441	0.9772	0.0670

Table 6.9: Oxidized bis-ferrocene molecule : dot charges (mulliken) as function of the switching field.

Author in [35] did the same simulation with gaussian09 but with the base LANL2DZ. The results of this simulation are shown in the figure. To compare the results correctly, it would have been necessary to re-propose the exact same simulation on gamess, but this base is not present in its basis-set. It was then tried to manually build this base, however with this base the SCF did not converge.
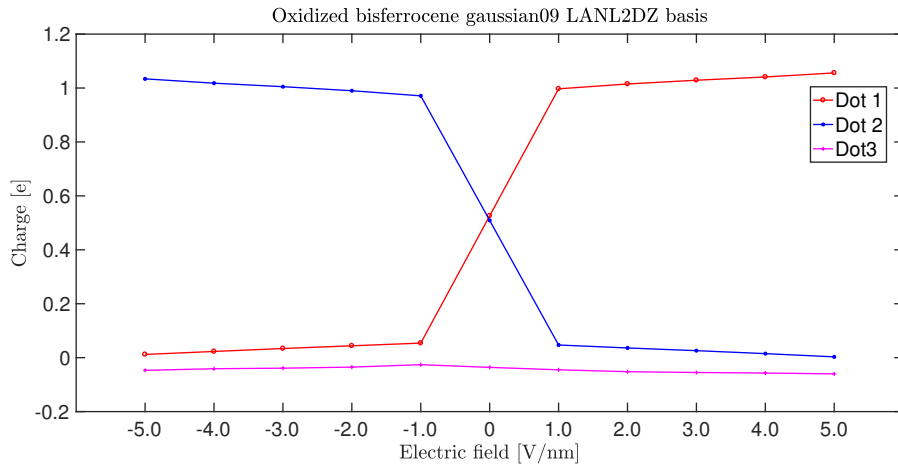
Figure 6.16: Oxidized bis-ferrocene: dot charges as function of the switching field in gaussian09 [35].

The behaviour of the molecule in presence of two point charges is shown in Fig. 6.17. Since the molecule switches with a switching field of $5\,V/nm$, in this case the molecule can't switch. This is due to the fact that two point charges creae a potential difference of $\pm0.5\,V$.
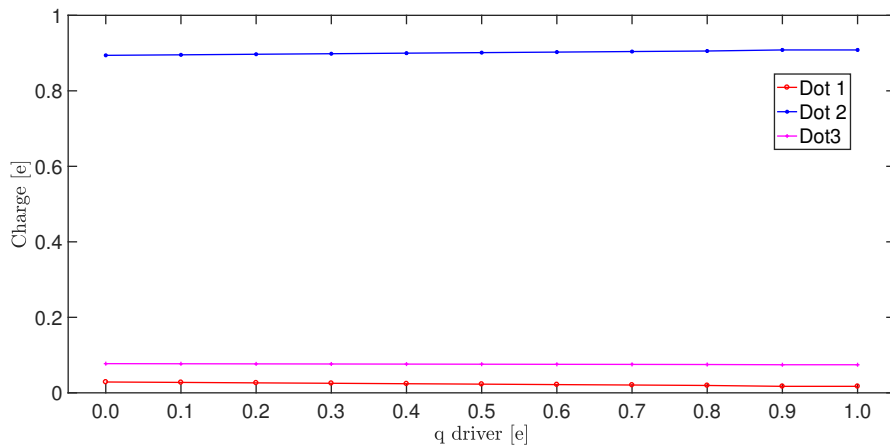
Figure 6.17: Oxidized bis-ferrocene: dot charges as function of the driver's polarization.

Driver 1	Driver 2	Dot 1	Dot 2	Dot 3
0.0	1.0	0.0287	0.8940	0.0773
0.1	0.9	0.0276	0.8954	0.0770
0.2	0.8	0.0264	0.8969	0.0767
0.3	0.7	0.0253	0.8983	0.0764
0.4	0.6	0.0241	0.8998	0.0761
0.5	0.5	0.0230	0.9012	0.0758
0.6	0.4	0.0218	0.9026	0.0755
0.7	0.3	0.0207	0.9041	0.0753
0.8	0.2	0.0195	0.9055	0.0750
0.9	0.1	0.0172	0.9083	0.0744
1.0	0.0	0.0172	0.9083	0.0744

Table 6.10: Oxidized decatriene molecule : dot charges as function of the driver polarization.

6.3   Clocked molecule

The clock field is used to move the charge present in the third dot in the two active dots to make the switch more efficient; on the contrary for the relax phase where an electric field of opposite sign is needed. In this case the clock field has a positive sign, but this obviously depends on the orientation of the molecule in the space, which changes from software to software.
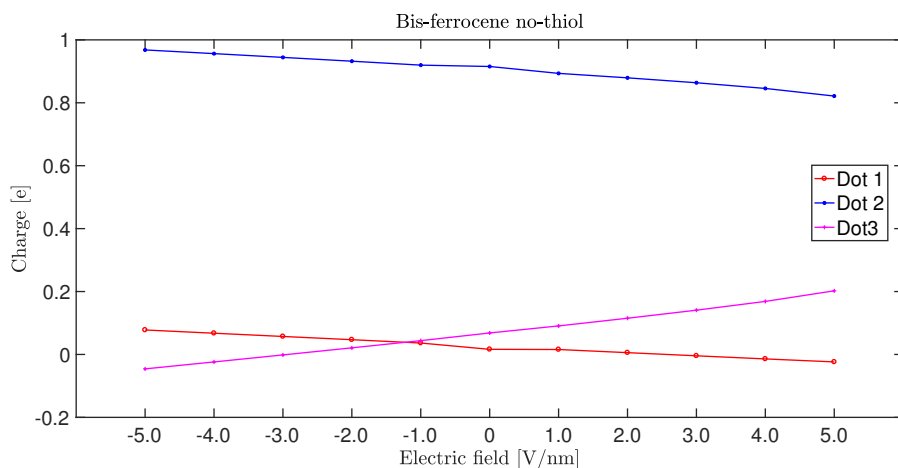
Figure 6.18: Oxidized bis-ferrocene: dot charges as function of the clock field.

Clock Field [V/nm]	Dot 1	Dot 2	Dot 3
-5.0	-0.0237	0.8214	0.2023
-4.0	-0.0142	0.8456	0.1686
-3.0	-0.0043	0.8637	0.1407
-2.0	0.0057	0.8793	0.1151
-1.0	0.0157	0.8935	0.0907
0	0.0163	0.9154	0.0683
+1.0	0.0363	0.9197	0.0439
+2.0	0.0469	0.9322	0.0210
+3.0	0.0572	0.9443	-0.0015
+4.0	0.0675	0.9563	-0.0238
+5.0	0.0778	0.9680	-0.0459

Table 6.11: Oxidized bis-ferrocene molecule : dot charges (mulliken) as function of the clock field.

The behaviour of the charge in the three dots are shown in Fig. 6.18. As we can notice, the value of $5\,\mathrm{V/nm}$ is not sufficient to move the charge from the two active dots to the third one. In particular, in this case a clock field of $10\,\mathrm{V/nm}$ is needed.

Figure 6.19: Bis-ferrocene oxidized scheme: at the equilibrium (a), with a clock field of $10\,\mathrm{V/nm}$ (b).

6.4 V_{out}

Authors in [35], [39] defined the *output voltage* V_{out}: this parameter is calculated as a difference voltage $V_2 - V_1$ imagining to place a receiver at a distance equal to the distance between the two active dots, which is for the diallyl butane $0.7\,\mathrm{nm}$, as shown in the Fig. 6.20. The algorithm for this calculation was developed in MATLAB and says that for every charges in a molecule $\{q_1, q_2, ..., q_N\}$ and their position in the space $\{P_1, P_2, ..., P_N\}$, the electric potential at distance d is equal to:
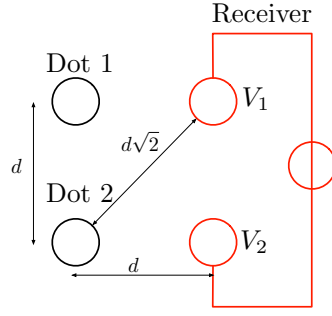
Figure 6.20: Molecule - receiver scheme.

$$V\left(\vec{d}\right) = \frac{1}{4\pi\varepsilon_0}\left(\frac{q_1}{\mid P_1 - \vec{d}\mid} + ... + \frac{q_N}{\mid P_2 - \vec{d}\mid}\right) \tag{6.1}$$

In the case shown in Fig. 6.20, if we consider the active dots as point charges, we have:

$$V_1 = \frac{1}{4\pi\varepsilon_0 \cdot d}\left(q_1 + \frac{q_2}{\sqrt{2}}\right) \tag{6.2}$$

$$V_2 = \frac{1}{4\pi\varepsilon_0 \cdot d}\left(\frac{q_1}{\sqrt{2}}_1 + q_1\right) \tag{6.3}$$
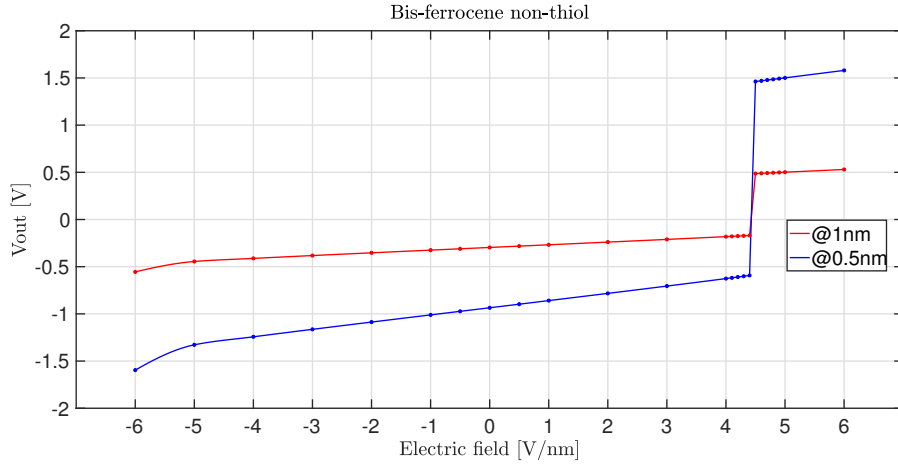
Figure 6.21: V_{out} in function of the switching field at distance of 1 nm and 0.5 nm.

The V_{out} characteristic in function of the switching field is shown in Fig. 6.21. The ideal receiver is set at a distance of 1 nm and 0.5 nm. In these cases, the V_{out}

is included between $\pm 0.5\,\mathrm{V/nm}$ and $\pm 1.5\,\mathrm{V/nm}$. The sign of V_{out} changes for a switching field of $4.5\,\mathrm{V/nm}$, as for the mulliken charges. In particular we don't have potential for a switching field of $4.5\,\mathrm{V/nm}$ since the simulation doesn't converge.

Chapter 7

Conclusions and future study

In conclusion, GAMESS is a good software for ab-initio simulations, also if it has some shortcomings. In particular, the absence of a default action for the point charges is really disabling for future works. In fact, in this work we used some tricks to simulate them and this produced some errors in the evaluation of the system energy.

Future studies could be to understand how GAMESS handles the oxidation of a molecule and the differences with gaussian09, to look for a new basis that can reproduce the simmetry of the bis-ferrocene molecule, as for gaussian09. It could be interesting to study the molecules in a dynamic point of wiev (introducing time also during the switch), to study a complete QCA cell and to see how the molecules interacts with each other and finally analyzing a QCA wire and its consumption in terms of power and energy.

After this, some logic component can be studied and analyzed.

Appendix A

Mulliken charge comparison

Atom	Gaussian09	Gamess	Error
C1	-0.092065	-0.096216	0.004151
C2	-0.092065	-0.096216	0.004151
C3	-0.098441	-0.102622	0.004181
C4	-0.098441	-0.102622	0.004181
H5	0.056792	0.055832	-0.00096
H6	0.056784	0.055831	-0.000953
H7	0.056792	0.055832	-0.00096
H8	0.056784	0.055831	-0.000953
H9	0.052050	0.052632	0..000582
H10	0.052048	0.052632	0.000584
H11	0.052050	0.052632	0.000582
H12	0.052048	0.052632	0.000584
C13	0.000463	0.001109	0.000646
C14	-0.125606	-0.123333	-0.002273
C15	-0.125615	-0.123332	-0.002283
H16	0.053773	0.056583	0.00281
H17	0.058023	0.057151	-0.000872
H18	0.053769	0.056582	0.002813
H19	0.058026	0.057151	-0.000875
C29	0.000463	0.001109	0.000646
C21	-0.125606	-0.123333	-0.002273
C22	-0.125615	-0.123332	-0.002283
H23	.053773	0.056583	0.00281
H24	0.058023	0.057151	-0.000872
H25	0.053769	0.056582	0.002813
H26	0.058026	0.057151	-0.000875

Table A.1: Mulliken charge comparison for a Diallyl butane molecule at the equilibrium.

Atom	Gaussian09	Gamess	Error
C1	-0.095807	-0.095791	0.000016
C2	-0.096626	-0.096643	0.000017
C3	-0.102682	-0.102695	0.000013
C4	-0.102557	-0.102545	-0.000012
H1	0.053031	0.053162	0.000131
H2	0.053030	0.053161	0.000131
H3	0.058627	0.058496	-0.000131
H4	0.058626	0.058494	0.000132
H5	0.052926	0.052801	-0.000125
H6	0.052927	0.052802	-0.000125
H7	0.052337	0.052462	0.000125
H8	0.052335	0.052460	0.000125
C5	-0.000895	-0.000932	0.000037
C6	-0.097411	-0.097333	-0.000078
C7	-0.097408	-0.097330	-0.000078
H9	0.070150	0.070154	0.000004
H10	0.073413	0.073538	0.000125
H11	0.070147	0.070151	0.000004
H12	0.073412	0.073538	0.000126
C8	0.003113	0.003151	0.000038
C9	-0.149272	-0.149350	0.000078
C10	-0.149269	-0.149347	0.000078
H13	0.043031	0.043028	-0.000003
H14	0.040894	0.040769	0.000125
H15	0.043031	0.043028	-0.000003
H16	0.040894	0.040769	0.000125

Table A.2: Mulliken charge comparison with an external electric field of 0.5 V/nm

Appendix B

Electric potential comparison with an external electric field of $0.5\,\mathrm{V/nm}$.

Atom	Gaussian09	Gamess	Error
C1	-14.540419	-14.540452	0.00033
C2	-14.532074	-14.532042	0.000032
C3	-14.545358	-14.545338	0.00002
C4	-14.522107	-14.522128	0.000021
H1	-1.179047	-1.178929	0.000118
H2	-1.179049	-1.178931	0.000118
H3	-1.156583	-1.156700	0.000117
H4	-1.156584	-1.156701	0.000117
H5	-1.176205	-1.176340	0.000135
H6	-1.176205	-1.176340	0.000135
H7	-1.166866	-1.166731	0.000135
H8	-1.166865	-1.166730	0.000135
C5	-14.525094	-14.525053	0.000041
C6	-14.540743	-14.540626	0.000117
C7	-14.540745	-14.540627	0.000118
H9	-1.118863	-1.118802	0.000061
H10	-1.115423	-1.115252	0.000171
H11	-1.118865	-1.118804	0.000061
H12	-1.115423	-1.115252	0.000171
C8	-14.573726	-14.573768	0.000042
C9	-14.620710	-14.620828	0.000118
C10	-14.620710	-14.620828	0.000118
H13	-1.181810	-1.181870	0.00006
H14	-1.188241	-1.188412	0.000171
H15	-1.181807	-1.181867	0.00006
H16	-1.188239	96-1.188410	0.000171

Appendix C

Input file for Gamess

C.1 Diallyl butane input files

C.1.1 Neutral at the equilibrium

```
$BASIS  GBASIS=STO NGAUSS=3 $END
$CONTRL  SCFTYP=UHF RUNTYP=OPTIMIZE COORD=ZMT $END
$STATPT  OPTTOL=0.0001 NSTEP=20 $END

$DATA
Title
C1
C
C     1     B1
C     1     B2     2     A1
C     2     B3     1     A2     3     D1
H     3     B4     1     A3     2     D2
H     3     B5     1     A4     2     D3
H     4     B6     2     A5     1     D4
H     4     B7     2     A6     1     D5
H     1     B8     2     A7     4     D6
H     1     B9     2     A8     4     D7
H     2     B10    1     A9     3     D8
H     2     B11    1     A10    3     D9
C     4     B12    2     A11    1     D10
C     13    B13    4     A12    2     D11
C     13    B14    4     A13    2     D12
H     14    B15    13    A14    4     D13
H     14    B16    13    A15    4     D14
H     15    B17    13    A16    4     D15
H     15    B18    13    A17    4     D16
C     3     B19    1     A18    2     D17
C     20    B20    3     A19    1     D18
C     20    B21    3     A20    1     D19
H     21    B22    20    A21    3     D20
H     21    B23    20    A22    3     D21
H     22    B24    20    A23    3     D22
H     22    B25    20    A24    3     D23

   B1                1.54219718
   B2                1.54715028
```

97

B3	1.54715028
B4	1.08772095
B5	1.08771964
B6	1.08772095
B7	1.08771964
B8	1.08843697
B9	1.08843680
B10	1.08843697
B11	1.08843680
B12	1.53585525
B13	1.37770630
B14	1.37772504
B15	1.08001478
B16	1.08038854
B17	1.08001487
B18	1.08038819
B19	1.53585525
B20	1.37770630
B21	1.37772504
B22	1.08001478
B23	1.08038854
B24	1.08001487
B25	1.08038819
A1	112.18495797
A2	112.18495797
A3	109.25301425
A4	109.25298930
A5	109.25301425
A6	109.25298930
A7	109.48180141
A8	109.48122967
A9	109.48180141
A10	109.48122967
A11	111.24431029
A12	118.62285258
A13	118.61999817
A14	121.66720440
A15	121.41761015
A16	121.66666901
A17	121.41779191
A18	111.24431029
A19	118.62285258
A20	118.61999817
A21	121.66720440
A22	121.41761015
A23	121.66666901
A24	121.41779191
D1	180.00000000
D2	−58.69919355
D3	58.71180363
D4	−58.69919355
D5	58.71180363
D6	−58.61861781
D7	58.61814219
D8	−58.61861781
D9	58.61814219
D10	−179.99339158
D11	−88.92015591
D12	88.87856924
D13	−2.31385877
D14	178.35611866
D15	2.31545807
D16	−178.35545484

```
   D17          −179.99339158
   D18           −88.92015591
   D19            88.87856924
   D20            −2.31385877
   D21           178.35611866
   D22             2.31545807
   D23          −178.35545484

$END
```

C.1.2 Neutral with the switching field

```
$BASIS GBASIS=STO NGAUSS=3 $END
$CONTRL SCFTYP=UHF RUNTYP=FFIELD COORD=ZMT MAXIT =200 ICHARG=1
MULT=2 $END
$SCF CONV=1d−5 $END
$STATPT OPTTOL=0.0001 NSTEP=20 $END
$EFIELD EVEC(1)=−0.006,0,0 $END

$DATA
Title
 C1

 C
 C      1     B1
 C      1     B2      2      A1
 C      2     B3      1      A2      3      D1
 H      3     B4      1      A3      2      D2
 H      3     B5      1      A4      2      D3
 H      4     B6      2      A5      1      D4
 H      4     B7      2      A6      1      D5
 H      1     B8      2      A7      4      D6
 H      1     B9      2      A8      4      D7
 H      2     B10     1      A9      3      D8
 H      2     B11     1      A10     3      D9
 C      4     B12     2      A11     1      D10
 C     13     B13     4      A12     2      D11
 C     13     B14     4      A13     2      D12
 H     14     B15    13      A14     4      D13
 H     14     B16    13      A15     4      D14
 H     15     B17    13      A16     4      D15
 H     15     B18    13      A17     4      D16
 C      3     B19     1      A18     2      D17
 C     20     B20     3      A19     1      D18
 C     20     B21     3      A20     1      D19
 H     21     B22    20      A21     3      D20
 H     21     B23    20      A22     3      D21
 H     22     B24    20      A23     3      D22
 H     22     B25    20      A24     3      D23

   B1           1.54219718
   B2           1.54715028
   B3           1.54715028
   B4           1.08772095
   B5           1.08771964
   B6           1.08772095
   B7           1.08771964
   B8           1.08843697
   B9           1.08843680
   B10          1.08843697
   B11          1.08843680
   B12          1.53585525
   B13          1.37770630
```

99

```
B14             1.37772504
B15             1.08001478
B16             1.08038854
B17             1.08001487
B18             1.08038819
B19             1.53585525
B20             1.37770630
B21             1.37772504
B22             1.08001478
B23             1.08038854
B24             1.08001487
B25             1.08038819
A1            112.18495797
A2            112.18495797
A3            109.25301425
A4            109.25298930
A5            109.25301425
A6            109.25298930
A7            109.48180141
A8            109.48122967
A9            109.48180141
A10           109.48122967
A11           111.24431029
A12           118.62285258
A13           118.61999817
A14           121.66720440
A15           121.41761015
A16           121.66666901
A17           121.41779191
A18           111.24431029
A19           118.62285258
A20           118.61999817
A21           121.66720440
A22           121.41761015
A23           121.66666901
A24           121.41779191
D1            180.00000000
D2            −58.69919355
D3             58.71180363
D4            −58.69919355
D5             58.71180363
D6            −58.61861781
D7             58.61814219
D8            −58.61861781
D9             58.61814219
D10          −179.99339158
D11           −88.92015591
D12            88.87856924
D13            −2.31385877
D14           178.35611866
D15             2.31545807
D16          −178.35545484
D17          −179.99339158
D18           −88.92015591
D19            88.87856924
D20            −2.31385877
D21           178.35611866
D22             2.31545807
D23          −178.35545484

$END
```

C.1.3   Neutral with the driver

```
$BASIS GBASIS=STO NGAUSS=3 $END
$CONTRL SCFTYP=UHF RUNTYP=ENERGY COORD=CART UNITS=BOHR
MAXIT =200 ICHARG=1 MULT=2 $END
$STATPT OPTTOL=0.0001 NSTEP=20 $END
$SYSTEM MWORDS=50 $END

 $DATA
 Title
C1
C   6.0     1.3332368711     −0.0002526451     −0.5880556204
C   6.0    −1.3332368711     −0.0002526451      0.5880556204
C   6.0     3.4358660887     −0.0002526451      1.4434251503
C   6.0    −3.4358660887     −0.0002526451     −1.4434251503
H   1.0     3.2227946107      1.6578397290      2.6394134677
H   1.0     3.2230477325     −1.6585651191      2.6391490900
H   1.0    −3.2227946107      1.6578397290     −2.6394134677
H   1.0    −3.2230477325     −1.6585651191     −2.6391490900
H   1.0     1.5533761233     −1.6556908607     −1.7887575775
H   1.0     1.5533514007      1.6551827736     −1.7887654158
H   1.0    −1.5533761233     −1.6556908607      1.7887575775
H   1.0    −1.5533514007      1.6551827736      1.7887654158
C   6.0    −6.0717882763      0.0000593591     −0.2287136680
C   6.0    −7.1866398826     −2.2847192418      0.3325699278
C   6.0    −7.1854907850      2.2851711012      0.3336581671
H   1.0    −6.2846283303     −4.0578002243     −0.1234590242
H   1.0    −9.0163919699     −2.3834287213      1.2328758142
H   1.0    −6.2825836824      4.0579984242     −0.1215847979
H   1.0    −9.0151818102      2.3843934114      1.2340302771
C   6.0     6.0717882763      0.0000593591      0.2287136680
C   6.0     7.1866398826     −2.2847192418     −0.3325699278
C   6.0     7.1854907850      2.2851711012     −0.3336581671
H   1.0     6.2846283303     −4.0578002243      0.1234590242
H   1.0     9.0163919699     −2.3834287213     −1.2328758142
H   1.0     6.2825836824      4.0579984242      0.1215847979
H   1.0     9.0151818102      2.3843934114     −1.2340302771
 $END
 $EFRAG
 POSITION=FIXED COORD=CART
 fragname=WATER1
W1O1  −7.1861  −14.372  −0.333
W1H2  −3.2131   5.376   −0.12
W1H3  −3.2131   4.763   −0.23
 fragname=CO21
C1C1   7.1861  −14.372  −0.333
C1O2  −6.3131   5.376   −0.12
C1O3  −6.2131   4.763   −0.23
 $END
 $WATER1
WATER1 as DR1
COORDINATES(BOHR)
W1O1  −7.1861  −14.372  −0.333  0.0  0.0
W1H2  −3.2131   5.376   −0.12   0.0  0.0
W1H3  −3.2131   4.763   −0.23   0.0  0.0
 STOP
 MONOPOLES
W1O1 0.7  0.0
W1H2 0.0  0.0
W1H3 0.0  0.0
 STOP
 REPULSIVE POTENTIAL
W1O1
```

```
0 ,0
 STOP
 $END
 $CO21
Carbon as DR2
COORDINATES(BOHR)
C1C1   7.1861  −14.372  −0.333  0.0  0.0
C1O2   −6.3131  5.376  −0.12  0.0  0.0
C1O3   −6.2131  4.763  −0.23  0.0  0.0
 STOP
 MONOPOLES
C1C1  0.3  0.0
C1O2  0.0  0.0
C1O3  0.0  0.0
 STOP
 REPULSIVE  POTENTIAL
C1C1
0 ,0
 STOP
 $END
 $FRGRPL
 PAIR=WATER1 CO21
W1O1 C1C1  0  0
 STOP
 $END
```

C.2   Decatriene input files

C.2.1   Oxidized at the equilibrium

```
$BASIS GBASIS=N31 NGAUSS=6 $END
$CONTRL SCFTYP=UHF RUNTYP=OPTIMIZE COORD=ZMT MAXIT=200 ICHARG=1
 MULT=2 $END
$SCF CONV=1d−5 $END
$STATPT OPTTOL=0.0001 NSTEP=120 $END

$DATA
 Title
 C1
 C
 C      1      B1
 C      1      B2      2      A1
 C      2      B3      1      A2      3      D1
 C      1      B4      3      A3      2      D2
 C      5      B5      1      A4      3      D3
 C      3      B6      1      A5      5      D4
 C      4      B7      2      A6      1      D5
 C      7      B8      3      A7      1      D6
 C      8      B9      4      A8      2      D7
 H      1      B10     5      A9      6      D8
 H      1      B11     5      A10     6      D9
 H      2      B12     1      A11     5      D10
 H      2      B13     1      A12     5      D11
 H      3      B14     1      A13     5      D12
 H      3      B15     1      A14     5      D13
 H      4      B16     2      A15     1      D14
 H      4      B17     2      A16     1      D15
 H      5      B18     1      A17     3      D16
 H      6      B19     5      A18     1      D17
```

```
H      7    B20    3    A19    1    D18
H      8    B21    4    A20    2    D19
H      9    B22    7    A21    3    D20
H      9    B23    7    A22    3    D21
H     10    B24    8    A23    4    D22
H     10    B25    8    A24    4    D23

    B1              3.01058963
    B2              1.53227957
    B3              1.53217342
    B4              1.50254935
    B5              1.34117397
    B6              1.50163317
    B7              1.50172885
    B8              1.33749439
    B9              1.33753740
    B10             1.09866234
    B11             1.09568545
    B12             1.09783298
    B13             1.09340648
    B14             1.09740350
    B15             1.09739758
    B16             1.09757238
    B17             1.09674183
    B18             1.08660537
    B19             1.08682579
    B20             1.08685195
    B21             1.08689350
    B22             1.08453091
    B23             1.08424531
    B24             1.08447326
    B25             1.08437389
    A1            102.49156352
    A2            102.38588864
    A3            112.68687569
    A4            123.76688167
    A5            112.73884559
    A6            112.76640511
    A7            123.94514055
    A8            123.93093691
    A9            107.27487803
    A10           111.94999824
    A11           149.36574713
    A12            66.41768628
    A13           109.71657120
    A14           109.38042250
    A15           109.50606020
    A16           108.79635032
    A17           117.37854216
    A18           118.79143636
    A19           117.37532487
    A20           117.39400725
    A21           120.41698865
    A22           121.57894236
    A23           120.41132646
    A24           121.56908684
    D1            141.70493867
    D2            −58.38396524
    D3             90.15088170
    D4            179.38361590
    D5           −121.63560653
    D6            123.83394343
    D7            123.83941343
```

```
D8            −149.74946798
D9             −35.69924519
D10             65.04827083
D11            144.94742397
D12            −57.29573822
D13             59.14444985
D14              2.03583153
D15            118.06137418
D16            −88.60340061
D17           −179.09463140
D18            −57.25941520
D19            −57.33234676
D20            179.45913830
D21             −0.60143634
D22            179.43625357
D23             −0.63938009

$END
```

C.2.2 Oxidized with the switching field

```
$BASIS GBASIS=N31 NGAUSS=6 $END
$CONTRL SCFTYP=UHF RUNTYP=ENERGY COORD=CART MAXIT=200 ICHARG=1
 MULT=2 $END
$SCF CONV=1d−5 $END
$EFIELD EVEC(1)=0.008,0,0 $END

$DATA
 Title
C1
C     6.0     1.4077421114    −0.6099878945    −0.7211454165
C     6.0    −1.4103554140    −0.6054306245     0.7234133917
C     6.0     2.6147211034    −0.3675706950     0.2667154670
C     6.0    −2.6159800022    −0.3609911734    −0.2655294792
C     6.0     0.6343451538    −1.7935760604    −0.3006175310
C     6.0    −0.6397955938    −1.7915315546     0.3047978910
C     6.0     3.4424451357     0.7943232453    −0.2045827673
C     6.0    −3.4419129741     0.8025438757     0.2046580313
C     6.0     3.5739917360     1.9350905960     0.4628050034
C     6.0    −3.5707754269     1.9433248731    −0.4633542805
H     1.0     1.8265231880    −0.7980097485    −1.7046600307
H     1.0     0.8075305812     0.2852756252    −0.7722006204
H     1.0    −1.8304818069    −0.7911823989     1.7067517013
H     1.0    −0.8078804400     0.2882086579     0.7740274032
H     1.0     2.2345003628    −0.1795078667     1.2636867785
H     1.0     3.2186049642    −1.2681063244     0.3080741334
H     1.0    −2.2345491097    −0.1741985975    −1.2622556257
H     1.0    −3.2217084718    −1.2602210851    −0.3069751625
H     1.0     1.0998560386    −2.7544354789    −0.4425950370
H     1.0    −1.1076917379    −2.7510434523     0.4481717254
H     1.0     3.9567118324     0.6570273353    −1.1401541884
H     1.0    −3.9574865198     0.6665620630     1.1396979959
H     1.0     4.1889445163     2.7315273049     0.0926872726
H     1.0     3.0869574988     2.1082293798     1.4050135547
H     1.0    −4.1847549979     2.7409927201    −0.0940955756
H     1.0    −3.0824886896     2.1151702588    −1.4051841977
$END
```

C.2.3 Oxidized with the driver

```
$BASIS GBASIS=N31 NGAUSS=6 $END
```

```
$CONTRL SCFTYP=UHF RUNTYP=ENERGY COORD=CART MAXIT =200 ICHARG=1
  MULT=2 $END
$SCF CONV=1d−5 $END
$SYSTEM MWORDS=50 $END

$DATA
Title
C1
C    6.0    1.4077421114   −0.6099878945   −0.7211454165
C    6.0   −1.4103554140   −0.6054306245    0.7234133917
C    6.0    2.6147211034   −0.3675706950    0.2667154670
C    6.0   −2.6159800022   −0.3609911734   −0.2655294792
C    6.0    0.6343451538   −1.7935760604   −0.3006175310
C    6.0   −0.6397955938   −1.7915315546    0.3047978910
C    6.0    3.4424451357    0.7943232453   −0.2045827673
C    6.0   −3.4419129741    0.8025438757    0.2046580313
C    6.0    3.5739917360    1.9350905960    0.4628050034
C    6.0   −3.5707754269    1.9433248731   −0.4633542805
H    1.0    1.8265231880   −0.7980097485   −1.7046600307
H    1.0    0.8075305812    0.2852756252   −0.7722006204
H    1.0   −1.8304818069   −0.7911823989    1.7067517013
H    1.0   −0.8078804400    0.2882086579    0.7740274032
H    1.0    2.2345003628   −0.1795078667    1.2636867785
H    1.0    3.2186049642   −1.2681063244    0.3080741334
H    1.0   −2.2345491097   −0.1741985975   −1.2622556257
H    1.0   −3.2217084718   −1.2602210851   −0.3069751625
H    1.0    1.0998560386   −2.7544354789   −0.4425950370
H    1.0   −1.1076917379   −2.7510434523    0.4481717254
H    1.0    3.9567118324    0.6570273353   −1.1401541884
H    1.0   −3.9574865198    0.6665620630    1.1396979959
H    1.0    4.1889445163    2.7315273049    0.0926872726
H    1.0    3.0869574988    2.1082293798    1.4050135547
H    1.0   −4.1847549979    2.7409927201   −0.0940955756
H    1.0   −3.0824886896    2.1151702588   −1.4051841977
$END
$EFRAG
POSITION=FIXED COORD=CART
 fragname=WATER1
W1O1   3.57  −5.21  0.46
W1H2  −10.2131  30.376  −0.12
W1H3  −10.2131  30.763  −0.23
 fragname=CO21
C1C1  −3.57  −5.21  −0.46
C1O2  −10.3131  30.376  −0.12
C1O3  −10.2131  30.763  −0.23
 $END
 $WATER1
WATER1 as DR1
COORDINATES(BOHR)
W1O1   3.57  −5.21  0.46  0.0  0.0
W1H2  −10.2131  30.376  −0.12   0.0  0.0
W1H3  −10.2131  30.763  −0.23   0.0  0.0
 STOP
 MONOPOLES
W1O1  0.3  0.0
W1H2  0.0  0.0
W1H3  0.0  0.0
 STOP
 REPULSIVE POTENTIAL
W1O1
0 ,0
 STOP
 $END
```

```
 $CO21
Carbon  as  DR2
COORDINATES(BOHR)
C1C1   −3.57  −5.21  −0.46  0.0  0.0
C1O2   −10.3131  30.376  −0.12  0.0  0.0
C1O3   −10.2131  30.763  −0.23  0.0  0.0
 STOP
 MONOPOLES
C1C1  0.7  0.0
C1O2  0.0  0.0
C1O3  0.0  0.0
 STOP
 REPULSIVE  POTENTIAL
C1C1
0 ,0
 STOP
 $END
 $FRGRPL
 PAIR=WATER1  CO21
W1O1  C1C1  0  0
 STOP
 $END
```

C.3   Bis-ferrocene input file

C.3.1   Neutral at the equilibrium

```
 $BASIS  GBASIS=N31  NGAUSS=6  NDFUNC=1  NPFUNC=1  $END
 $CONTRL  SCFTYP=UHF  RUNTYP=OPTIMIZE  COORD=ZMT  MAXIT=200  $END
 $STATPT  OPTTOL=0.0001  NSTEP=120  $END
 $SYSTEM  MWORDS=125  $END

 $DATA
 Title
 C1
 C
 C     1    B1
 C     2    B2    1     A1
 C     3    B3    2     A2    1     D1
 C     4    B4    3     A3    2     D2
 Fe    1    B5    5     A4    4     D3
 C     6    B6    1     A5    5     D4
 C     7    B7    6     A6    1     D5
 C     8    B8    7     A7    6     D6
 C     9    B9    8     A8    7     D7
 C    10    B10   9     A9    8     D8
 C     8    B11   7     A10   6     D9
 C    12    B12   8     A11   7     D10
 C    12    B13   8     A12   7     D11
 C    14    B14   12    A13   8     D12
 C    15    B15   14    A14   12    D13
 C    16    B16   15    A15   14    D14
 C    17    B17   16    A16   15    D15
 C    18    B18   17    A17   16    D16
 C    16    B19   15    A18   14    D17
 C    20    B20   16    A19   15    D18
 N    17    B21   16    A20   15    D19
 C    20    B22   16    A21   15    D20
 C    23    B23   20    A22   16    D21
 C    24    B24   23    A23   20    D22
```

C	25	B25	24	A24	23	D23
C	24	B26	23	A25	20	D24
C	27	B27	24	A26	23	D25
C	27	B28	24	A27	23	D26
C	29	B29	27	A28	24	D27
C	30	B30	29	A29	27	D28
C	31	B31	30	A30	29	D29
C	32	B32	31	A31	30	D30
Fe	32	B33	31	A32	30	D31
C	34	B34	32	A33	31	D32
C	35	B35	34	A34	32	D33
C	36	B36	35	A35	34	D34
C	37	B37	36	A36	35	D35
C	35	B38	34	A37	32	D36
H	12	B39	8	A38	7	D37
H	13	B40	12	A39	8	D38
H	13	B41	12	A40	8	D39
H	13	B42	12	A41	8	D40
H	28	B43	27	A42	24	D41
H	28	B44	27	A43	24	D42
H	28	B45	27	A44	24	D43
H	36	B46	35	A45	34	D44
H	37	B47	36	A46	35	D45
H	38	B48	37	A47	36	D46
H	39	B49	35	A48	34	D47
H	35	B50	34	A49	32	D48
H	30	B51	29	A50	27	D49
H	33	B52	32	A51	31	D50
H	32	B53	31	A52	30	D51
H	31	B54	30	A53	29	D52
H	9	B55	8	A54	7	D53
H	10	B56	9	A55	8	D54
H	11	B57	10	A56	9	D55
H	7	B58	6	A57	1	D56
H	1	B59	5	A58	4	D57
H	5	B60	4	A59	3	D58
H	4	B61	3	A60	2	D59
H	3	B62	2	A61	1	D60
H	2	B63	1	A62	5	D61
H	15	B64	14	A63	12	D62
H	19	B65	18	A64	17	D63
H	18	B66	17	A65	16	D64
H	22	B67	17	A66	16	D65
H	26	B68	25	A67	24	D66
H	25	B69	24	A68	23	D67
H	23	B70	20	A69	16	D68
H	27	B71	24	A70	23	D69

B1	1.42432140
B2	1.42385704
B3	1.42463075
B4	1.42384447
B5	2.08459851
B6	2.08353753
B7	1.42873485
B8	1.42888278
B9	1.42268892
B10	1.42300740
B11	1.51172238
B12	1.53861482
B13	1.52877716
B14	1.39188103
B15	1.39494033

```
B16           1.41568887
B17           1.39071610
B18           1.38875239
B19           1.44907700
B20           1.41569620
B21           1.38557527
B22           1.39493330
B23           1.39188889
B24           1.40609326
B25           1.38875951
B26           1.52876654
B27           1.53861066
B28           1.51173418
B29           1.42888093
B30           1.42269326
B31           1.42301251
B32           1.42477709
B33           2.07809077
B34           2.08630376
B35           1.42417847
B36           1.42431745
B37           1.42386359
B38           1.42384347
B39           1.09423424
B40           1.09161746
B41           1.09116815
B42           1.09189287
B43           1.09161847
B44           1.09189298
B45           1.09116870
B46           1.07827234
B47           1.07838995
B48           1.07857541
B49           1.07838288
B50           1.07837063
B51           1.07899004
B52           1.07807904
B53           1.07848088
B54           1.07839866
B55           1.07898980
B56           1.07839841
B57           1.07847960
B58           1.07808027
B59           1.07827298
B60           1.07836994
B61           1.07838285
B62           1.07857378
B63           1.07838864
B64           1.08332259
B65           1.08458937
B66           1.08359593
B67           1.00464467
B68           1.08359663
B69           1.08458885
B70           1.08332472
B71           1.09423262
A1          107.98832088
A2          108.00649939
A3          107.99419900
A4           70.09766200
A5          157.37258679
A6           70.47889197
A7          106.92749439
```

A8	108.75166886
A9	107.81760282
A10	128.03571982
A11	112.99631494
A12	112.09494024
A13	121.69854015
A14	120.02011915
A15	119.53931805
A16	121.29465590
A17	117.72001719
A18	133.77882278
A19	106.67933896
A20	108.61749139
A21	133.77947148
A22	120.02032308
A23	119.02714625
A24	122.39844197
A25	121.69533968
A26	110.61033671
A27	112.09462869
A28	124.92639957
A29	108.75131922
A30	107.81771939
A31	107.89077475
A32	70.03962299
A33	108.52747933
A34	69.96906657
A35	108.01020745
A36	107.98846118
A37	70.07751394
A38	106.94805730
A39	111.10363706
A40	110.22845254
A41	111.12988947
A42	111.10263583
A43	111.13050995
A44	110.22817317
A45	125.99759718
A46	125.99017943
A47	125.96907648
A48	125.95822504
A49	124.59850256
A50	125.30228954
A51	125.42865194
A52	126.14786305
A53	126.06430118
A54	125.30079771
A55	126.06287414
A56	126.14718431
A57	124.42996574
A58	125.99739697
A59	125.99241800
A60	126.04151755
A61	125.96936989
A62	125.98903171
A63	119.93178095
A64	118.77656718
A65	121.51664779
A66	125.29231743
A67	120.76122417
A68	118.82449094
A69	120.04155665
A70	106.47738774

D1	-0.02630539
D2	0.05761447
D3	-60.01192633
D4	-48.53390094
D5	-163.88864144
D6	59.55195094
D7	0.18507789
D8	-0.27879090
D9	-124.18300498
D10	22.08131956
D11	-103.72104496
D12	41.48335946
D13	177.91113020
D14	0.01685779
D15	0.07690624
D16	-0.04136208
D17	179.36281550
D18	-179.40764070
D19	179.61525020
D20	0.00403170
D21	-179.36810327
D22	0.14227371
D23	-0.18335598
D24	-177.90806203
D25	85.59612133
D26	-41.49644772
D27	-71.91729979
D28	176.23869852
D29	0.27802356
D30	-0.26216300
D31	59.98819612
D32	121.83857251
D33	-118.04554140
D34	-60.06362139
D35	0.01630894
D36	123.13785780
D37	139.93912076
D38	55.95915065
D39	176.25827364
D40	-64.81624883
D41	177.44421629
D42	-61.78038705
D43	57.14602374
D44	118.86515404
D45	178.88926613
D46	179.32636937
D47	-119.12026929
D48	2.51618449
D49	-4.03547809
D50	178.67415052
D51	178.53923948
D52	178.66885262
D53	-179.54332556
D54	-178.66713159
D55	-178.53703408
D56	75.31266505
D57	-178.88039134
D58	-178.91097519
D59	-179.06827109
D60	-179.31952094
D61	-178.89008234
D62	-3.04587300
D63	179.65804780

```
        D64              179.48068500
        D65             −179.11727176
        D66              179.61536151
        D67              179.56466154
        D68               −0.32400050
        D69             −158.12256424

$END
```

C.3.2   Oxidized at the equilibrium

```
$BASIS GBASIS=N31 NGAUSS=6 NDFUNC=1 NPFUNC=1 $END
$CONTRL SCFTYP=UHF RUNTYP=OPTIMIZE COORD=ZMT MAXIT=200 ICHARG=1
 MULT=2 $END
$STATPT OPTTOL=0.0001 NSTEP=300 $END
$SCF CONV=1d−5 $END
$SYSTEM MWORDS=125 $END

$DATA
 Title
C1
C
C       1    B1
C       2    B2     1    A1
C       3    B3     2    A2     1    D1
C       4    B4     3    A3     2    D2
Fe      1    B5     5    A4     4    D3
C       6    B6     1    A5     5    D4
C       7    B7     6    A6     1    D5
C       8    B8     7    A7     6    D6
C       9    B9     8    A8     7    D7
C      10    B10    9    A9     8    D8
C       8    B11    7    A10    6    D9
C      12    B12    8    A11    7    D10
C      12    B13    8    A12    7    D11
C      14    B14   12    A13    8    D12
C      15    B15   14    A14   12    D13
C      16    B16   15    A15   14    D14
C      17    B17   16    A16   15    D15
C      18    B18   17    A17   16    D16
C      16    B19   15    A18   14    D17
C      20    B20   16    A19   15    D18
N      17    B21   16    A20   15    D19
C      20    B22   16    A21   15    D20
C      23    B23   20    A22   16    D21
C      24    B24   23    A23   20    D22
C      25    B25   24    A24   23    D23
C      24    B26   23    A25   20    D24
C      27    B27   24    A26   23    D25
C      27    B28   24    A27   23    D26
C      29    B29   27    A28   24    D27
C      30    B30   29    A29   27    D28
C      31    B31   30    A30   29    D29
C      32    B32   31    A31   30    D30
Fe     32    B33   31    A32   30    D31
C      34    B34   32    A33   31    D32
C      35    B35   34    A34   32    D33
C      36    B36   35    A35   34    D34
C      37    B37   36    A36   35    D35
C      35    B38   34    A37   32    D36
H      12    B39    8    A38    7    D37
H      13    B40   12    A39    8    D38
```

111

```
H    13   B41   12   A40    8   D39
H    13   B42   12   A41    8   D40
H    28   B43   27   A42   24   D41
H    28   B44   27   A43   24   D42
H    28   B45   27   A44   24   D43
H    36   B46   35   A45   34   D44
H    37   B47   36   A46   35   D45
H    38   B48   37   A47   36   D46
H    39   B49   35   A48   34   D47
H    35   B50   34   A49   32   D48
H    30   B51   29   A50   27   D49
H    33   B52   32   A51   31   D50
H    32   B53   31   A52   30   D51
H    31   B54   30   A53   29   D52
H     9   B55    8   A54    7   D53
H    10   B56    9   A55    8   D54
H    11   B57   10   A56    9   D55
H     7   B58    6   A57    1   D56
H     1   B59    5   A58    4   D57
H     5   B60    4   A59    3   D58
H     4   B61    3   A60    2   D59
H     3   B62    2   A61    1   D60
H     2   B63    1   A62    5   D61
H    15   B64   14   A63   12   D62
H    19   B65   18   A64   17   D63
H    18   B66   17   A65   16   D64
H    22   B67   17   A66   16   D65
H    26   B68   25   A67   24   D66
H    25   B69   24   A68   23   D67
H    23   B70   20   A69   16   D68
H    27   B71   24   A70   23   D69

   B1            1.42432140
   B2            1.42385704
   B3            1.42463075
   B4            1.42384447
   B5            2.08459851
   B6            2.08353753
   B7            1.42873485
   B8            1.42888278
   B9            1.42268892
   B10           1.42300740
   B11           1.51172238
   B12           1.53861482
   B13           1.52877716
   B14           1.39188103
   B15           1.39494033
   B16           1.41568887
   B17           1.39071610
   B18           1.38875239
   B19           1.44907700
   B20           1.41569620
   B21           1.38557527
   B22           1.39493330
   B23           1.39188889
   B24           1.40609326
   B25           1.38875951
   B26           1.52876654
   B27           1.53861066
   B28           1.51173418
   B29           1.42888093
   B30           1.42269326
   B31           1.42301251
```

B32	1.42477709
B33	2.07809077
B34	2.08630376
B35	1.42417847
B36	1.42431745
B37	1.42386359
B38	1.42384347
B39	1.09423424
B40	1.09161746
B41	1.09116815
B42	1.09189287
B43	1.09161847
B44	1.09189298
B45	1.09116870
B46	1.07827234
B47	1.07838995
B48	1.07857541
B49	1.07838288
B50	1.07837063
B51	1.07899004
B52	1.07807904
B53	1.07848088
B54	1.07839866
B55	1.07898980
B56	1.07839841
B57	1.07847960
B58	1.07808027
B59	1.07827298
B60	1.07836994
B61	1.07838285
B62	1.07857378
B63	1.07838864
B64	1.08332259
B65	1.08458937
B66	1.08359593
B67	1.00464467
B68	1.08359663
B69	1.08458885
B70	1.08332472
B71	1.09423262
A1	107.98832088
A2	108.00649939
A3	107.99419900
A4	70.09766200
A5	157.37258679
A6	70.47889197
A7	106.92749439
A8	108.75166886
A9	107.81760282
A10	128.03571982
A11	112.99631494
A12	112.09494024
A13	121.69854015
A14	120.02011915
A15	119.53931805
A16	121.29465590
A17	117.72001719
A18	133.77882278
A19	106.67933896
A20	108.61749139
A21	133.77947148
A22	120.02032308
A23	119.02714625

113

A24	122.39844197
A25	121.69553968
A26	110.61033671
A27	112.09462869
A28	124.92639957
A29	108.75131922
A30	107.81771939
A31	107.89077475
A32	70.03962299
A33	108.52747933
A34	69.96906657
A35	108.01020745
A36	107.98846118
A37	70.07751394
A38	106.94805730
A39	111.10363706
A40	110.22845254
A41	111.12988947
A42	111.10263583
A43	111.13050995
A44	110.22817317
A45	125.99759718
A46	125.99017943
A47	125.96907648
A48	125.95822504
A49	124.59850256
A50	125.30228954
A51	125.42865194
A52	126.14786305
A53	126.06430118
A54	125.30079771
A55	126.06287414
A56	126.14718431
A57	124.42996574
A58	125.99739697
A59	125.99241800
A60	126.04151755
A61	125.96936989
A62	125.98903171
A63	119.93178095
A64	118.77656718
A65	121.51664779
A66	125.29231743
A67	120.76122417
A68	118.82449094
A69	120.04155665
A70	106.47738774
D1	−0.02630539
D2	0.05761447
D3	−60.01192633
D4	−48.53390094
D5	−163.88864144
D6	59.55195094
D7	0.18507789
D8	−0.27879090
D9	−124.18300498
D10	22.08131956
D11	−103.72104496
D12	41.48335946
D13	177.91113020
D14	0.01685779
D15	0.07690624
D16	−0.04136208

114

```
D17            179.36281550
D18           −179.40764070
D19            179.61525020
D20              0.00403170
D21           −179.36810327
D22              0.14227371
D23             −0.18335598
D24           −177.90806203
D25             85.59612133
D26            −41.49644772
D27            −71.91729979
D28            176.23869852
D29              0.27802356
D30             −0.26216300
D31             59.98819612
D32            121.83857251
D33           −118.04554140
D34            −60.06362139
D35              0.01630894
D36            123.13785780
D37            139.93912076
D38             55.95915065
D39            176.25827364
D40            −64.81624883
D41            177.44421629
D42            −61.78038705
D43             57.14602374
D44            118.86515404
D45            178.88926613
D46            179.32636937
D47           −119.12026929
D48              2.51618449
D49             −4.03547809
D50            178.67415052
D51            178.53923948
D52            178.66885262
D53           −179.54332556
D54           −178.66713159
D55           −178.53703408
D56             75.31266505
D57           −178.88039134
D58           −178.91097519
D59           −179.06827109
D60           −179.31952094
D61           −178.89008234
D62             −3.04587300
D63            179.65804780
D64            179.48068500
D65           −179.11727176
D66            179.61536151
D67            179.56466154
D68             −0.32400050
D69           −158.12256424
```

$END

C.3.3   Oxidized with the switching field

```
$BASIS GBASIS=N31 NGAUSS=6 NDFUNC=1 NPFUNC=1 $END
$CONTRL SCFTYP=UHF RUNTYP=ENERGY COORD=CART MAXIT=200 ICHARG=1
 MULT=2 $END
$SCF CONV=1d−5 $END
```

```
$SYSTEM MWORDS=125 $END
$GUESS GUESS=MOREAD NORB=154 $END
$EFIELD EVEC(1)=0.012,0,0 $END

$DATA
Title
C1
C     6.0    −7.0164138183    3.2976923918   −0.5073977271
C     6.0    −7.4340771815    2.0256357170   −0.9523252460
C     6.0    −7.6229874382    1.2066451946    0.1819875317
C     6.0    −7.3224593538    1.9742121234    1.3288565237
C     6.0    −6.9471510149    3.2663805178    0.9020856871
FE   26.0    −5.3919697225    1.7724114586    0.0816213180
C     6.0    −3.4918419568    0.9933743069    1.1535956960
C     6.0    −3.8397291622    0.0309630307    0.1759132153
C     6.0    −3.7300118086    0.6644309455   −1.0853271419
C     6.0    −3.3090857563    1.9970151124   −0.8874008254
C     6.0    −3.1651263368    2.2031902716    0.4980489998
C     6.0    −4.1825291179   −1.4323827937    0.3857713847
C     6.0    −4.6449895372   −1.7394846179    1.8187057221
C     6.0    −3.0349096885   −2.3613731012   −0.0101268594
C     6.0    −1.7026698709   −2.0304007736    0.2382634963
C     6.0    −0.6910355827   −2.9426404074   −0.0952921515
C     6.0    −1.0193547461   −4.1832452497   −0.6753915221
C     6.0    −2.3402489430   −4.5334346940   −0.9322290570
C     6.0    −3.3305196182   −3.6105304849   −0.5924414059
C     6.0     0.7470956660   −2.9115041801    0.0182150217
C     6.0     1.2261565834   −4.1389084714   −0.4981827053
N     7.0     0.1513307286   −4.8847051730   −0.9158704840
C     6.0     1.6523068119   −1.9637850016    0.5022732126
C     6.0     3.0224420195   −2.2410223927    0.4692922306
C     6.0     3.4716334434   −3.4666583804   −0.0478372440
C     6.0     2.5846911645   −4.4286020315   −0.5336788540
C     6.0     4.0289289159   −1.2256766570    1.0066541542
C     6.0     4.0015990509   −1.1082050710    2.5348268861
C     6.0     3.8103408451    0.0964498039    0.3107374146
C     6.0     3.8242564936    0.2482520302   −1.1780554296
C     6.0     3.4917670902    1.5485110280   −1.4896045088
C     6.0     3.2341390979    2.2392065602   −0.2573239150
C     6.0     3.4914027300    1.3420773883    0.8307489367
FE   26.0     5.5325414044    1.6799706686   −0.3172045050
C     6.0     7.0703131731    3.3892489570   −0.3373824131
C     6.0     7.2967943242    2.5446026660   −1.4464127167
C     6.0     7.6334514836    1.2584859453   −0.9621685910
C     6.0     7.5948216759    1.3038764328    0.4520676530
C     6.0     7.2404084175    2.6198243277    0.8351589625
H     1.0    −5.0121480360   −1.6674302799   −0.2756822195
H     1.0    −5.4978591682   −1.1283156865    2.0957103062
H     1.0    −4.9342894684   −2.7809290929    1.9048210945
H     1.0    −3.8500363991   −1.5617271633    2.5355328633
H     1.0     4.7561958075   −0.4164253809    2.8981597299
H     1.0     3.0313148486   −0.7810689963    2.8910471314
H     1.0     4.2003350598   −2.0783484152    2.9717129544
H     1.0     7.2709938506    2.8395873181   −2.4771055680
H     1.0     7.9207503091    0.4165945825   −1.5607575043
H     1.0     7.8510648324    0.5032585646    1.1176273446
H     1.0     7.1659244341    2.9816591216    1.8418532862
H     1.0     6.8384358054    4.4352227018   −0.3780433307
H     1.0     4.0137730917   −0.5517477593   −1.8664813614
H     1.0     3.3614179790    1.5816061870    1.8665814483
H     1.0     2.9014834716    3.2552259239   −0.1662515367
H     1.0     3.3720372394    1.9589171524   −2.4723755406
H     1.0    −3.9070406727    0.1952101872   −2.0343293871
```

116

```
H       1.0    −3.1326685721    2.7222417754    −1.6579718179
H       1.0    −2.8591337705    3.1137892158     0.9756947365
H       1.0    −3.4702562079    0.8373422782     2.2143923092
H       1.0    −6.8183835639    4.1489496653    −1.1290736915
H       1.0    −6.6867410254    4.0890785663     1.5388374938
H       1.0    −7.3979501662    1.6439954421     2.3465089600
H       1.0    −7.9702855327    0.1918452882     0.1760687250
H       1.0    −7.6091621795    1.7404373673    −1.9712140124
H       1.0    −1.4572980942   −1.0780938204     0.6722033015
H       1.0    −4.3583551000   −3.8641521594    −0.7863771279
H       1.0    −2.5977608888   −5.4764293826    −1.3800560981
H       1.0     0.2005269185   −5.8069564576    −1.2760495704
H       1.0     2.9514139808   −5.3618071998    −0.9214062983
H       1.0     4.5267457220   −3.6797143631    −0.0642377320
H       1.0     1.2885657454   −1.0329006146     0.9032498809
H       1.0     5.0177075177   −1.5727519512     0.7142901192
$END
$VEC
1   1 1.54180469E−08  ...  −1.01175600E−08
1   2 3.38323391E−07  ...   1.12932931E−07
1   3 1.28007430E−07  ...  −6.15323336E−08
    .
    .
    .
    .
    .
54159 7.23323144E−05  ...  −7.73492112E−04
54160−9.63647063E−06  ...   1.36677534E−04
 $END
```

C.3.4 Oxidized with the clock field

```
$BASIS GBASIS=N31 NGAUSS=6 NDFUNC=1 NPFUNC=1 $END
$CONTRL SCFTYP=UHF RUNTYP=ENERGY COORD=CART MAXIT=200 ICHARG=1
 MULT=2 $END
$SCF CONV=1d−5 $END
$SYSTEM MWORDS=125 $END
$GUESS GUESS=MOREAD NORB=154 $END
$EFIELD EVEC(1)=0,−0.004,0 $END

$DATA
 Title
 C1
C       6.0    −7.0164138183    3.2976923918    −0.5073977271
C       6.0    −7.4340771815    2.0256357170    −0.9523252460
C       6.0    −7.6229874382    1.2066451946     0.1819875317
C       6.0    −7.3224593538    1.9742121234     1.3288565237
C       6.0    −6.9471510149    3.2663805178     0.9020856871
FE     26.0    −5.3919697225    1.7724114586     0.0816213180
C       6.0    −3.4918419568    0.9933743069     1.1535956960
C       6.0    −3.8397291622    0.0309630307     0.1759132153
C       6.0    −3.7300118086    0.6644309455    −1.0853271419
C       6.0    −3.3090857563    1.9970151124    −0.8874008254
C       6.0    −3.1651263368    2.2031902716     0.4980489998
C       6.0    −4.1825291179   −1.4323827937     0.3857713847
C       6.0    −4.6449895372   −1.7394846179     1.8187057221
C       6.0    −3.0349096885   −2.3613731012    −0.0101268594
C       6.0    −1.7026698709   −2.0304007736     0.2382634963
C       6.0    −0.6910355827   −2.9426404074    −0.0952921515
C       6.0    −1.0193547461   −4.1832452497    −0.6753915221
C       6.0    −2.3402489430   −4.5334346940    −0.9322290570
C       6.0    −3.3305196182   −3.6105304849    −0.5924414059
```

117

```
C       6.0     0.7470956660    −2.9115041801    0.0182150217
C       6.0     1.2261565834    −4.1389084714    −0.4981827053
N       7.0     0.1513307286    −4.8847051730    −0.9158704840
C       6.0     1.6523068119    −1.9637850016    0.5022732126
C       6.0     3.0224420195    −2.2410223927    0.4692922306
C       6.0     3.4716334434    −3.4666583804    −0.0478372440
C       6.0     2.5846911645    −4.4286020315    −0.5336788540
C       6.0     4.0289289159    −1.2256766570    1.0066541542
C       6.0     4.0015990509    −1.1082050710    2.5348268861
C       6.0     3.8103408451    0.0964498039     0.3107374146
C       6.0     3.8242564936    0.2482520302     −1.1780554296
C       6.0     3.4917670902    1.5485110280     −1.4896045088
C       6.0     3.2341390979    2.2392065602     −0.2573239150
C       6.0     3.4914027300    1.3420773883     0.8307489367
FE      26.0    5.5325414044    1.6799706686     −0.3172045050
C       6.0     7.0703131731    3.3892489570     −0.3373824131
C       6.0     7.2967943242    2.5446026660     −1.4464127167
C       6.0     7.6334514836    1.2584859453     −0.9621685910
C       6.0     7.5948216759    1.3038764328     0.4520676530
C       6.0     7.2404084175    2.6198243277     0.8351589625
H       1.0     −5.0121480360   −1.6674302799    −0.2756822195
H       1.0     −5.4978591682   −1.1283156865    2.0957103062
H       1.0     −4.9342894684   −2.7809290929    1.9048210945
H       1.0     −3.8500363991   −1.5617271633    2.5355328633
H       1.0     4.7561958075    −0.4164253809    2.8981597299
H       1.0     3.0313148486    −0.7810689963    2.8910471314
H       1.0     4.2003350598    −2.0783484152    2.9717129544
H       1.0     7.2709938506    2.8395873181     −2.4771055680
H       1.0     7.9207503091    0.4165945825     −1.5607575043
H       1.0     7.8510648324    0.5032585646     1.1176273446
H       1.0     7.1659244341    2.9816591216     1.8418532862
H       1.0     6.8384358054    4.4352227018     −0.3780433307
H       1.0     4.0137730917    −0.5517477593    −1.8664813614
H       1.0     3.3614179790    1.5816061870     1.8665814483
H       1.0     2.9014834716    3.2552259239     −0.1662515367
H       1.0     3.3720372394    1.9589171524     −2.4723755406
H       1.0     −3.9070406727   0.1952101872     −2.0343293871
H       1.0     −3.1326685721   2.7222417754     −1.6579718179
H       1.0     −2.8591337705   3.1137892158     0.9756947365
H       1.0     −3.4702562079   0.8373422782     2.2143923092
H       1.0     −6.8183835639   4.1489496653     −1.1290736915
H       1.0     −6.6867410254   4.0890785663     1.5388374938
H       1.0     −7.3979501662   1.6439954421     2.3465089600
H       1.0     −7.9702855327   0.1918452882     0.1760687250
H       1.0     −7.6091621795   1.7404373673     −1.9712140124
H       1.0     −1.4572980942   −1.0780938204    0.6722033015
H       1.0     −4.3583551000   −3.8641521594    −0.7863771279
H       1.0     −2.5977608888   −5.4764293826    −1.3800560981
H       1.0     0.2005269185    −5.8069564576    −1.2760495704
H       1.0     2.9514139808    −5.3618071998    −0.9214062983
H       1.0     4.5267457220    −3.6797143631    −0.0642377320
H       1.0     1.2885657454    −1.0329006146    0.9032498809
H       1.0     5.0177075177    −1.5727519512    0.7142901192
$END
$VEC
1   1  1.54180469E−08  ...  −1.01175600E−08
1   2  3.38323391E−07  ...   1.12932931E−07
1   3  1.28007430E−07  ...  −6.15323336E−08
.
.
.
.
.
```

118

```
54159  7.23323144E−05  ...  −7.73492112E−04
54160 −9.63647063E−06  ...   1.36677534E−04
 $END
```

C.3.5   Oxidized with the driver

```
 $BASIS  GBASIS=N31 NGAUSS=6 NDFUNC=1 NPFUNC=1 $END
 $CONTRL SCFTYP=UHF RUNTYP=ENERGY COORD=CART MAXIT=200 ICHARG=1
  MULT=2 $END
 $SCF CONV=1d−5 $END
 $SYSTEM MWORDS=125 $END
 $GUESS GUESS=MOREAD NORB=154 $END

 $DATA
 Title
 C1
 C    6.0   −7.0164138183    3.2976923918   −0.5073977271
 C    6.0   −7.4340771815    2.0256357170   −0.9523252460
 C    6.0   −7.6229874382    1.2066451946    0.1819875317
 C    6.0   −7.3224593538    1.9742121234    1.3288565237
 C    6.0   −6.9471510149    3.2663805178    0.9020856871
 FE  26.0   −5.3919697225    1.7724114586    0.0816213180
 C    6.0   −3.4918419568    0.9933743069    1.1535956960
 C    6.0   −3.8397291622    0.0309630307    0.1759132153
 C    6.0   −3.7300118086    0.6644309455   −1.0853271419
 C    6.0   −3.3090857563    1.9970151124   −0.8874008254
 C    6.0   −3.1651263368    2.2031902716    0.4980489998
 C    6.0   −4.1825291179   −1.4323827937    0.3857713847
 C    6.0   −4.6449895372   −1.7394846179    1.8187057221
 C    6.0   −3.0349096885   −2.3613731012   −0.0101268594
 C    6.0   −1.7026698709   −2.0304007736    0.2382634963
 C    6.0   −0.6910355827   −2.9426404074   −0.0952921515
 C    6.0   −1.0193547461   −4.1832452497   −0.6753915221
 C    6.0   −2.3402489430   −4.5334346940   −0.9322290570
 C    6.0   −3.3305196182   −3.6105304849   −0.5924414059
 C    6.0    0.7470956660   −2.9115041801    0.0182150217
 C    6.0    1.2261565834   −4.1389084714   −0.4981827053
 N    7.0    0.1513307286   −4.8847051730   −0.9158704840
 C    6.0    1.6523068119   −1.9637850016    0.5022732126
 C    6.0    3.0224420195   −2.2410223927    0.4692922306
 C    6.0    3.4716334434   −3.4666583804   −0.0478372440
 C    6.0    2.5846911645   −4.4286020315   −0.5336788540
 C    6.0    4.0289289159   −1.2256766570    1.0066541542
 C    6.0    4.0015990509   −1.1082050710    2.5348268861
 C    6.0    3.8103408451    0.0964498039    0.3107374146
 C    6.0    3.8242564936    0.2482520302   −1.1780554296
 C    6.0    3.4917670902    1.5485110280   −1.4896045088
 C    6.0    3.2341390979    2.2392065602   −0.2573239150
 C    6.0    3.4914027300    1.3420773883    0.8307489367
 FE  26.0    5.5325414044    1.6799706686   −0.3172045050
 C    6.0    7.0703131731    3.3892489570   −0.3373824131
 C    6.0    7.2967943242    2.5446026660   −1.4464127167
 C    6.0    7.6334514836    1.2584859453   −0.9621685910
 C    6.0    7.5948216759    1.3038764328    0.4520676530
 C    6.0    7.2404084175    2.6198243277    0.8351589625
 H    1.0   −5.0121480360   −1.6674302799   −0.2756822195
 H    1.0   −5.4978591682   −1.1283156865    2.0957103062
 H    1.0   −4.9342894684   −2.7809290929    1.9048210945
 H    1.0   −3.8500363991   −1.5617271633    2.5355328633
 H    1.0    4.7561958075   −0.4164253809    2.8981597299
 H    1.0    3.0313148486   −0.7810689963    2.8910471314
 H    1.0    4.2003350598   −2.0783484152    2.9717129544
```

```
H      1.0    7.2709938506    2.8395873181   −2.4771055680
H      1.0    7.9207503091    0.4165945825   −1.5607575043
H      1.0    7.8510648324    0.5032585646    1.1176273446
H      1.0    7.1659244341    2.9816591216    1.8418532862
H      1.0    6.8384358054    4.4352227018   −0.3780433307
H      1.0    4.0137730917   −0.5517477593   −1.8664813614
H      1.0    3.3614179790    1.5816061870    1.8665814483
H      1.0    2.9014834716    3.2552259239   −0.1662515367
H      1.0    3.3720372394    1.9589171524   −2.4723755406
H      1.0   −3.9070406727    0.1952101872   −2.0343293871
H      1.0   −3.1326685721    2.7222417754   −1.6579718179
H      1.0   −2.8591337705    3.1137892158    0.9756947365
H      1.0   −3.4702562079    0.8373422782    2.2143923092
H      1.0   −6.8183835639    4.1489496653   −1.1290736915
H      1.0   −6.6867410254    4.0890785663    1.5388374938
H      1.0   −7.3979501662    1.6439954421    2.3465089600
H      1.0   −7.9702855327    0.1918452882    0.1760687250
H      1.0   −7.6091621795    1.7404373673   −1.9712140124
H      1.0   −1.4572980942   −1.0780938204    0.6722033015
H      1.0   −4.3583551000   −3.8641521594   −0.7863771279
H      1.0   −2.5977608888   −5.4764293826   −1.3800560981
H      1.0    0.2005269185   −5.8069564576   −1.2760495704
H      1.0    2.9514139808   −5.3618071998   −0.9214062983
H      1.0    4.5267457220   −3.6797143631   −0.0642377320
H      1.0    1.2885657454   −1.0329006146    0.9032498809
H      1.0    5.0177075177   −1.5727519512    0.7142901192
 $END
 $VEC
 1   1  1.54180469E−08  ...  −1.01175600E−08
 1   2  3.38323391E−07  ...   1.12932931E−07
 1   3  1.28007430E−07  ...  −6.15323336E−08
 .
 .
 .
 .
 .
54159  7.23323144E−05  ...  −7.73492112E−04
54160 −9.63647063E−06  ...   1.36677534E−04
 $END
 $EFRAG
 POSITION=FIXED COORD=CART
 fragname=WATER1
W1O1   −5.391969  1.772411  11
W1H2   −10.2131  30.376  −0.12
W1H3   −10.2131  30.763  −0.23
 fragname=CO21
C1C1   5.532541  1.6799  10.60
C1O2   10.3131  30.376  −0.12
C1O3   10.2131  30.763  −0.23
 $END
 $WATER1
WATER1 as DR1
COORDINATES(BOHR)
W1O1   −5.391969  1.772411  11   0.0  0.0
W1H2   −10.2131  30.376  −0.12   0.0  0.0
W1H3   −10.2131  30.763  −0.23   0.0  0.0
 STOP
 MONOPOLES
W1O1  1.0  0.0
W1H2  0.0  0.0
W1H3  0.0  0.0
 STOP
 REPULSIVE POTENTIAL
```

```
W1O1
0 ,0
 STOP
 $END
 $CO21
Carbon  as  DR2
COORDINATES(BOHR)
C1C1    5.532541  1.6799  10.60  0.0  0.0
C1O2    10.3131  30.376  −0.12  0.0  0.0
C1O3    10.2131  30.763  −0.23   0.0  0.0
 STOP
 MONOPOLES
C1C1  0.0  0.0
C1O2  0.0  0.0
C1O3  0.0  0.0
 STOP
 REPULSIVE  POTENTIAL
C1C1
0 ,0
 STOP
 $END
 $FRGRPL
 PAIR=WATER1 CO21
W1O1  C1C1  0  0
 STOP
 $END
```

Bibliography

[1] Gordon E. Moore. "Cramming more components onto integrated circuits". In: *Proceedings of the IEEE* 86.1 (1998), pp. 82–85. ISSN: 00189219. DOI: 10.1109/JPROC.1998.658762.

[2] Scott E. Thompson and Srivatsan Parthasarathy. "Moore's law: the future of Si microelectronics". In: *Materials Today* 9.6 (2006), pp. 20–25. ISSN: 13697021. DOI: 10.1016/S1369-7021(06)71539-5.

[3] Craig S. Lent, P. Douglas Tougaw, and Wolfgang Porod. *Bistable saturation in coupled quantum dots for quantum cellular automata*. Vol. 62. 7. 1993, pp. 714–716. DOI: 10.1063/1.108848.

[4] Craig S. Lent et al. *Quantum cellular automata*. Vol. 4. 1. 1993, pp. 49–57. DOI: 10.1088/0957-4484/4/1/004.

[5] C.S. Lent, P.D. Tougaw, and W. Porod. *Quantum cellular automata: the physics of computing with arrays of\nquantum dot molecules*. 1994, pp. 5–13. DOI: 10.1109/PHYCMP.1994.363705.

[6] Yuhui Lu and Craig S. Lent. *A metric for characterizing the bistability of molecular quantum-dot cellular automata*. Vol. 19. 15. 2008. DOI: 10.1088/0957-4484/19/15/155703.

[7] P. Douglas Tougaw and Craig S. Lent. "Logical devices implemented using quantum cellular automata". In: *Journal of Applied Physics* 75.3 (1994), pp. 1818–1825. ISSN: 00218979. DOI: 10.1063/1.356375.

[8] Mehdi Askari and Maryam Taghizadeh. "Logic Circuit Design in Nano-Scale using Quantum-Dot Cellular Automata". In: *European Journal of Scientific Research* 48 (2011), pp. 516–526.

[9] K. Walus and G.A. Jullien. "Quantum-dot cellular automata adders". In: *2003 Third IEEE Conference on Nanotechnology, 2003. IEEE-NANO 2003.* Vol. 2. 2003, pp. 461–464. DOI: 10.1109/NANO.2003.1231818. URL: http://ieeexplore.ieee.org/lpdocs/epic03/wrapper.htm?arnumber=1231818.

[10] Heumpil Cho and Earl E. Swartzlander. "Adder designs and analyses for quantum-dot cellular automata". In: *IEEE Transactions on Nanotechnology* 6.3 (2007), pp. 374–383. ISSN: 1536125X. DOI: 10.1109/TNANO.2007.894839.

[11] K. Walus et al. "Simple 4-bit processor based on Quantum-dot Cellular Automata (QCA)". In: *Proceedings of the International Conference on Application-Specific Systems, Architectures and Processors*. 2005, pp. 288–293. DOI: 10.1109/ASAP.2005.58.

[12] M.J. Kontz M.T. Niemier and P.M. Kogge. "A design of and design tools for a novel quantum dot based microprocessor". In: *Proceedings of 27th Design Automation Conference* (2000), pp. 227–232.

[13] P. Douglas Tougaw. "A device architecture for computing with quantum dots". In: *Proceedings of the IEEE* 85.4 (1997), pp. 541–557. ISSN: 00189219. DOI: 10.1109/5.573740.

[14] Alexei O Orlov et al. "Experimental demonstration of clocked single-electron switching in quantum-dot cellular automata". In: *Appl. Phys. Lett.* 77.2 (2000), pp. 295–297. ISSN: 00036951. DOI: 10.1063/1.126955. URL: http://link.aip.org/link/?APL/77/295/1.

[15] V. Vankamamidi, M. Ottavi, and F. Lombardi. "Clocking and cell placement for QCA". In: *2006 6th IEEE Conference on Nanotechnology, IEEE-NANO 2006* 1.c (2006), pp. 343–346. URL: http://www.scopus.com/inward/record.url?eid=2-s2.0-42549103185%7B%5C&%7DpartnerID=tZOtx3y1.

[16] G. Toth and C.S. Lent. "Quasi-adiabatic Switching for Metal-Island Quantum-dot Cellular Automata". In: *Journal of Applied Physics* 85 (1999), pp. 2977–2984.

[17] I Amlani et al. "Demonstration of a functional quantum-dot cellular automata cell". In: *Journal of Vacuum Science and Technology B: Microelectronics and Nanometer Structures* 16.6 (1998), pp. 3795–3799. ISSN: 10711023. DOI: 10.1116/1.590410. URL: http://www.scopus.com/inward/record.url?eid=2-s2.0-0343705344%7B%5C&%7DpartnerID=40%7B%5C&%7Dmd5=.

[18] W. Porod G. Csaba. "Simulation of field coupled computing architectures based on magnetic dot arrays". In: *Journal of Computational Electronics* 1 (2002), pp. 87–91.

[19] Craig S Lent. "Bypassing the transistor paradigm". In: *Science* 288.5471 (2000), pp. 1597–1599. ISSN: 00368075. DOI: 10.1126/science.288.5471.1597. URL: http://science.sciencemag.org/content/288/5471/1597.abstract.

[20] Kevin Hennessy and Craig S Lent. "Clocking of molecular quantum-dot cellular automata". In: *J. Vac. Sci. Technol. B* 19.5 (2001), pp. 1752–1755. ISSN: 0734211X. DOI: 10.1116/1.1394729. URL: http://dx.doi.org/10.1116/1.1394729.

[21] Craig S. Lent and Beth Isaksen. "Clocked molecular quantum-dot cellular automata". In: *IEEE Transactions on Electron Devices* 50.9 (2003), pp. 1890–1896. ISSN: 00189383. DOI: `10.1109/TED.2003.815857`.

[22] Craig S. Lent, Beth Isaksen, and Marya Lieberman. "Molecular quantum-dot cellular automata". In: *Journal of the American Chemical Society* 125.4 (2003), pp. 1056–1063. ISSN: 00027863. DOI: `10.1021/ja026856g`.

[23] Yuhui Lu and Craig S. Lent. "Theoretical study of molecular quantum-dot cellular automata". In: *Journal of Computational Electronics* 4.1-2 (2005), pp. 115–118. ISSN: 15698025. DOI: `10.1007/s10825-005-7120-y`.

[24] Yuhui Lu and Craig Lent. "Self-doping of molecular quantum-dot cellular automata: mixed valence zwitterions." In: *Physical chemistry chemical physics : PCCP* 13.33 (2011), pp. 14928–36. ISSN: 1463-9084. DOI: `10.1039/c1cp21332f`. URL: `http://www.ncbi.nlm.nih.gov/pubmed/21755091`.

[25] Xingyong Wang et al. "Exploring the possibility of noncovalently surface bound molecular quantum-dot cellular automata: Theoretical simulations of deposition of double-cage fluorinated fullerenes on Ag(100) surface". In: *Journal of Physical Chemistry C* 117.3 (2013), pp. 1308–1314. ISSN: 19327447. DOI: `10.1021/jp306903w`.

[26] Yuhui Lu, Mo Liu, and Craig Lent. "Molecular quantum-dot cellular automata: From molecular structure to circuit dynamics". In: *Journal of Applied Physics* 102.3 (2007). ISSN: 00218979. DOI: `10.1063/1.2767382`.

[27] Valentina Arima et al. "Toward quantum-dot cellular automata units: thiolated-carbazole linked bisferrocenes". In: *Nanoscale* 4.3 (2012), pp. 813–823. ISSN: 2040-3364. DOI: `10.1039/C1NR10988J`. URL: `http://xlink.rsc.org/?DOI=C1NR10988J`.

[28] A. Pulimeno et al. "Molecular QCA: A write-in system based on electric fields". In: *Proceedings - International NanoElectronics Conference, INEC*. 2011. DOI: `10.1109/INEC.2011.5991702`.

[29] A. Pulimeno et al. "Towards a molecular QCA wire: Simulation of write-in and read-out systems". In: *Solid-State Electronics* 77 (2012), pp. 101–107. ISSN: 00381101. DOI: `10.1016/j.sse.2012.05.022`.

[30] Azzurra Pulimeno, Mariagrazia Graziano, and Gianluca Piccinini. "Molecule interaction for QCA computation". In: *Proceedings of the IEEE Conference on Nanotechnology*. 2012. DOI: `10.1109/NANO.2012.6322051`.

[31] Azzurra Pulimeno et al. "Bis-ferrocene molecular QCA Wire: Ab initio simulations of fabrication driven fault tolerance". In: *IEEE Transactions on Nanotechnology* 12.4 (2013), pp. 498–507. ISSN: 1536125X. DOI: `10.1109/TNANO.2013.2261824`.

[32] Michael W. Schmidt et al. "General atomic and molecular electronic structure system". In: *Journal of Computational Chemistry* 14.11 (1993), pp. 1347–1363. ISSN: 1096987X. DOI: 10.1002/jcc.540141112.

[33] Mark S. Gordon and Michael W. Schmidt. "Advances in electronic structure theory: GAMESS a decade later". In: *Theory and Applications of Computational Chemistry*. 2005, pp. 1167–1189. ISBN: 9780444517197. DOI: 10.1016/B978-044451719-7/50084-6.

[34] M.J. Frisch et al. *Gaussian09*. 2009.

[35] A. Pulimeno. "Molecular Quantum-dot Cellular Automata (QCA) - Characterization of the bis-ferrocene molecule as a QCA device". PhD thesis. Politecnico di Torino, 2013, p. 114.

[36] Hua Qi et al. "Molecular Quantum Cellular Automata Cells. Electric Field Driven Switching of a Silicon Surface Bound Array of Vertically Oriented Two-Dot Molecular Quantum Cellular Automata". In: *Journal of the American Chemical Society* 125.49 (2003), pp. 15250–15259. ISSN: 00027863. DOI: 10.1021/ja0371909.

[37] Ira N. LEVINE. *Quantum Chemistry*. 2014. DOI: 10.1007/978-4-431-54825-6. arXiv: arXiv:1011.1669v3. URL: http://www.gnresearch.org/doi/10.5935/1984-6835.20090007%7B%5C%%7D5Cnhttp://link.springer.com/10.1007/978-4-431-54825-6%7B%5C%%7D5Cnhttp://ebooks.cambridge.org/ref/id/CBO9781107415324A009%7B%5C%%7D5Cnhttp://www.scielo.br/scielo.php?script=sci%7B%5C_%7Darttext%7B%5C&%7Dpid=S0100-40422011000300028%7B%5C%%7Dlng.

[38] *GAMESS User's Guide*. 2016. URL: http://www.msg.ameslab.gov/gamess/GAMESS_Manual/input.pdf.

[39] Yuri Ardesi. "Energy Analysis and Bistability Study of Molecular FCN". Politecnico di Torino, 2017, p. 137.

[40] Ruiyu Wang. "Analysis and Modulation of Molecular Quantum-dot Celluar Automata (QCA) Wire Acknowledgments". PhD thesis. Politecnico di Torino, 2013, p. 102.

[41] Ruiyu Wang. "Analysis and Modulation of Molecular Quantum-dot Celluar Automata (QCA) Wire Acknowledgments". PhD thesis. Politecnico di Torino, 2017, p. 188.

[42] R. S. Mulliken. "Electronic Population Analysis on LCAO,ÄìMO Molecular Wave Functions. I". In: *The Journal of Chemical Physics* 23.10 (1955), pp. 1833–1840. ISSN: 0021-9606. DOI: 10.1063/1.1740588. URL: http://aip.scitation.org/doi/10.1063/1.1740588.

[43]   Kubelka Group. *Population analysis*. 2017. URL: http://www.uwyo.edu/
        kubelka-chem/mm_notes_16.pdf.

[44]   URL: http://encyclopedia2.thefreedictionary.com/neutral+molecule.